DETECTION OF CROP WATER STRESS AND ITS IMPACT ON PRODUCTIVITY OF CROPLAND ECOSYSTEM

Thesis submitted to the Andhra University, Visakhapatnam in partial fulfillment of the requirement for the award of

Master of Technology in Remote Sensing and Geographic Information System

By

Nitika Dangwal,
M.Tech (Remote Sensing and GIS)
Agriculture & Soils Department

Under the Supervision of

Dr. N. R. Patel,
Scientist/Engineer-SF
Agriculture and Soils Department

Under the Co-Supervision of

Mamta Kumari
Scientist-SD
Agriculture & Soils Department

Agriculture and Soils Department
Indian Institute of Remote Sensing,
Indian Space Research Organization
Dept. of Space, Govt. of India, Dehradun – 248001
Uttarakhand, India

August-2014

DISCLAIMER

This document describes work undertaken as part of a programme of study at the Indian Institute of Remote Sensing of Indian Space Research Organization, Department of Space, and Government of India. All views and opinions expressed therein remain the sole responsibility of the author, and do not necessarily represent those of the Institute.

CERTIFICATE

This is to certify that Ms. Nitika Dangwal has carried out the thesis entitled "**Detection of Crop Water Stress and Its Impact on Productivity of Cropland Ecosystem**" in partial fulfillment for the award of degree of Master of Technology (M. Tech.) in Remote Sensing and GIS. The thesis has been carried out in Agriculture and Soils Department and is the original work of the candidate under the guidance of Dr.N.R.Patel, Scientist/Engineer-SF and co-guidance of Ms. Mamta Kumari, Scientist-SD, Agriculture and Soils Department, Indian Institute of Remote Sensing, Dehradun, India.

Dr.N.R.Patel,
(Supervisor)
Scientist/Engineer- SF,
Agriculture and Soils Department

Ms. Mamta Kumari
(Co-Supervisor)
Scientist-SD,
Agriculture and Soils Department

Dr S.K Saha
Dean (Academics)

ACKNOWLEDGEMENT

I express my sincere gratitude and respect to my thesis Supervisor, Dr. N.R. Patel, Scientist-SF, Agriculture and Soils department, IIRS and Ms. Mamta Kumari (Scientist-SD, ASD) for their valuable guidance, constant encouragement throughout the course of this study, and untiring help without which this research would not have attained its shape.I extent my gratefulness to Dr. Y.V.N. Krishna Murthy, Director, IIRS, for his excellent strategic administration. Apart from that highly appreciative expert comments during project discussions helped a lot to improve the standards of the project.

I would also like to thank Dr. S.K. Saha, Dean (Academics),IIRS, Dr. Suresh Kumar, HOD, Agriculture and Soils department, IIRS, for unrelenting nature to transfer their expertise. The way they trained us in the Agriculture and Soils division has made the whole period a great learning process.

It would be unfair if I proceed without thanking our course-coordinator Mrs. Shefali Agarwal for her concern on us and efficient management of academic activities that helped us complete our course curriculum with ease and in time. I could never miss to thank Dr. Hari Shankar Srivastava (Scientist-SF, ASD), and Mr. Justin George (Scientist-SC, ASD) for their care, intellectual help and resourceful supervision. I sincerely express my gratitude to all my colleagues in the ASD lab who were always a team and created the best working environment in all possible ways.

Friends make our life loom or gloom. I am very lucky to have encouraging, supportive and cheering friends always giving me positive energy to go ahead with my project and life. Mr. A.Ponraj, Ms. Suman Roy, Ms. Hemanti Sharma, Mr.Joyson, Mr.Trinadh and my all M.Tech batch mates.

I also thank my well-wishers and friends whom I might have not made a special mention here, but always stays with a special mention in my life. Yet importantly, I extend my

salutations to my beloved parents, my husband and in-laws for their everlasting encouragement and support.

Last but not the least, I wish to record my gratitude, with utmost reverence and gracious faithfulness to the Almighty God, for his indomitable lead and guidance throughout my life.

Thank You all,

Nitika Dangwal

ABSTRACT

Detection of crop water stress is crucial for efficient irrigation water management. Satellite monitoring of vegetation water stress is very important for precision agriculture, which relies on timing of irrigation to ensure crops will not suffer from water stress and produce maximum potential yield under limited water conditions. Potential of Satellite data to provide spatial and temporal dynamics of crop growth conditions under water stress and its impact over productivity of wheat. This study was conducted in western Uttar Pradesh and some parts of Haryana. Multi-temporal Landsat data was used for detecting water stress using thermal and optical based indices. Use of vegetation water stress index (VWSI), land surface wetness index (Ws_LSWI),

Water stress index (WSI) and SEBS for ET was used. For estimating productivity light use efficiency model (LUE model) was used. Water stress was validated with flux tower data. For yield validation crop cutting experiment was done. The main objective of this study was to detect crop water stress using different optical and thermal based indices and observing its impact on productivity of wheat. Stress factor was incorporated into LUE model for assessing impact over productivity.

The results indicated that Ws_LSWI was superior over other indices showing RMSE 0.12, R^2 0.65. Whereas, Ws_VWSI showed over estimated values with Mean RD = 4%. SEBS derived daily ET values were over estimated for all months.LUE derived using two different water scalar. Ws_LSWI based estimated LUE showed better results for February month than Ws_VWSI. Productivity derived by using water scalar (Ws_LSWI) had 0.65 R^2 and 0.46 for Ws_VWSI In conclusion, Ws_LSWI was found useful in detecting crop water stress and has proved to be a robust index.

Keywords: Water Stress, Crop Productivity, Light Use Efficiency, Energy balance

Table of Contents

LIST OF TABLES

LIST OF FIGURES

LIST OF ABBREVIATIONS

Abbreviation	Description
NDVI	Normalized Difference Vegetation Index
ET	Evapotranspiration
SEBS	Surface Energy Balance System
LUE	Light Use Efficiency
LAI	Leaf Area Index
LST	Land Surface Temperature
LSWI	Land Surface Wetness Index
VWSI	Vegetation Water Stress Index
WSI	Water Stress Index
EF	Evaporative Fraction
PAR	Photosynthetically Active Radiation
FAPAR	Fraction of Absorbed Photosynthetically Active Radiation
APAR	Absorbed Photosynthetically Active Radiation
LULC	Land Use/Land Cover
SEBAL	Surface Energy Balance Algorithm
SEBI	Surface Energy Balance Index
ILWIS	Integrated Land and Water Information System
LUEmax	Maximum Light Use Efficiency
CCE	Crop Cutting Experiment
NPP	Net Primary productivity
GPP	Gross Primary Productivity
HI	Harvest Index
Ws	Water Stress Scalar
R2	Coefficient of determination
RMSE	Root Mean Square Error

INTRODUCTION *Chapter1*

1.1 BACKGROUND

Biosphere's continued exposure to abiotic stresses viz., extreme temperature, chemical toxicity, salinity, drought etc has led to imbalance in natural status of environment. Any kind of stress can reduce average yield to more than 50%. Water stress condition arises due to inability to meet human and ecological demand of water whereas water scarcity refers to lack of available water or lack of water supply. An important point is that water scarcity is one of the many aspects that contribute to water stress. Thus, an area can be highly water stressed but not necessarily water scarce.

Agriculture is the major sector of all economic sectors which has relevance by water scarcity. Currently agriculture accounts 70% of global freshwater withdrawals. Water is a crucial component for food production. Since the biomass production requires huge amount of water to be transpired, it won't be incorrect, if we say that agriculture is both cause and victim of water scarcity. Growing demands with population growth has lead to large environmental cost. There is an uncertain impacts of climate change on water resources and water demand and similarly impact of bio energy production on agriculture and Climate change alter hydrological regimes and the availability of freshwater, with impact on rain fed and irrigated agriculture (UN-Water,2009,2012; FAO, 2008;FAO,2011a). Increase in precipitation in temperate zones, reduction in precipitation in Semi-arid areas, extreme variability in rainfall distribution and overall increase in temperature has been seen. All this has a particular impact on tropical and sub-tropical agriculture (IPCC, 2008). The availability of water is also affected by changes in runoff in rivers and aquifers recharge which will add to human pressure on water resources.

1.2 PROBLEM STATEMENT

Each year, in different parts of the world stress disrupt agriculture production and food supply resulting to famine conditions. 80-90% of biomass of non woody plants comprises of water. When there is a limited water supply to the roots of a plant it directly influence transpiration resulting in water stressed conditions. Availability of less water causes physical limitation in plants. Movement of water, oxygen and carbon dioxide in and out of plant is governed by Stomata. During water stress, stomata close to conserve water which result into closing the pathway for the exchange of oxygen, water and carbon dioxide which result into decrease of photosynthesis (Porporato et al., 2001). Hence, growth of leaves is affected by water stress more than root growth because roots can compensate more for moisture stress. Water stress causes reduction in photosynthesis which ultimately leads to reduction in growth and development

crop.Factors influencing crop water stress include soil moisture, canopy temperature/evapotranspiration (ET), leaf water content and leaf water potential (LWP).

Detection of water stress can help farmers in taking proper measure for reducing negative impacts on productivity. Water stress can be detected using Ground based techniques and remote sensing based techniques.

The traditional ground based techniques of stress measurement are based on measurement of predawn leaf water potential (Dixon, 1914), leaf pigment concentration (Lichtenthaler, 1987), leaf chlorophyll fluorescence (Muller, 1874) and evapotranspiration (ET) (Priestley and Taylor, 1972).Predawn leaf water potential technique uses pressure chamber for estimating leaf water potential. Since past 4 decades, Scholander et al. used this technique to measure trees and shrubs water relations. It requires manual operation and is slow and time consuming.Leaf water content technique, measures relative leaf water content which assesses the water status of plants. Most of the water resides in mesophyll cells of the plant. Relative leaf water content can be determined by taking ratio of three weight determinants i.e. fresh weight, dry weight ,turgid weight of leaf sample. It is also a time consuming method, comparative difference between stressed and non stressed plant are done during morning as the difference between water potential is greatest between plants at that time. Leaf pigment concentration technique, the theory behind it is that plant pigment concentration varies with species and phenology; with natural as well as anthropogenic stress. Healthy plants have generally high chlorophyll content than unhealthy plants; reduced chlorophyll is generally associated with stressed condition of plant. Two common approaches for quantifying pigments are: (a) conventional chemical method which require destructive sampling and time taking laboratory analyses; (b) chlorophyll meters that are simple and portable instrument which carryout rapid measurement. Leaf chlorophyll fluorescence technique is used more extensively to provide information on the functioning of photosynthetic apparatus. This method uses portable optical system and compact fluorescence meter. The functioning of the apparatus depends on photosynthesis, several environmental factors viz., light, water, nutrients affect this process and lead to plant stress. Therefore, this apparatus is recognized as the good indicator of plant stress also because changes occur in Chlorophyll fluorescence before any physical sign of deterioration in tissue is detected in the plants so stress can be detected before any physical damage done to plants. The disadvantage of this technique is that instruments are not made for commercial use. Lysimeter is a device which is used to measure actual ET released by plants.

All ground based measurement can be used successfully for measuring plant water stress at ground level or local regional level, but they are not applicable for large spatial scale like remote sensing does. Either ground measurement can be used for ground truthing of remote sensing applications.

Remote sensing studies have become widely popular for plant and environmental studies during 1980s.Remote sensing helps in providing reliable, quantitative, timely information on latest crop condition in a cost-effective manner instead of cost-and-time consuming conventional field methods (Bouman, 1995; Le Toan *et al.,* 1997; Shen *et al.,* 2009). Remote sensing derived information is used to evaluate spatial and temporal variations in crop growth, crop stress and supports for decision making for agricultural development (Shen *et al.,* 2009). The spectral characteristic of vegetation is governed by absorption and scattering characteristic of leaf internal structure and constituents like water, nitrogen, cellulose and lignin. Cellular structure and water content of leaves are detected in near infrared and mid infrared region of wavelength, whereas, leaf pigments are detected by visible band.

Chlorophyll and water content of vegetation are used as major indicator of plant stress. In stressed vegetation, chlorophyll content decreases which results in overall variation in absorption of light by leaf pigments. Consequently, it directly affects spectral signature of plant by decreasing reflection in green band and increasing in blue and red band resulting in changing normal spectral signature of plants (Murtha, 1982; Zarco-Tejada et al., 2000). Therefore, water stress can be detected using Visible, Near Infrared (NIR), shortwave infrared (SWIR) and Thermal infrared (TIR) bands. There are different water stress based indices using Visible, NIR, SWIR and TIR bands viz., Vegetation water stress index(VWSI), Land Surface Wetness Index(LSWI) are SWIR and NIR based indices (Ghulam *et al*.,2007) while Crop Water Stress Index(CWSI),Water Stress Index(WSI) are TIR based indices (Jackson *et al*., 1977; Jiang and Islam, 2001).

During the past decades, significant efforts have been made in the use of satellite data to assess the interactions between land surface and atmospheric processes over a wide range of scales(spatial and temporal). Remote sensing based models are an effective way to detect water stress for a large area. These models are based on Surface energy balance and turbulent fluxes theory through processes associated with surface radiation and energy balance which estimate physical properties of land surface like ET and Evaporative fraction (EF) (Su *et al.,* 2001). It determines water deficit status of the required area. Examples of such model are SEBI (Surface Energy Balance Index), SEBAL (Surface Energy Balance Algorithm), and SEBS (Surface Energy Balance System).

Water stress, being the most significant environmental stress, negatively affects crop growth and development, finally limits crop production, more than any other environmental factor (Shao *et al*., 2009).Water stress at flowering stage commonly results in severe reduction in crop yield. A major reason of this is a decline in assimilate flux to the developing ear head (Yadav *et al*., 2004). The influence of water stress over productivity of a crop can be assessed by using different productivity models, several process based models such as Biome BGC, BEPS and LUE based models require input variables derived from remote sensing. The light use efficiency

based model elaborated by Monteith has been widely used in estimating productivity based on remote sensing. Different factors are used as an input in this model including water stress scalar (Ws). This water stress scalar is incorporated into LUE model by water stress indices derived through remote sensing to observe impact of water stress on productivity.

Satellite monitoring of vegetation water stress is very important for precision agriculture, which relies on timing of irrigation to ensure crops will not suffer from water stress and produce maximum potential yield under limited water conditions. In this study, water stress for wheat crop was detected using optical and thermal data in parts of western UP and Haryana. Moreover, water stress impact on wheat crop productivity was also observed using light use efficiency model (LUE model).

1.3 RESEARCH OBJECTIVE

- ❖ To assess performance of different approaches of water stress detection from satellite data and validation with Eddy Covariance measurements.
- ❖ To analyze importance of water stress factor in controlling cropland productivity over space and time.
- ❖ To refine and validate LUE based algorithm for estimating cropland productivity.

1.4 RESEARCH QUESTIONS

- How well different approaches of stress detection from satellite data (VIS, NIR, SWIR & TIR) could capture water stress in cropland ecosystem under sub-tropical environment?
- How much water stress does control estimation of cropland productivity in sub-tropical ecosystem?
- Can refined LUE model improve accuracy of crop yield/productivity estimation?

LITERATURE REVIEW *Chapter2*

Detection of crop water stress and analysis of its impact on crop production is very important step to determine quantitative loss in crop yield. To assess the temporal and spatial variations in crop water stress and its impact on wheat productivity, stress indices, crop growth and yield has to be understood and assessed at regional scale. Satellite remote sensing by virtue of its synoptic view coverage, repetivity and multispectral information becomes an important source of spatial information and agriculture resource crop acreage, crop condition and crop growth to evaluate this abiotic stress of crop during various crop growth stages. Literature pertaining to the objectives of the present investigation is reviewed and presented under following sections:

2.1 ATMOSPHERIC CORRECTION OF SATELLITE DATA

Satellite images require atmospheric correction before proceeding for any study or undergoing further processing to derive different earth surface parameters with space borne imagery it is necessary to convert digital numbers into radiance and reflectance, since the data which provided to the user is in the digital numbers (DN). Studies that intend to use remote sensing data to determine ground surface characteristics such as biomass, phonological changes, leaf area index and yield estimation requires the conversion of digital numbers into target reflectance. To make multi-temporal and multi-sensor images comparable, digital numbers(DN) should be converted into physical units (Price, 1987).

There are several atmospheric correction techniques available (i.e. SMAC algorithm,6S code, FLAASH etc.) but the major disadvantages with them is that they require information other than satellite data product like path radiance, atmospheric transmittance at several locations collected within the image area during the satellite overpass. Under such conditions, a new but efficient tool ATCOR (atmospheric correction technique) is better option, it even consider topographic effect and has the capability to process thermal data. It also has an advantage of supporting all major commercial sensors with a sensor specific database of look up table (LUTs) which contains results of pre-calculated radiative transfer calculations. Integral part of ATCOR is its large database which contains results of radiative transfer calculations based on Modtran5 code.

The atmosphere influences the amount of electromagnetic energy that is sensed by detectors of an imaging system and these effects are wavelength dependent (Sabins Jr, n.d.);(Slater, 1980). The radiance received at the satellite is affected by the atmosphere by refraction, scattering and absorbing of light. Hence for correction of such effects and sensor gain and

offset solar zenith angle and solar irradiance must be included in radiometric corrections procedure that convert DN values to ground reflectance (Chavez, 1996). Liang et al., 2001 showed that atmospheric correction is a necessary step to extract quantitative information from Landsat Thematic Mapper-Plus imagery .ATCOR has also been used for atmospheric correction of airborne hyper spectral data of Antarctic region (Black et al., 2014).

2.2 CROP INVENTORY MAPPING FOR CROP STRESS DETECTION

In Agriculture Sector inventory of crop acreage and production at regional environment condition is the basic need for studying spatial and temporal characteristic of sustainable agriculture productivity. The conventional techniques for crop production estimation are timely reporting scheme and yield estimation from crop cutting experiment (CCE). Such reports are costly ,contains large errors, subjective and time consuming due to incomplete ground observation .which leads to poor area and crop yield estimation(Reynolds et al., 2000). Remote sensing data has great potential in mapping and doing inventory of different crops and Land use Land cover classes because satellite sensors has advantage of synoptic view and temporal repetivity.

DeFries et al., 1995 described the utility of multi temporal AVHRR dataset for land cover classification. Use of coarse resolution satellite data for distinguishing irrigated and rainfed agriculture in ecological modeling, water resource management and primary productivity assessment in a regional scale (Hooda and DYE, 1995). Patel et al., 2001 carried out study using LISS-III in Solani Watershed to derive agriculture land use for both Kharif and Rabi season along with other land cover categories. Both Kharif and Rabi season crop were identified using visual interpretation of LISS-III images acquired for Kharif and Rabi season and the statistics of that area was derived by integrating the two season maps on pixel by pixel basis in GIS environment. Further, Patel and Pande (2002) revealed that NDVI derived from multispectral AVHRR data was a good indicator of vegetation vigor and non-parametric classifier such as the rule based or hierarchical classification procedure could be easily employed with temporal NDVI for generating broad land use/land cover characteristic. Field based crop classification was also done using temporal profile of NDVI from Landsat data by rule based classifier(ŞENCAN, 2004).

2.3 REMOTE SENSING DERIVED WATER STRESS INDICES

There are several remote sensing based indices which consist of NIR, SWIR and TIR bands and can be used for detecting water stress for different crops. Water stress indices are often used in assisting farmer to maximize the crop yield when optimizing the irrigation system (López López et al., 2009). With thermal infra-red remote sensing surface temperature can be

monitored and can be related with crop water stress (Idso et al., 1977); (Jackson et al., 1981); (Idso, 1982); (Clawson and Blad, 1982). Transpiration makes leaf surface cooler because net radiation is consumed to evaporate plant water, this fact is used in detecting vegetation stress with canopy temperature (Usman et al., 2009). There are various successful examples of use of water stress indices viz., Critical Temperature Variability(CTV),(Clawson and Blad, 1982),Crop Water Stress Index(CWSI),(Jackson,1982) and Water Deficit Index(WDI),(Moran et al., 1994)for crop water stress detection.

2.3.1 WATER STRESS INDEX FROM THERMAL REMOTE SENSING

This index was introduced by Jiang–Islam (2013) by interpretation of relationship of normalized difference vegetation index and land surface temperature. (NDVI-Ts)which provide the basis to estimate Evapotranspiration (ET) by modifying Priestley and Taylor's equation (Priestley and Taylor, 1972).This was modified Water Deficit Index(WDI) which was proposed by Moran *et al*., 1994 where instead of potential evapotranspiration concept wet environment transpiration was used. This method is based on the NDVI-Ts scatter plot. Price, 1990 was the first to introduce the idea of deriving spatially explicit maps of latent heat fluxes via mathematical description of how remotely sensed measurement points fell within NDVI-Ts scatter plot. Knowledge of sensible (H) heat fluxes , Latent (LE) heat fluxes and soil water content are of great importance to many environment application including the monitoring of crop growth , productivity and crop water requirement and also for the procedures such as irrigation and cultivation management (Kustas *et al*., 2004) ; (Dodds *et al*., 2005)(Consoli *et al*., 2006). Such data are also very important for numerical modeling and for predicting atmospheric and hydrological cycles(Jacob *et al*., 2002).

The ability of satellite remote sensing to provide synoptic views in a spatially contiguous fashion without disturbing the area to be surveyed make it attractive for retrieval of such parameters (De Troch *et al*., 1996). The combined use of satellite data in from optical and thermal radiometers has been promising for retrieval of LE and H and soil surface water deviations.(Sandholt *et al.*, 2002);(Stisen *et al*., 2008).There are some residual methods which are based on information derived from scatter plot relation between vegetation indices(VI) and surface temperature (Ts). Ts /VI group of methods require relatively few parameters measurable over larger areas. They have a great ability to deal with surface heterogeneity and contain potential to provide easy transformation between instantaneous and averaged daytime flux. Taking measures from heterogeneous areas and plotting a feature space between remote sensing derived Ts /VI to form a scatterplot in triangular or trapezoidal shape for analysis of biophysical properties closed in the Ts /VI envelope and also for the estimation of land surface energy fluxes. Goward *et al.*, 2002 suggested the potential of using scatter plot derived rate of change of Ts with vegetation amount to diagnose the surface resistance to moisture fluxes. Hope *et al*.,

1986 used simulations from canopy reflectance model to conform that increase in vegetation amount as indicated by satellite derived vegetation indices measured, resulted in decrease in area averaged minimum canopy resistance and to increase in latent heat flux. Nemani and Running, 1989 used AVHRR data to relate slope of Ts/VI relationship over a coniferous forest in USA to the regional surface resistance. Carlson and Buffum, 1989 studied Ts/VI feature space properties using one dimensional boundary layer model of Goward et al., (1985). Carlson *et al.*, 1990 showed that the sensitivity of Ts to soil moisture variations differs for the leaf and surface soil around the plants, and tends to be much greater between areas of bare soil rather than across the leaves.

Ridd, 1995, Carlson *et al.*, 1995a and Gillies and Carlson, 1995 further illustrated how different parts of the Ts/VI triangle/ trapezoidal space correspond to different biophysical properties. Moran *et al.*, 1994 ,Carlson *et al.*, 1995b and Gillies and Carlson, 1995 used different spatial data sets to demonstrate that the boundaries of the triangular shape might be used to infer the physical constraints for the solution of the surface energy fluxes and surface soil moisture availability. Figure.2.1demonstrates Ts/VI feature space.

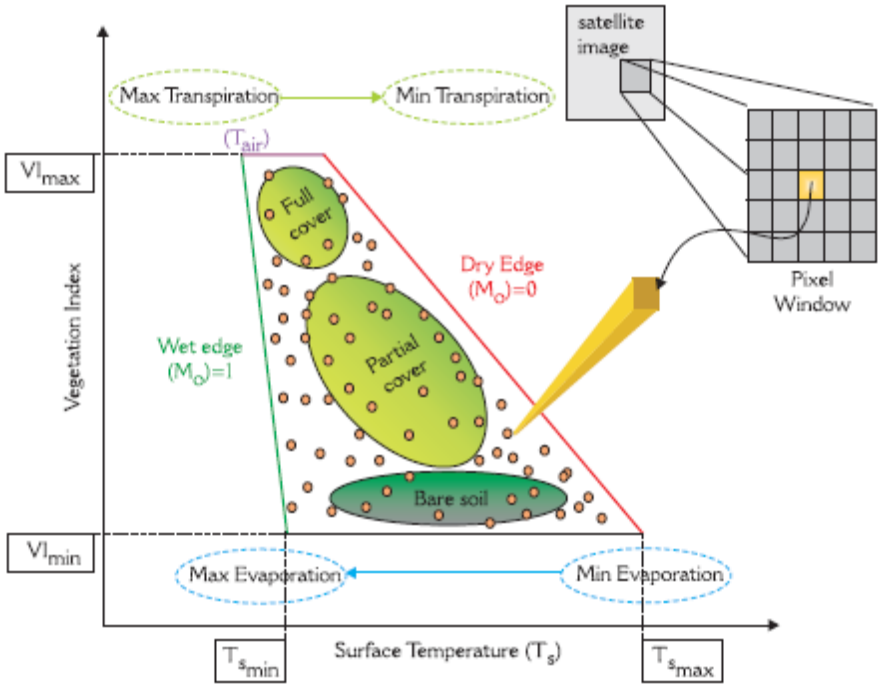

Figure 2.1: .Summary of the key descriptors and physical interpretation of Ts/VI feature space or scatterplot. (Source: synthesized from previous work of (Lambin and Ehrlich, 1996), (Sandholt et al., 2002) and (Nishida et al., 2003).

2.3.2 WATER STRESS INDEX FROM OPTICAL REMOTE SENSING

As an alternative to thermal measurement, various water stress indices have been introduced using Short wave infrared band (SWIR) and near infrared index (NIR), SWIR band is sensitive to equivalent water thickness while NIR band is sensitive to variations in dry matter content.NIR and SWIR bands are used to detect effects of drought on vegetation water content and water stress (Ghulam *et al*., 2008a);(Claudio *et al*., 2006);(Cohen, 1991);(Hardisky *et al*., 1983);(Hunt Jr *et al*., 1987);(Ripple, 1986);(Tucker, 1980). The water indices using SWIR band is appeared more useful in extracting information about vegetation water status, water sustainability studies and in draught detection (Kim, 2006). SWIR region is least affected by ozone and Rayleigh scattering moreover, it is also less affected by water vapor and aerosol content.(Vermote *et al*., 2002)

Vegetation water stress index(VWSI) uses NIR and SWIR reflectance band to form trapezoid to create minimal and maximal waterlines for slope and intercept which is crop specific. Ghulam et al., 2008a created a statistical method which was based on Scatter plot of NIR and SWIR in trapezoidal shape which surrounds the data to determine the amount of water stress for one pixel which is compared with other pixel in scatter plot.

Land surface wetness index (LSWI) is a measure of interaction of liquid molecules in a plant canopy (Gao, 1996) ,that is why it is sensitive to the total liquid in crop. The index derived from SWIR and NIR has different nomenclature for different author (Gao,1996) and (Chen *et al*., 2005) called it as NDWI(Normalized Difference Water Index). Xiao *et al*., 2004 called it LSWI (Land Surface Water Index).

2.4 USE OF WATER BALANCE AND ENERGY BALANCE CONCEPT FOR EVAPOTRANSPIRATION ESTIMATION

The water availability at root zone is very important for supporting growth and productivity of crop. When rain water or irrigation reaches soil surface it undergo many processes some of it infiltrate into soil, some of it moves out as surface runoff. Water which infiltrate may also directly evaporate from soil surface to the atmosphere. Most of it is consumed by plant roots for growth and transpiration, water also accumulate within root zone and can also moves downward beyond rootzone.When rainfall and irrigation water content is not sufficient, the soil water content gets reduced to such levels which cannot tolerate crop water requirement. This led to less actual evapotranspiration than crop water requirement and hence plants experience water stress.

Actual evapotranspiration is a fraction of crop water requirement which depends on soil moisture availability. Mostly actual evapotranspiration approaches to crop water requirement during active growth stages of crop when sufficient moisture is present in soil.
However, it also falls below crop water requirement in earlier stages of growth before full canopy coverage and at the end of crop growing stage. As a result, rainfed crops covering more than 80 % of global cropped area and 60-70 % of global crop production is frequently limited by moisture stress (Biggs et al., 2008).

Evapotranspiration is a process which governs hydrological cycle and energy transport between soil-water-vegetation system and atmosphere(Senay *et al*., 2008). The process combines two separate and simultaneous process evaporation and transpiration. Evaporation occurs on open water bodies surfaces, bare ground and vegetation whereas transpiration transpires water from soil through plant roots and leaf (Senay *et al*., 2011). The two processes occur simultaneously and require a source of water ,energy and slope of vapor (Kalma *et al*., 2008). Natural hazards, global warming and species extinction are the main cause of global environment change which is the matter of today's concern. Evapotranspiration governs these processes and play important role in agriculture and hydrology for prediction and estimation of global climate change. For determining crop water stress the spatial distribution and accurate quantification of evapotranspiration is important. Understanding the rate and amount of evapotranspiration is important for monitoring hydrological and agricultural systems (Elhag *et al.*, 2011). Due to its important role in agriculture, meteorology and hydrology it can be used as an important in determining water stress.

Crop characteristics, radiation, air temperature are weather parameters affecting ET. Although ET can't be measured directly, there are some conventional Evapotranspiration estimation techniques i.e. pan measurement, eddy correlation system, Bowen ratio, weighing Lysimeter. Conventional techniques are field based and provide better ET estimation for homogenous area(Li and Singh, 2009). Most of these techniques require surface and land parameters which are difficult to obtain for larger area and thus restrict its applicability to large area. However, remote sensing based estimation of ET provide consistent and economic feasibility on regional scales (Irmak, 2008), Beside this it also provide continuous spatial information within shorter time period and practically useful for inaccessible areas. Work has been done to derive evapotranspiration from remote sensing without site specific relationship by using Priestly-Taylor equation and Grangers complementary relationship. Such relationship incorporates atmospheric conditions in relative evaporation coefficient without getting dependent on in-situ conditions. But this approach does not distinguish between soil and vegetation temperature profile (Venturini *et al.*, 2008). ET can also be estimated by using surface temperature-vegetation index (Ts-VI) triangle approach. This approach determines quantitatively the dry and wet edges of triangle space using MODIS dataset. However, determining these edges require high rate of uncertainty especially in arid and semi-arid areas also in cloudy conditions it

become difficult to determine dry pixels and wet pixels moreover it was difficult to determine dry pixels in short duration after rainfall which will give maximum evapotranspiration (Tang *et al*., 2010).

MODIS global terrestrial ET was developed by Mu *et al.*, (2007) however its algorithm was modified in 2011 by simplifying the calculation of vegetation cover fraction. ET was calculated as the sum of day and night time components by adding calculations of soil heat flux and by improving estimates of stomatal conductance, boundary layer resistance, aerodynamic resistance and also by separating dry canopy surface from wet canopy surface, it also divided soil surface into moisture surface and saturated wet surface. This modification provided very critical information on global terrestrial water and energy cycles and environment change. However this modification hasn't been validated yet (Mu *et al*., 2011).

Zhang *et al*., 2008 have estimated evapotranspiration by using three different models namely Pennmen-Monteith, Clumping model and Shuttle-Wallace. Shuttle worth-Wallace model assumes that there is blending of heat fluxes from leaves and soil whereas clumping model use Shuttle worth Wallace model by separating soil surface into fractional area inside and outside the influence of canopy. Out of these three, clumping model derived best ET correlated with in-situ observation but overestimates after rainfall duration. However, these results were site-specific. MODIS NDVI data and Global Land Data Assimilation System(GLDAS) meteorological data was used to calculate ET in ungauged basins making it completely independent of field data.Ts-NDVI method has the limitation in range of NDVI, so this can be only applied for wide range of NDVI to make expected trapezoid from Ts-NDVI space moreover it is unable to consider ET during night time and cloudy daytime (Du and Sun, 2012).

Kalma *et al.*, 2008 pointed out that solutions of surface energy budget are surface energy models. There are several other models which are remote sensing and field measurement based such as surface energy balance algorithm (SEBAL) which was developed by (Bastiaanssen *et al.*, 1998), ET derived from SEBAL was spatially distributed and calculated sensible heat flux by using wind speed from single weather station it also used hot and cold points of satellite image to provide empirical temperature difference equation. Zhang et al., 2011 modified SEBAL approach. Almhab and Busu, n.d derived ET by using SEBAL approach from Advanced Very High Resolution Radiometer (AVHRR) onboard NOAA-14 satellite and Landsat TM in Mountainous terrain of Sana's basin in Yemen. Results showed that AVHRR derived ET are reasonable however ET derived from Landsat shows better results because of high resolution. Similarly other models are-The Surface energy balance index (SEBI) (Menenti and Choudhury, 1993),The Simplified surface energy balance index (S-SEBI) (Roerink *et al*., 2000), Mapping Evapotranspiration with internalized calibration (METRIC) (Allen *et al*., 2007).

The SEBS (Su, 1999) was introduced to estimate atmospheric turbulent fluxes, actual evapotranspiration (ET) and evaporative fraction using satellite image and meteorological information at proper scale. SEBS includes a set of tool for deriving physical parameter of land surface such as albedo, land surface emissivity and land surface temperature from spectral radiance and reflectance of satellite earth observation data. Ma *et al*., 2012 derived actual ET from Landsat 5 TM by using SEBS on irrigated area. They used multi-temporal satellite image for obtaining daily ET and then compared the results with ground measurement data in which they found SEBS results to be very similar to ground measurements.

2.5 CROP YEILD ESTIMATION USING REMOTE SENSING

The two important criteria for sustainable land management are crop yield and crop variability (Smyth and Dumanski, 1993). The average crop yields are often used to assess yield performance, but are not used for evaluating sustainable farming system. The reason behind it is that average yield signifies long term normal yield without providing information on performance over space and time. Hence crop yield modeling is challenge for many researchers. Agriculture is a major user of satellite remote sensing data. Projects like Crop acreage and Production estimation (CAPE) was in process for more than a decade to estimate crop production using satellite observations in India for crops like wheat,sorghum,groundnut,cotton and mustard in their major growing areas (Navalgund *et al.*, 1991a). Other project is FASAL (Forecasting Agricultural Outputs Using Space Agrometeorology and Land based observation) which strengthened the current capability from econometric and weather based techniques with remote sensing applications (Parihar, 1999). Emergence of yield forecasting came into existence due to (i) the ability of satellite to supply observations over large areas which led to provide crop monitoring techniques with possible spatial extent and (ii) strong correlation between satellite derived vegetation indices and different crop parameters.

Using remote sensing data yield modeling can be done by two approaches firstly, satellite based derived parameters are directly related to yield (Dubey *et al.*, 1991). Maximum linear relation has been seen for NDVI with yield for various crops in Punjab and Haryana. Secondly, remotely sensed data derived biophysical parameter like LAI are used in yield model (Saha and Bairagi, 1998). Moreover temporal profiles of remote sensing data used in estimating spectral growth parameters are highly correlated to crop yield (Dubey *et al*., 1991). There are number of crop yield prediction models using remote sensing developed for wheat and used in crop forecast (Parihar, 1999).

2.6 CROP YIELD ESTIMATION USING REMOTE SENSING AND LIGHT USE EFFICIENCY MODEL

The light use efficiency of a plant canopy is defined as ratio of net primary productivity to absorbed photosynthetically active radiation. Net primary productivity is approximately constant with respect to changes in Absorbed photosynthetically active radiation (APAR) which means that Net primary productivity can be modeled by making linear relationship with (APAR). Common Light use efficiency model was originated with (Monteith, 1972),(Monteith and Moss, 1977) who found linear relationship between net primary productivity and APAR for different range of crops in Britain which led him to conclude that photosynthetic radiation use efficiency was a conservative parameter. Such linear relationship was observed by (Gallagher and Biscoe, 1978) for several field crops.

The effects of environmental factors like water stress, temperature and nitrogen availability is focus of theoretical (Hunt and Running, 1992)(Runyon *et al.*, 1994),(Sands, 1996) and experimental work (Gallagher and Biscoe, 1978)(Legg *et al*., 1979),(Wright *et al.*, 1993). LUE models have been used to estimate regional and global patterns of GPP and NPP at various spatial and temporal (Potter *et al*., 1993)(Prince and Goward, 1995),(Landsberg and Waring, 1997).

The major parameter of a LUE model is fraction of absorbed PAR (FAPAR). In general, FAPAR can be derived from remote sensing data due to the link between absorbed solar energy and satellite derived vegetation indices (Myneni and Williams, 1994). Linear relationship between FAPAR and NDVI has been shown in different studies for different biomes(Ruimy *et al*., 1994);(Saugier,1994);(Myneni and Williams, 1994);(Law and Waring, 1994). This linear relationship between FAPAR and NDVI can be applied in LUE model for addressing temporal and spatial variation in gross primary productivity (GPP).

There are different models used for assessment of GPP- the Global Production Efficiency Model (GLO-PEM) (Prince and Goward, 1995) which simulates global GPP and NPP by directly retrieving APAR from Satellite data, the 3-PG model(Physiological Principles in Predicting Growth) (Landsberg and Waring, 1997) which was used to calculate forest GPP using APAR and LUE, the Vegetation Production Model(VPM) (Xiao et al., 2004) in which potential Light Use Efficiency is affected by leaf phenology, temperature and land surface moisture conditions. The C-Fix model (Veroustraete *et al*., 2002),CASA model (Potter *et al.*, 1993) for deriving Net Primary Productivity. The input parameters of LUE model derived from remote sensing are discussed below:

2.6.1 FRACTION OF ABSORBED PAR (FAPAR)

Spatial and temporal scales information on PAR is needed for applications dealing with productivity (Running *et al*., 2004). The proper observation of FAPAR is suitable to monitor the

seasonal cycle and inter-annual variability of activities of vegetation related to photosynthesis. FAPAR varies in space and time due to difference between species and ecosystem, human activities and weather and climate processes(Myneni and Williams, 1994) defined FAPAR as fraction of incident PAR absorbed by photosynthesizing tissue in a canopy fraction of PAR absorbed by vegetation (Chen, 1996);(Gower *et al.*, 1999);(Tian *et al.*, 2000). It is difficult to measure FAPAR directly, but it can be derived from models which describe the transfer of solar radiation in plant canopies, using remote sensing observation as component.

Absorption of radiation by leaves is of greater concern than any other part of plants in environmental application. Ground based estimation of FAPAR requires simultaneous measurement of PAR above and below canopy as well as architecture information to account for the no leaves absorption. FAPAR is also retrieved from space remote sensing platforms by numerically inverting physically based models. Most of the derived products represent only the fraction absorbed by green part of leaf canopy. Since it is a ratio of two radiation quantities FAPAR is a dimensionless variable.

2.6.2 VEGETATION INDICES TO DERIVE FAPAR

A single spectral band contains insufficient information for characterization of vegetation structure and status (i.e. health, canopy geometry) so combination of two or more spectral bands by band ratios and development of vegetation indices took place to incorporate more information on vegetation (Qi *et al*., 1994). Most of the vegetation indices use red and near infrared band (NIR) (Baret and Guyot, 1991). Vegetation indices are quantitative measurements indicating vigour of vegetation (Campbell, 1987), they show better sensitivity than individual spectral bands for detection of biomass (Asrar *et al*., 1984). Most common used indices to derive FAPAR, LAI and other surface parameters from space-borne and air-borne remote sensing data are Simple ratio(SR) and normalized difference vegetation index (NDVI) (Rouse Jr *et al.*, 1974). These vegetation indices have been found very well correlated with various vegetation variables like green leaf area(Asrar *et al.*, 1984), standing biomass(Tucker, 1979),FAPAR(Sellers, 1985) and productivity(Asrar *et al.*, 1985).

2.6.3 LIGHT USE EFFICIENCY

LUE can be expressed as dry mass formed per unit of absorbed photosynthetically active radiation (APAR). All crops don't have similar efficiency for utilizing intercepted sunlight. Crop geometry, structure, spatial distribution of leaves and their angle are factors that affect LUE. NPP studies at regional and global scale require accurate estimation of APAR and LUE. LUE is known to exhibit both spatial variation across vegetation types(Gower *et al*., 1999);Turner *et al.*,2002) and temporal variations at individual sites(Campbell *et al*.,2001; (Nouvellon *et al.*, 2000), Consequently generating valid representations of LUE is specially

difficult in regions with substantial cropping because native vegetation and crops often have different LUE value which create spatial heterogeneity which can't be captured by remotely sensed reflected observations (Gower *et al.*, 1999). Hence a common approach is to incorporate information about vegetation type , temperature and water availability conditions for LUE calculations (Ruimy *et al*., 1994). LUE values are generally highest for C4 crops ,lower for C3 crops and lowest in grassland (Gower *et al*., 1999);(Ruimy *et al*., 1994).

Individual studies have shown that LUE varies with factors such as species composition, stand age, foliar nutrients and soil fertility (Gower *et al.*, 1999). Moreover the relationship between optical remote sensing based NDVI and FAPAR is generally considered to be near linear(Sellers, 1985);(Ruimy *et al*., 1994) and consequently NDVI is frequently used with an estimate of maximum light use efficiency (LUEmax) in models to calculate productivity (Ruimy *et al*., 1999). To assess the impact of water stress over productivity, water stress scalar is used as one of the important factor in LUE model(Monteith, 1972). Variations in water situation can cause reduction in LUE and thus finally affect productivity. Satellite based derived water stress index can be used as a proxy for water stress (Ws = 1-ET/ETm) which is defined as the function of ratio of actual ET to potential ET rates on the earth surface in LUE model for estimating productivity affected by water stress.

3.1 STUDY AREA

Study area comprises of Western Uttarpradesh and some parts of Haryana. Western U.P contributes to 34 percent of total food grain production at state level and 6 percent at national level. Sugarcane is the dominant crop of this region and Wheat is the dominant crop of Haryana. Major population of this area depends upon agriculture Wheat, Rice, oilseeds, pulses and potatoes are major agriculture product. It also supports 15% of India's total livestock population.

3.2 LOCATION

The study area is located between 26.4 deg and 30.21deg latitude and 77.3 deg and 80.4 deg longitude. The holy river Ganga provides the boundary to the north region separating it from hilly areas and Tarai regions of U.P, western area is separated by river Yamuna which separates it from Haryana and Delhi. The study was conducted in five districts of western UP (Meerut,Ghaziabad,Baghpat, Gautambudhnagar and Muzzafarnagar) and small area of Haryana (i.e. Sonipat and Panipat). Haryana state is bounded on Northwest by the state of Punjab and union territory of Chandigarh from North and Northeast by Himachal Pradesh and Uttarakhand and on south and south west by Rajasthan.

3.3 SOILS

Soil of Western UP is alluvium, coarse to medium in texture and moderately alkaline. They appear dark grey which indicate high organic matter composition. Region is spread with loam and silty to silty clay loam in most part of the region.Whereas in Haryana soils are generally deep and fertile exception occurs in Northeast and south west area where eroded and sandy land occur.

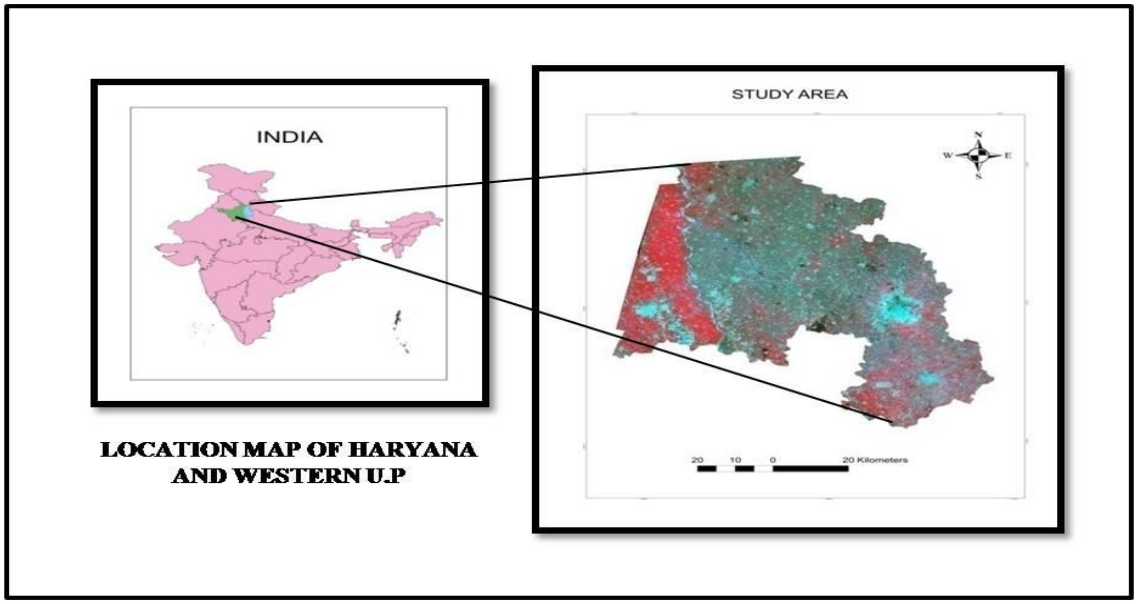

Figure 3.1: Location Map of the study area

3.4 CLIMATE

In Western UP rainfall is highly irregular, uncertain and unevenly distributed. About 80% of total rainfall is received in June to September. Long dry spells are usually experienced during Rabi season. A small amount of precipitation is received during dry spells of Rabi season provide boost to Rabi season crops. The maximum and minimum temperature increase from January to April in both weather station of western Uttarpradesh, January month is the coolest month with minimum temperature of 5.0 and 5.6 degree in Meerut and Muzzafarnagar respectively. In Haryana in summers maximum temperature raise to 45 degree Celsius in May and June and January is the coldest month where temperature may fall below freezing point. Precipitation averages around 450 mm annually between July and September.

3.5 FARMING SYSTEM

Crop production is the major enterprise of farming community. Dairying forms another farming enterprise in this region. Agro-horticulture and agro-forestry are also emerging enterprises of farming system in this region. Sugarcane is the pre dominant commercial crop cultivation of this region. Field preparation for wheat cultivation generally starts in the month of November and continues till second fortnight of December because of delayed harvesting of

sugarcane. More than 90% of area is covered with irrigated wheat with average of 4 to 5 irrigation is provided to the crop. Haryana contributes a good production of Wheat and Rice .In addition cotton, pearl millet, mustard and rapeseed, Chickpeas, Sugarcane, Sorghum and corn. Dairy cattle, Buffaloes and bullock are used in field work. Haryana is well known for its contribution in Green Revolution.

3.6 CROPPING SYSTEM

Double cropping is the most popular practice. Dominant cropping system is Sugarcane-Ratoon-Wheat. Other cropping systems practiced in west UP are sorghum-wheat, rice-wheat, and pearl millet-wheat. Wheat and Sugarcane both cover more than 57% of cropped area. Other important crops are Rice, Rapeseed and Mustard. In Haryana region, major cropping system is Rice-Wheat. Other cropping systems are Cotton-Wheat, Rice-other crops, Bajra/Jowar/Gwar-Wheat, Bajra-Mustard, Bajra-Pulses.

3.7 CROP ROTATION

Crop Rotation followed in Western Uttarpradesh is:

- ✓ Sugarcane-Ratoon—Wheat + Mustard
- ✓ Sugarcane-Ratoon-Oat
- ✓ Fodder Sorghum-Sugarcane-Wheat
- ✓ Rice-Berseem+Mustard
- ✓ Fodder Sorghum – Rapeseed and Mustard
- ✓ Fodder Sorghum –Potato –Moong

Crop Rotation followed in Haryana is:

- ✓ Pearl millet – Wheat
- ✓ Pearl millet – Chickpea
- ✓ Pearl millet – Sorghum
- ✓ Wheat - Rice

Many studies were carried out in India and abroad to demonstrate usefulness of remote sensing data to quantify different biophysical parameters and agricultural studies. Looking at potential of remote sensing various methods and techniques are developed in relating remotely sensed signatures from satellite sensors to crop parameters, crop water stress and final yield of wheat is discussed in following sections.

4.1 DATA USED

To achieve the objective in present study the following satellite products, ancillary data and software have been used.

4.1.1 REMOTE SENSING DATA

Satellite dataset used for this study was Landsat 5-TM, Awifs, Landsat 8. Details are given in following table 4.1

Table 4.1: Details of satellite data products used in this Study

S.no.	Data Type	Date of acquisition	Path/Row	Resolution
1.	Landsat 5 TM	11th November 2009 14th February 2010 4th April 2010	146/40	30m
2.	Awifs	24th December 2009 31st January 2010 20th March 2010	95/52 93/52 93/49	56m
3.	Landsat 8	21st November 2013 7th December 2013 8th January 2014 9th February2014 13th March 2014 14th April 2014	146/40	30m

4.1.2 ANCILLARY DATA

Survey of India topographic sheets of numbers 53G, 53K, 53H and 53L at 1:250,000 scales have been used for this study. Weather data for 2009-10 and for 2013-14 was obtained from Department of agriculture, Sardar Vallabhai Patel University of Agriculture and Technology (SVPUAT).

4.1.3 INSTRUMENT USED

- **PAR/LAI Ceptometer (AccuPAR model LP-80)** - It is a portable linear photosynthetically active radiation (PAR) sensor used to calculate canopy PAR interception and LAI of vegetation canopy non-destructively in real time. It consists of an integrated microprocessor driven data logger with a probe in which 80 sensors are placed at 1 cm of distance. Instrument is capable of taking hand-held or unattended measurements
- **Garmin GPS –** It is used for tracking coordinates for sample site and data collection.

4.1.4 SOFTWARE USED

- Erdas Imagine 9.2, 2013 for image processing
- ENVI 4.5 for image processing
- ArcGIS 10 for database creation and analysis
- ILWIS 3.8.3 for SEBS
- Microsoft Office 2007
- MATLAB for statistical and graphical analysis

The Methodology adopted for this study can be understood by the following flowchart

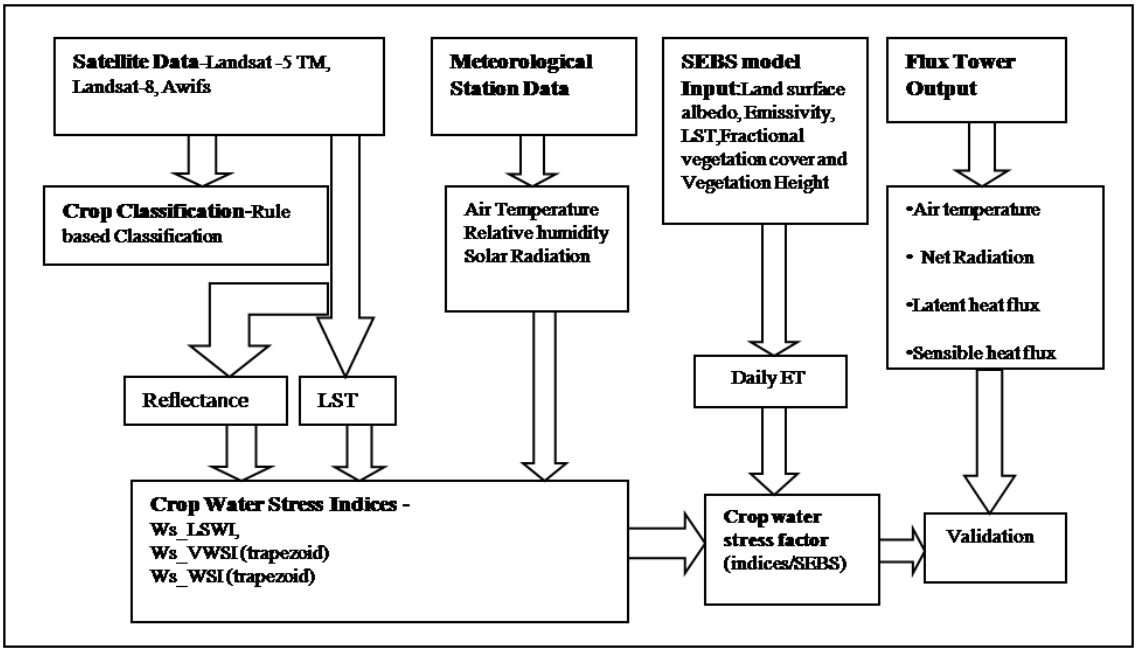

Figure 4.1: Methodology (Part-1)

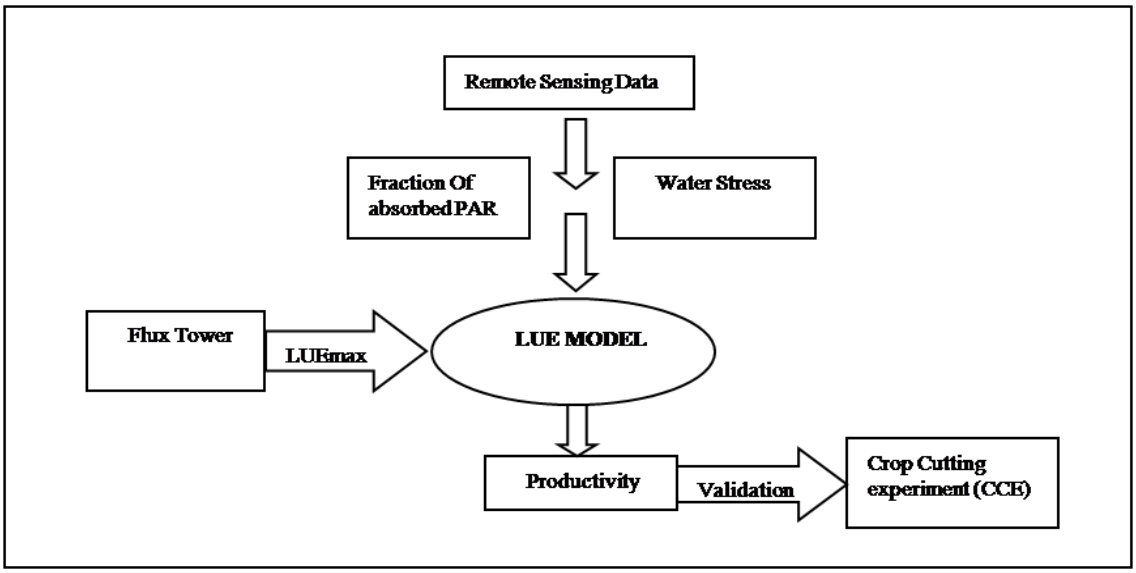

Figure 4.2: Methodology (Part-2)

4.2 GROUND MEASUREMENTS

Leaf area index and Fraction of photosynthetically active radiation are important ground measurement property. Leaf area index can be defined as one sided leaf area per unit ground area. It is an important structural property of a plant canopy. FAPAR measures the proportion of available radiation in the photosynthetically active wavelength (400-700nm). In ground, LAI and FAPAR were measured in randomly selected samples sites which have homogeneity and sufficient aerial extent. GPS coordinates were also recorded for the sample sites for accurate identification of particular locations and for further analysis. Ground measurement site map is shown in figure 4.4.

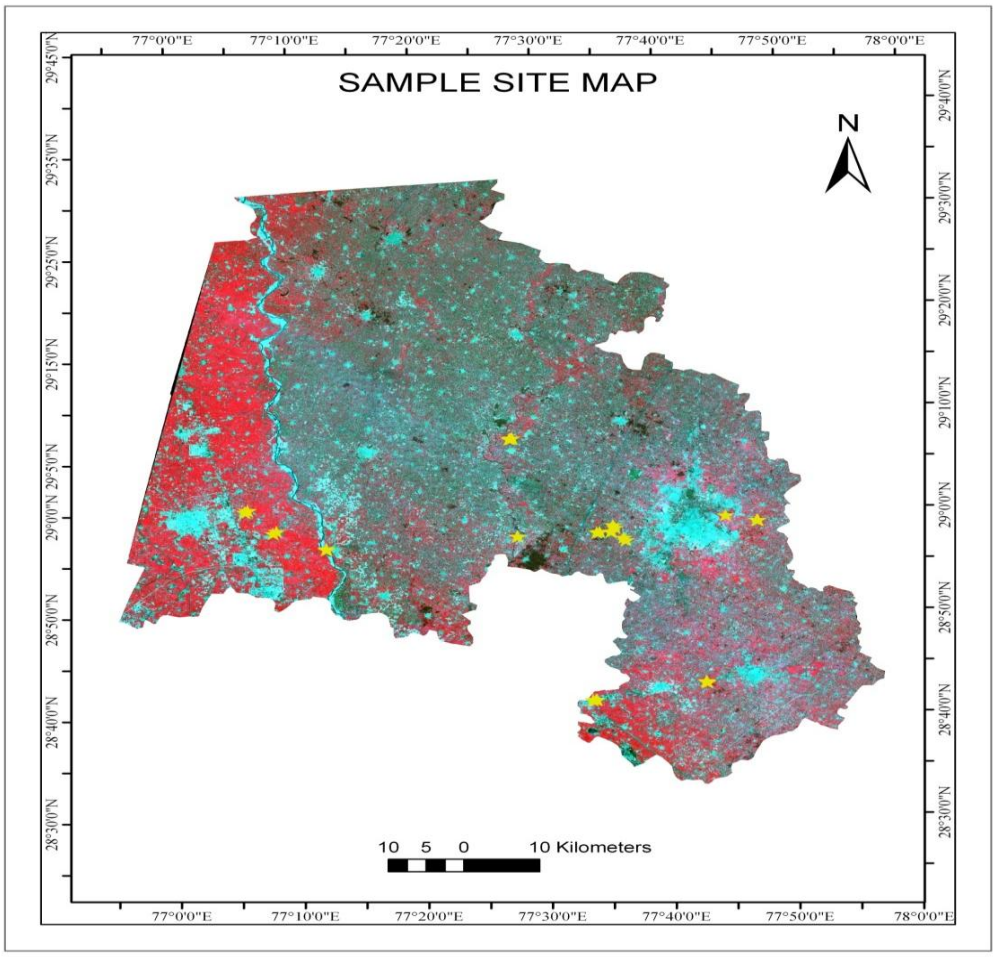

Figure 4.2: Ground measurement site map

Figure.4.4: Ground data measurement

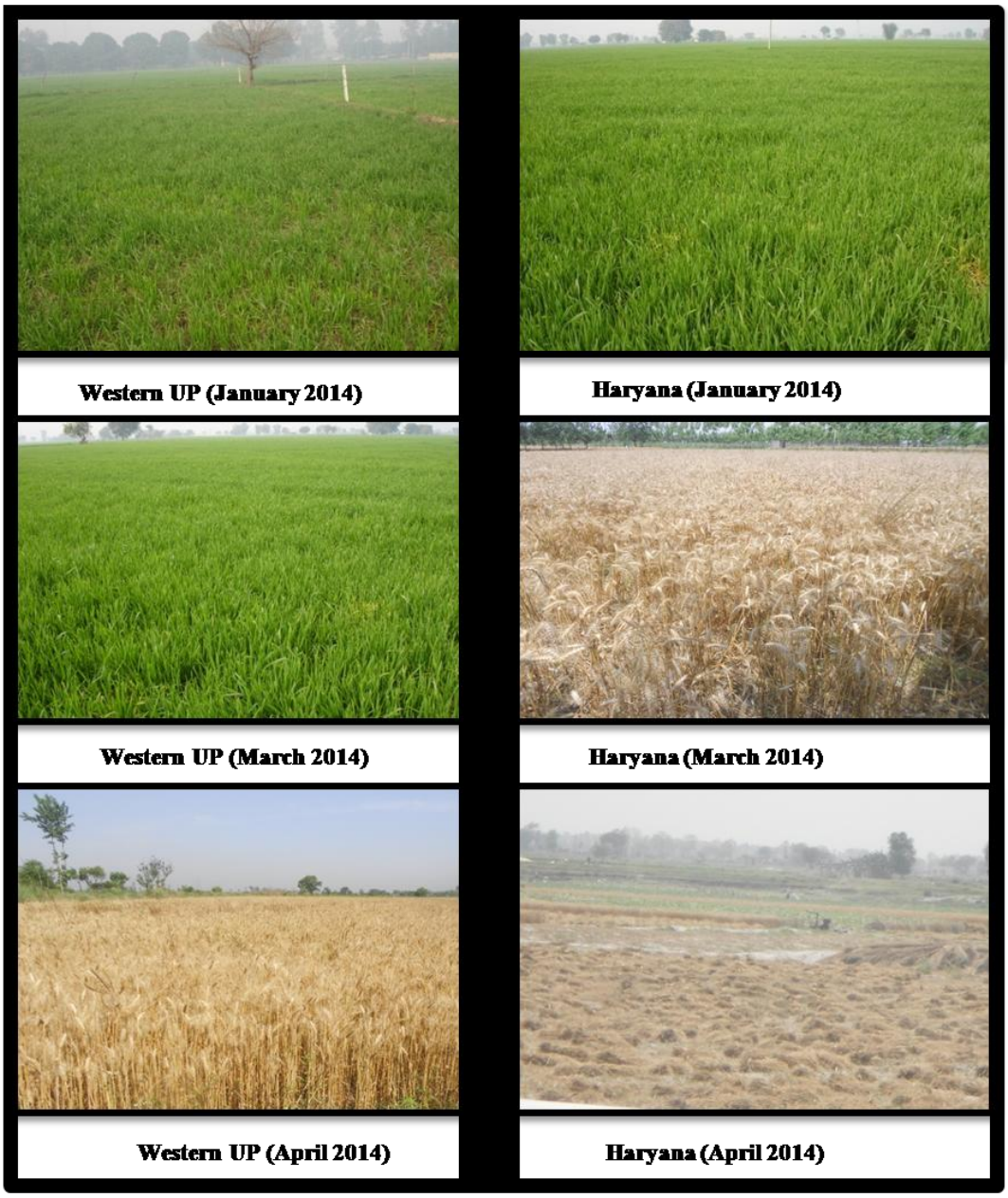

Figure 4.5: Vegetative growth of wheat during different months in Western UP and Haryana

4.2.1 FRACTIONOFABSORBED PHOTOSYNTHETICALLY ACTIVE RADIATION (FAPAR) MEASUREMENTS

FAPAR was measured by using AccuPAR instrument, this instrument record the amount of PAR intercepted above canopy and below canopy in an open field. Hence the radiation falling Above the canopy can be absorbed and reflected even at the soil surface. For estimation of FAPAR above phenomenon was used:

I is the incoming PAR reading above canopy,

B is the incoming PAR below canopy,

With these readings we can derive absorbed photosynthetically active radiation (APAR)

APAR= I – B …… (4.2.1.1)

Further, The Fraction of absorbed PAR can be derived by:

FAPAR = APAR / I ……. (4.2.1.2)

4.2.2 LEAF AREA INDEX (LAI) GROUND MEASUREMENT

LAI was measured by placing instrument once above canopy and three times below canopy. From every sample site two three readings of LAI was measured. The estimated LAI was then averaged out to represent field LAI.

4.3 PRE-PROCESSING OF SATELLITE DATA

Satellite data need to be converted to reflectance values from raw digital numbers and also needs haze removal if haze exists, for better visuality of the image.

4.3.1 HAZE REMOVAL

In many of the satellite imagery the scenes contain haze and their removal can be performed in ATCOR before atmospheric correction. In radiance signal, haze is an additive component. Since the algorithm for haze removal runs fully automatic in ATCOR. It is a combination of Richter (1996 b) and Zhang et al (2002). Haze removal consists of five major steps:

- Clear and hazy areas are masked with the tasseled cap haze transformation (Crist and Cicone1984)

  TC= x1*BLUE + x2*RED ……. (4.3.1.1)

Where BLUE and RED are blue, red bands and x1 and x2 are weighing coefficients. Clear area pixels are taken as those pixels where tasseled cap (TC) is less than mean value of TC.

Calculation of regression between blue and red band for clear areas, if no blue band exist than green band is used as a substitute.

- Haze areas are orthogonal to "clear line",i.e haze optimized transform which is called HOT and can be defined as (Zhang et al.,2002)

HOT=BLUE *sinα – RED*cosα ……. (4.3.1.2)

- Then histogram of HOT is calculated for haze areas
- Histograms are calculated for each HOT level j below 800nm band. The haze signal Δ which has to be subtracted is computed as digital number corresponding to HOT (level j) minus digital number corresponding to 2% lower histogram threshold of HOT(haze areas).Finally the dehaze new numbers will be

DN (new) = DN - Δ ……. (4.3.1.3)

4.3.2 ATMOSPHERIC CORRECTION OF SATELLITE DATA (IN ATCOR)

In ATCOR, atmospheric correction function database have been compiled, which enables the conversion if raw data (DN values) into ground reflectance images. The atmospheric correction functions are saved as a look up tables (LUT) in the database and consist of the following parameters:

- **Standard atmosphere** –where air temperature, altitude profiles of pressure, water vapor content and ozone concentration is taken from model MODTRAN-2, presently the following atmospheres are available:
    1. Midlatitude summer atmosphere
    2. Tropical atmosphere
    3. US standard atmosphere 1976
    4. Fall atmosphere
    5. Midlatitude winter
- **Aerosol type**-Rural, Urban and other(maritime and desert)
- Range of aerosol concentration- we need to define aerosol optical depth in the form of visibility range which is 5-120 km.
- **Solar zenith angles**- solar zenith angle is also required which ranges between 0 -70.
- **Range of ground elevations**- calculations are performed for elevation above sea level corresponding to pressure levels. In this way, the Rayleigh optical depth for places of different elevations is considered.
- The atmospheric correction functions also depend on spectral response of sensor, thus there are different function for each sensor and each band.

- The atmospheric correction here also depends upon sensor view angle.

4.4 CROP DISCRIMINATION

Discrimination of crops in remote sensing images can be done by adopting any classification technique which can generate a classified map. The theory is based upon the fact that each crop has unique spectral signatures. Spatial, spectral and radiometric characteristic of the sensor, date of image acquisition and classification technique influences crop identification using remote sensing data. In this study Rule based classification technique was adopted using high resolution data i.e. Landsat. Since study was focused on wheat crop various land use and land cover classes was prepared and crop inventory was carried out. Rule based classification was performed using temporal NDVI images prepared from Landsat data.

Accuracy assessment of classified map was also done using independent reference sites of study area. Overall accuracy was defined as percentage of total independent referenced pixels that were correctly classified by rule based classifier. Producer's accuracy was also calculated by dividing the number of pixels correctly classified for each crop by the total number of independent referenced pixels for that crop. While the user accuracy is the fraction of number of classified pixels with respect to total number of classified pixels for the crop. Kappa coefficient was also calculated to measure the importance of classification result relative to chance agreement. A kappa value of one indicates perfect agreement between training pixels and their prescribed classes (Lillesand *et al*., 2004) and kappa value of zero indicate bad classification.

4.5 DERIVING PARAMETERS

Different parameters were derived in the study for further use in SEBS model and stress indices. Like land surface temperature, surface albedo.

4.5.1 LAND SURFACE TEMPERATURE RETRIEVAL

For Land surface temperature retrieval from Landsat TM thermal data, Quin et al.Mono window algorithm was adopted. Following steps were used in this algorithm to derive LST:

- First step involves digital number to radiance conversion-

  L6 = 0.1238 + 0.005632156 *DN …… (4.5.1.1)

  Where, L6 denote radiance of thermal band which is 6^{th} in number.
- Second step involves conversion of radiance into brightness temperature, which is an important component for retrieval of land surface temperature-

  BT=1260.56/ln (1+60.776/L6) ……. (4.5.1.2)

- Finally Mono-window algorithm is applied for land surface temperature retrieval-

$$\mathbf{Ts}=\mathbf{1}/\boldsymbol{C6}\{\boldsymbol{a6}*(\mathbf{1}-\boldsymbol{C6}-\boldsymbol{D6})+[\boldsymbol{b6}*(\mathbf{1}-\boldsymbol{C6}-\boldsymbol{D6})+\boldsymbol{C6}+\boldsymbol{D6}]*\boldsymbol{T6}-\boldsymbol{D6}*\boldsymbol{Ta} \quad \text{…… (4.5.1.3)}$$

Where, $\boldsymbol{C6}=\boldsymbol{\varepsilon 6}*\boldsymbol{\tau 6}$

$\boldsymbol{D6}=(\mathbf{1}-\boldsymbol{\tau 6})*[\mathbf{1}+(\mathbf{1}-\boldsymbol{\varepsilon 6})*\boldsymbol{\tau 6}]$

$\boldsymbol{a6}=-\mathbf{67.355353}$

$\boldsymbol{b6}=\mathbf{0.458606}$

$\boldsymbol{\varepsilon 6}$ ***and*** $\boldsymbol{\tau 6}$ ***are emmisivity and total atmospheric transmissivity***

4.5.2 ALBEDO RETRIEVAL

Albedo is an important component of radiation budget. Sun's energy falling over earth is not fully absorbed instead only partial quantity is absorbed by earth rest reflects back into the space that reflected energy is albedo. In other words albedo is the fraction of incoming radiation that is reflected by the earth surface. In this study, albedo is an important component which is used as one of the SEBS input. Using Landsat data albedo can be retrieved using this equation:

Albedo= [(0.160*band1+0.291*band2+0.243*band3+0.116*band4+0.112*band5+0.081*band7)-0.0015]

4.5.3 EMISSIVITY RETRIEVAL

The ability of a surface to emit energy through radiation is called emissivity of a material. It is an important factor to measure Land surface temperature. Emissivity calculations have various methods but for this study equation proposed by Vande Griend, Owe, 1993 was used. Given as follows:

Emissivity = 1.0094+0.047*lnNDVI

4.6 DERIVINGWATER STRESS INDICES

For detection of water stress in this study,NIR,SWIR and TIR bands were used in the form of three major indices were used Vegetation water stress index(VWSI) , Land surface wetness index (LSWI) and Water stress index(WSI).

4.6.1 VEGETATION WATER STRESS INDEX (VWSI)

Vegetation water stress index was introduced by(Ghulam et al., 2008a). This index made use of Near Infrared and Short wave infrared wavelength for fuel moisture content modeling(FMC) because FMC depends upon leaf dry matter content and leaf water content which is expressed in equivalent water thickness (EWT,g/m2). It has been proved by sensitivity analysis from radiative transfer modeling that variation in dry matter of leaf and canopy is mostly expressed in NIR domain while variation of equivalent water thickness exhibits in SWIR range. Hence, reflectance bands of NIR and SWIR were used as new index in the form of VWSI. 2-D trapezoidal scatter plot was formed using NIR and SWIR reflectance. A baseline (CD) which is also named as soil line in the plot is an indication of water status of bare surfaces. Since FMC is only relational with fully and partially vegetated areas. So pure pixels corresponding to water were removed and a hypothetical trapezoidal plot was formed (fig.4.3) where all four vertices i.e. A corresponded to full cover with high canopy water content, B corresponds to full cover with low canopy water content, C corresponds to saturated bare soil and D corresponded to dry bare soil. The line which is orthogonal to baseline represents changes in surface vegetation fraction from bare soil to partial and full canopy cover. The direction of vegetation water stress can be expressed and understood by line EF in the plot, at E and F vegetation fraction is similar but at E canopy water content is higher than F. Thus these two vectors which are orthogonal and parallel to NIR-SWIR baseline determine the vegetation water stress.

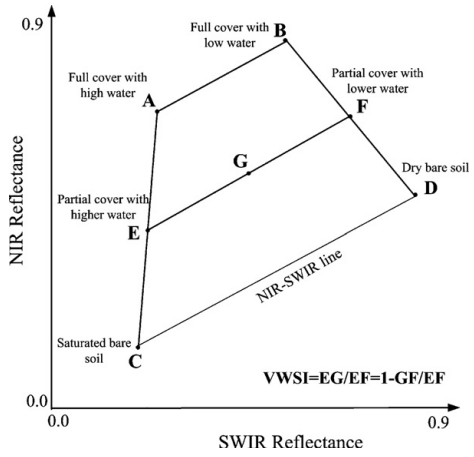

Figure 4.6: Sketch map of VWSI (source: (Ghulam et al., 2008b))

Vegetation water stress index can be calculated by using the following equations:

VWSI = EG/EF = 1-GF/EF ……. (4.6.1.1)

Now, if we assume that NIR and SWIR baseline exist, then it can be mathematically expressed as-

$$\mathbf{RNIR = MRSWIR \pm 1 \ldots\ldots\ldots\ldots (4.6.1.2)}$$

Where**, RNIR** and **RSWIR** are reflectance of NIR and SWIR bands

M refers to slope of NIR and SWIR baseline

I is the interception on vertical axis

Hence, according to the relationship between NIR-SWIR baseline and maximal and minimal waterlines, VWSI is expressed as:

$$\mathbf{VWSI=1-\frac{(M1-M)*(NIR-M2*SWIR-I2)}{(M1-M2)*(NIR-M*SWIR)-(M1-M)*I2+(M2-M)*I1} \ldots\ldots (4.6.1.3)}$$

Where, **M1, M2, I1** and **I2** refers to slope and intercept of maximal and minimal waterlines (i.e according to figure 4.3 is AC and BD)

4.6.2 WATER STRESS INDEX (WSI)

WSI is the modified form of water deficit index (WDI) which was proposed by(Moran et al., 1994). The index is based on NDVI-Ts scatter plot. NDVI and surface temperature is widely used to derive water stress and evapotranspiration. Jiang and Islam, (2001) estimated evapotranspiration from NDVI-Ts scatter plot by modifying Priestly and Taylor's Equation. Jiang and Islam modified equation by replacing Priestly Taylor coefficient α with ϕ which defined unsaturated areas. The resultant equation was-

$$\boldsymbol{ETj-i=\ \emptyset\left[\frac{\Delta}{\Delta+\gamma}\right](Rn-G)} \ldots\ldots\ldots\ldots \mathbf{(4.6.2.1)}$$

Where, ∅ = jiang Islam parameter

γ =Psychrometric constant

Δ= slope of the saturation vapor pressure curve

Rn=net radiation at surface level

G=soil heat flux

The jiang and Islam parameter ∅ ranges from 0 to 1.26 for dry bare soil to well vegetated surface.This parameter can be calculated by linear interpolation between the limits of NDVI-Ts plot (fig.4.7). Jiang and Islam, (2001) interpreted the upper edge with high temperature and low values of ∅ as the minimum value of ET for each class of NDVI ,while the cold edge is associated with low Ts and maximum values of ∅. Therefore the values of Jiang and Islam parameter varies within the limits of NDVI-Ts plot (fig.4.7). NDVI-Ts plot is applied to derive ∅ by using normalized temperature.

$$\emptyset i = 1.26 \frac{Tmax - Ti}{Tmax - Tmin} \quad \text{..... (4.6.2.2)}$$

Where,

Tmax = maximum temperature for vegetation class obtained by extrapolating upper edge to intersect Ts axis where NDVI=0

Tmin = minimum temperature for vegetation class obtained by averaging surface temperature of pixels identified as water.

Ti = radiometric temperature for given pixels

WSI which is being used in this study has taken concept of WDI by Moran et al. who showed relation between water stress and actual and potential ET (Ws=1-ET/ETm). Since maximum ET is closer to wet environment ETm was changed into Ew. Then according Straschnoy et al., (2006) ET/Ew is a good indicator of water deficit. Thus the major equation for WDI became

WDI = 1-ET/Ew ..... (4.6.2.3)

So, in this form of WDI ET can be replaced by Jiang and Islam equation given above and Ew will be replaced by Priestly-Taylor equation. So WSI can be given as:

$$\text{WSI} = 1 - \emptyset/\alpha \quad \text{..... (4.6.2.4)}$$

Now, by assuming α as 1.26 and replacing ∅ by above given equation the final equation which we used for our study will be:

$$\text{WSI} = 1 - \frac{Ti - Tmin}{Tmax - Tmin} \quad \text{..... (4.6.2.5)}$$

Where, Tmax = maximum temperature for vegetation class obtained by extrapolating upper edge to intersect Ts axis where NDVI=0

Tmin = minimum temperature for vegetation class obtained by averaging surface temperature of pixels identified as water.

Ti = radiometric temperature for given pixels.

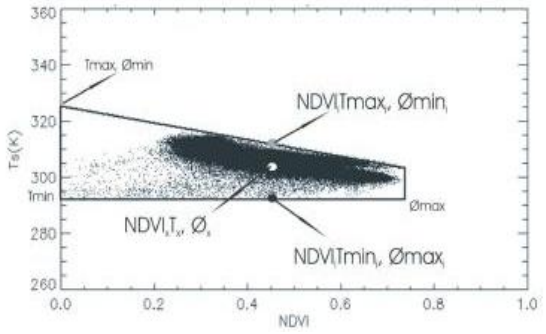

Figure 4.7: NDVI-Ts plot (source: (Jiang and Islam, 2001))

4.6.3 LAND SURFACE WETNESS INDEX (LSWI)

LSWI uses NIR and SWIR regions of electromagnetic spectrum for stress assessment. This index is sensitive for the total amount of vegetation liquid and also for soil background. So, LSWI was estimated by following equation:

$$\boldsymbol{LSWI = \frac{NIR-SWIR}{NIR+SWIR}} \text{ ..... (4.6.3.1)}$$

Estimated LSWI was further used in deriving water stress scalar (Ws) (Xiao et al., 2005).

$$\boldsymbol{Ws = \frac{1+LSWI}{1+LSWImax}} \text{ ..... (4.6.3.2)}$$

Where**, LSWI** is value of particular pixel

LSWImax is maximum LSWI value of particular pixel

4.7 SURFACE ENERGY BALANCE SYSTEM (SEBS)

Surface energy balance system is the remote sensing model for estimating daily ET per pixel based on the resolution of a thermal band of image data. (Su, 2002). This model can utilize satellite dataset like Landsat, MODIS, and ASTER with a combination of ground meteorological data which are used as inputs in surface energy balance. Generally, SEBS require following input:

- **Remote sensing inputs**-The first set of input comprises of land surface temperature, Surface emissivity, Albedo and normalized difference vegetation index (NDVI).
- **Meteorological data-** Second set of inputs includes specific humidity, air pressure at reference height (reference height is the measurement height), temperature.

- Third set of data include instantaneous downward solar radiation (downwards shortwave and downwards long wave).

In this study, for deriving ET from SEBS, ILWIS 3.8.3 version was used. Above shown inputs were derived for Landsat data. However, model has a limitation that all inputs should have same projection and coordinate system. Then after, all images were brought to same projection and coordinate system after exporting to ILWIS.

- After placing all inputs SEBS follows following equations to derive ET (Su, 2002)

Main energy balance equation is represented as:

$$R = G_0 + H + LE \quad \text{..... (4.7.1)}$$

Where,

R = Net radiation in W/m2,

G_0= Soil heat flux in W/m2,

H = Turbulent sensible heat flux in W/m2, and

L*E*= Turbulent latent heat flux where L is latent heat of vaporization and E is AET

Net radiation is derived by the formula:

$$R_n = (1 - \alpha) * R_{swd} + \varepsilon * R_{lwd} - \varepsilon * \sigma * To\text{^}4 \text{..... (4.7.2)}$$

Where,

R_n = Net radiation in W/m2,

α= Albedo which is unit less,

R_{swd} = Downward solar radiation in W/m^2

ε = Emissivity which is unit less

R_{lwd} = Downward long wave radiation in W/m^2

σ= Stefan-Boltzmann constant

T_0 = Land surface temperature in Kelvin

- Soil heat is obtained by:

$$Go = Rn * [Tc + (1 - fc) * (Ts - Tc)] \text{..... (4.7.3)}$$

Where,

Go = soil heat flux

Rn = net radiation

Tc = ratio of soil heat flux to net radiation

fc = fractional canopy coverage

Ts = 0.3115 for bare soil.

- Latent heat flux can be written as:

$$\lambda * E = \Lambda (Rn - Go) \text{..... (4.7.4)}$$

Where,

Λ= evaporative fraction

Rn= net radiation
Go = Soil heat flux

- Finally, Actual Evapotranspiration is derived by this equation:

$$\textbf{ETdaily} = 8.64 * 10^{7} * \Lambda o^{24} * \frac{Rnavg - Goavg}{\lambda * \rho w} \text{ ..... (4.7.5)}$$

Where,
ETdaily = daily evapotranspiration (mm/day)
$Rnavg$ = daily average of net radiation (MJ $m^{-2}d^{-1}$)
$Goavg$ = soil heat flux assumed for 24 hours (MJ $m^{-2}d^{-1}$)
Λ = latent heat of vaporization (MJ $m^{-2}d^{-1}$)
ρw = density of water

4.8 VALIDATION OF ESTIMATED WATER STRESS

4.8.1 FLUX TOWER DATA

The energy balance method and eddy covariance technique provide alternative measurement of Latent heat flux equivalent to ET and moreover it provide promising estimates for closing the water balance of ecosystem. Eddy covariance technique provides measurement regarding vertical turbulent fluxes within atmospheric boundary layer. Full surface energy balance profile viz., Air temperature, relative humidity, wind speed, net radiation estimated Latent and Sensible heat flux data which was obtained from flux tower situated at Meerut. The obtained Latent energy and sensible energy was processed through Edi-pro software to obtain actual evapotranspiration (ET actual).

4.8.2 ET_{ref} ESTIMATE FROM PENNMEN MONTEITH METHOD

ET_{ref} was computed by Pennmen Monteith Program. The program used standardized equation from ASCE Pennmen Monteith (ASCE-PM) method of ASCE Manual 70 (Jensen et al., 1990). The standardized reference ET equation is simplify and clarified presentation of the method. It is a reduced form of ASCE-PM equation which is similar to the form used in FAO irrigation and Drainage Paper No.56. As used in EWRI (2001) equation is presented as-

$$ETref = \frac{0.4.8\Delta(Rn - G) + \gamma \frac{Cn}{T+273} u2\ (es - ea)}{\Delta + \gamma\ (1 + Cdu2)}$$

Where, ET_{ref} = Standardized reference crop evapotranspiration (mm day^{-1})
Rn = net radiation at crop surface (MJ $m^{-2}d^{-1}$)

G = Soil heat flux density at soil surface (MJ $m^{-2}d^{-1}$)

T = Mean daily air temperature (^{o} c)

U_2 = Mean daily or hourly wind speed (ms^{-1})

es = Saturation vapor pressure (kPa)

ea = Mean actual vapor pressure (kPa)

Δ = Slope of saturation vapor pressure temperature curve ($kPa^{o}C^{-1}$)

Cn = Numerator constant that change with reference type and calculation time step.

Cd = Denominator constant that changes with reference type and calculation time step

4.8.3 WATER STRESS FACTOR

Meteorological data viz., latent heat flux (LE), sensible heat flux (H) obtained from flux-tower were used for deriving actual evapotranspiration (ETactual) whereas reference evapotranspiration (ETref) obtained using Pennmen Monteith program. Derived ETactual and ET ref were used for calculating water stress factor (Ws) which was further used for validation. Equation for calculating water stress factor (Ws) is given as-

$$\mathbf{Ws = 1 - \frac{ETactual}{ETref}}$$

4.9 PREPARING INPUTS FOR LUE MODEL

- **LUE MODEL:** light use efficiency model estimate productivity and predict that APAR and maximum light use efficiency is directly proportional. To observe the affects of water stress over wheat growing regions LUE model was used for this study. Equation for LUE model is given below:

$$\textbf{PRODUCTIVITY} = [(\sum \boldsymbol{PAR} * \boldsymbol{FAPAR} * \boldsymbol{LUE}) * \boldsymbol{HI}]$$

For productivity estimation, Light use efficiency model is used in this study. Inputs required for LUE model are as follows:

- **Photosynthetically active radiation (PAR):** Radiation data was downloaded from this link http://rredc.nrel.gov/solar/new_data/india/nearest_cell.cgi at block level at half hourly basis. The radiation data was then processed and converted into PAR images by doing interpolation.
- **Fraction of absorbed PAR(FAPAR):** FAPAR for one year (i.e. 2009-10) was derived by the above given equation (Mohamed,2005).

FAPAR=0.014*exp^5.005*NDVI

For present year i.e. 2013-14 FAPAR was estimated by establishment of logarithmic relationship between NDVI and Ground measured FAPAR. The equation so obtained was used for calculating FAPAR –

FAPAR = 0.285*ln (NDVI) +0.929

- **Light use efficiency**

  LUE is a function of maximum light use efficiency (Emax), Temperature scalar (Ts) and Water scalar (Ws). Since this study focus on wheat, so E.max value used for wheat was 2.8 g /MJ PAR .Temperature scalar was estimated by using the equation developed for terrestrial ecosystem model, In Water scalar different water stress indices which was derived in this study were used one by one (Ws_LSWI,Ws_VWSI, Ws_WSI).Ts equation is as follows:

$$\mathbf{Ts} = \frac{(T-Tmin)*(T-Tmax)}{[(T-Tmin)*(T-Tmax)]-(T-Topt)^2}$$

Where,

T = interpolated surface of mean monthly temperature from stations

Tmin = minimum temperature of photosynthetic activities

Tmax = maximum temperature of photosynthetic activities

Topt = optimum temperature of photosynthetic activities

- **Harvest Index**

  Harvest index is the ratio of grain yield and above ground biomass at maturity. For calculating productivity, harvest index was used in LUE model. In this study Harvest index values were estimated from field by Crop cutting experiment. Crop cutting experiment was carried out at selected sample sites. From every selected field wheat was harvested in 1m *1m range. Biomass and grain were removed separately and individual weights were taken for each sample. Then with the calculated weight harvest index was calculated for all plots. All values were then averaged and a mean value was taken to be used in LUE model. Equation for Harvest index is given below -

Harvest index=Grain yield / Total plant wt

4.10 STATISTICAL PARAMETERS USED FOR EVALUATION

The performance of indices and models used for detecting water stress and productivity were evaluated based on various statistical measures viz., root mean square error (RMSE), agreement index (AI) and mean relative deviation (RD).

- The RMSE serves to aggregate the magnitudes of the errors in predictions for various times into a single measure of predictive power. RMSE is a good measure of accuracy, but only to compare errors of different models for a particular variable and not between variables, as it is scale-dependent. (same units as the quantities measured). The equation for calculating RMSE is given as –

$$\textbf{RMSE} = \sqrt{\frac{1}{N}\sum_{i=1}^{N}(p_i - O_i)^2}$$

Where, p_i is the predicted data, O_i is the observed data, N is the number of observations

- The Agreement index describes that how much the forecast agrees with the actual data. (in scale of 0 to 1). The equation for calculating AI is given as-

$$\textbf{AI} = 1 - \frac{\sum_{i=1}^{N}(p_i - O_i)^2}{\sum_{i}^{n}(|p_i - \bar{x}| + |O_i - \bar{x}|)^2}$$

Where, p_i is the predicted data, O_i is the observed data, $\bar{x}$ is the mean observed values.

- The mean relative deviation error (mean RD) is useful for comparing the precision of different measurements. It also makes error propagation calculations much simpler.

$$\textbf{Mean RD} = \left(\frac{f_i - O_i}{O_i}\right) * 1$$

The present study attempts to evaluate performance of different water stress indices for estimating crop water stress and to assess the impact on productivity of wheat. The inputs from remote sensing has been effectively used and integrated with GIS databases for estimating water stress and productivity for wheat keeping in view the usefulness of remotely sensed signatures to quantify crop water stress and estimating yield in wheat crop to assess its impact over it. The present study was undertaken in wheat region of western Uttarpradesh and some adjacent regions of Haryana. To manifold objectives mention in Chapter-1.The results obtained in this research are described in this Chapter.

5.1 CROP DISCRIMINATION

Crop discrimination using remotely sensed data is based upon the fact that each crop has unique spectral signature. Typical spectral reflectance of crop shows absorption due to pigments in visible region (0.62-0.68μm) and high reflectance in the near infrared regions because of internal cellular structure of leaves. Vigor of crop is manifest in the absorption in the red and reflectance in near infrared region (Navalgund et al., 1991b).

A study was carried out to identify and discriminate wheat crop from others land use / land cover classes using Rule based classification approach. A rule based approach provides an effective way to take decisions for feature selection by applying simple mathematical logics. Temporal NDVI obtained from Landsat- 5 TM of three months (November, February and April) were used for crop discrimination where separate rules were formed based on NDVI values of different months and different classes were assigned. Classification criteria developed for this classification is described below:

- If (nd1 <=0.4),(nd1 >=0), (nd2>=0.5), (nd3>=0.2) & (nd3 <=0.6) –**Wheat**
- If (nd1>0.3), 9nd2 <=0.6), (nd2>=0), (nd3 <=0.7) & (nd3>=0) – **Sugarcane**
- If (nd1>=0.1),(nd2<=0.6), (nd3<=0.4),(nd3>=0),(nd1<=0.4) & (nd2>=0.2) – **Vegetable**
- If (nd> -0.05) ,(nd2>-0.05),(nd3>-0.05) ,(nd1<0.3), (nd2<0.3) &(nd3<0.3) – **Settlement**
- If (nd1<=0) , (nd2<=0) & (nd3<=0) - **Water body**

Where, nd1 = NDVI (November), nd2=NDVI (February) and nd3=NDVI (April).
(Figure 5.1) shows the crop inventory map of respective study area.

Accuracy assessment of classified map was carried out. The accuracy assessment matrix is presented in the table 5.1. The overall accuracy and kappa coefficient was found 90.12 percent and 0.87 respectively. The performance of this classifier was good for wheat discrimination,

Producer's accuracy for wheat was found to be 85% which mean that 15% is mixed with vegetable since they are grown in same time period. Similarly, mixing is also observed in orchard and sugarcane classes. With rule based classification we were able to discriminate wheat from other classes for further use.

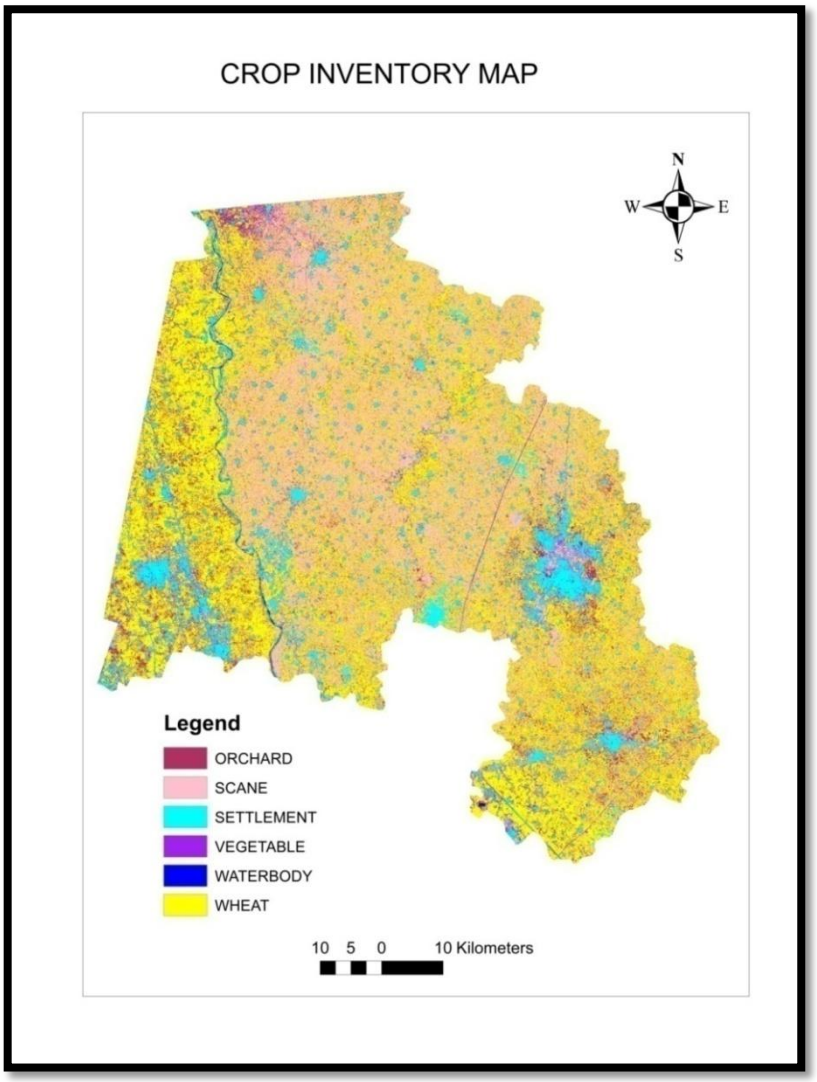

Figure 5.1: Crop inventory map

Table 5.1: Classification Accuracy assessment table

Classes	Refer. total	Classified total	Correctly classified	Producer's accuracy	User's accuracy
Wheat	80	77	68	85%	88.3%
Sugarcane	62	63	56	90.3%	88.89%
Vegetable	10	8	7	70%	87.50%
Non vegetation	23	23	21	91.30%	91.30%
Orchard	13	16	12	92.31%	75%
Overall accuracy	90.12%				
Overall kappa statistics	0.87				

5.2 METEOROLOGICAL AND BIOPHYSICAL PARAMETERS OBTAINED FROM GROUND

Meteorological parameters were obtained from agriculture university (S.V.P.U.A.T) for 2009-10 and 2013-14, which included minimum and maximum daily temperature and Relative humidity for two years (Figure 5.2), (Figure 5.3). Radiation data was downloaded on half hourly basis for 9 blocks which was processed and converted to PAR data (figure 5.4).These parameters were used for water stress derivation and also in productivity calculation.

Biophysical parameters (PAR, FAPAR, and LAI) were also obtained from ground measurements for three months (January 2014, March 2014, and April 2014); details are given in table 5.2.

Table 5.2: Details about ground measured parameters

PARAMETERS	JANUARY_2014	MARCH_2014	APRIL_2014
PAR	498.9±2.19	829.9±3.34	1298.27±4.08
FAPAR	0.46±0.06	0.74±0.05	0.64±0.05
LAI	0.91±0.10	2.11±0.12	1.78±0.11

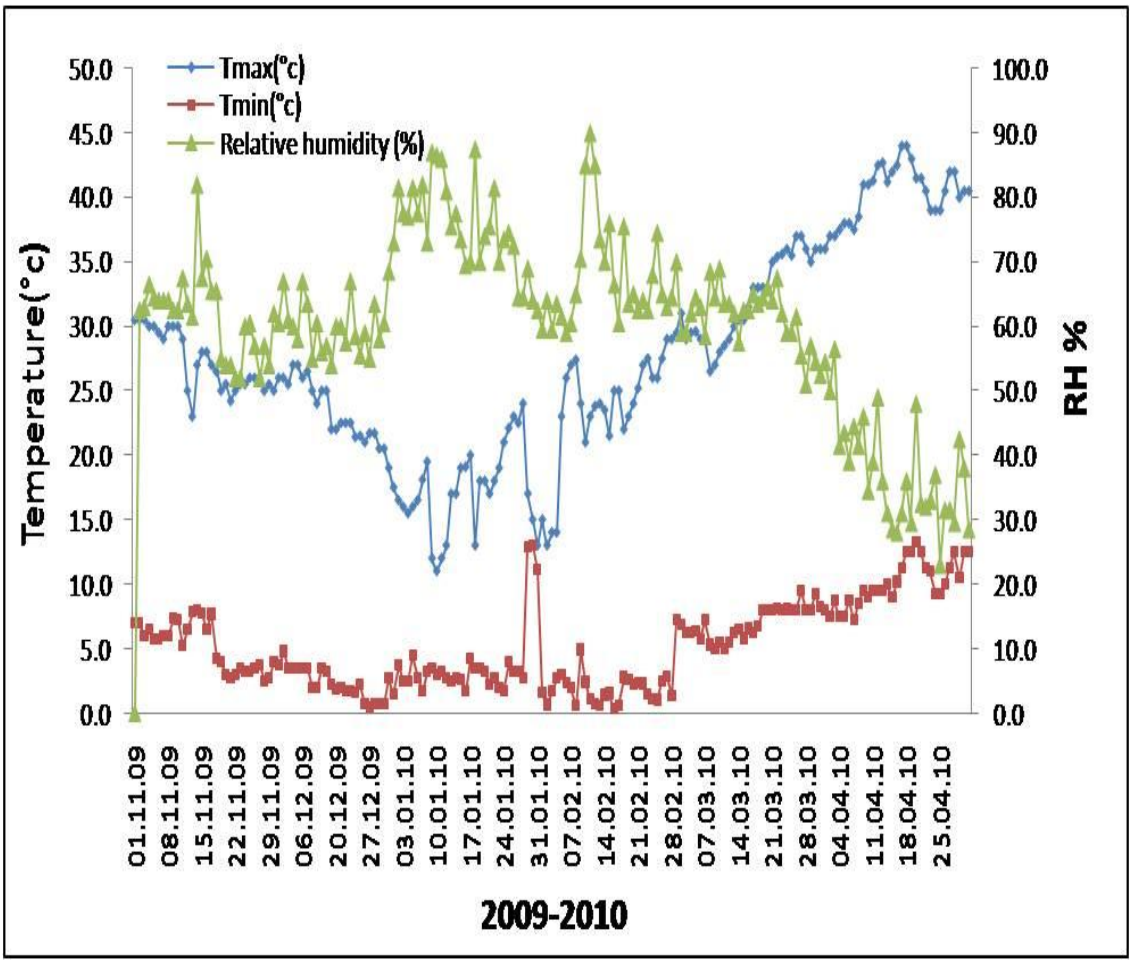

Figure 5.2: Meteorological data obtained for 2009-10

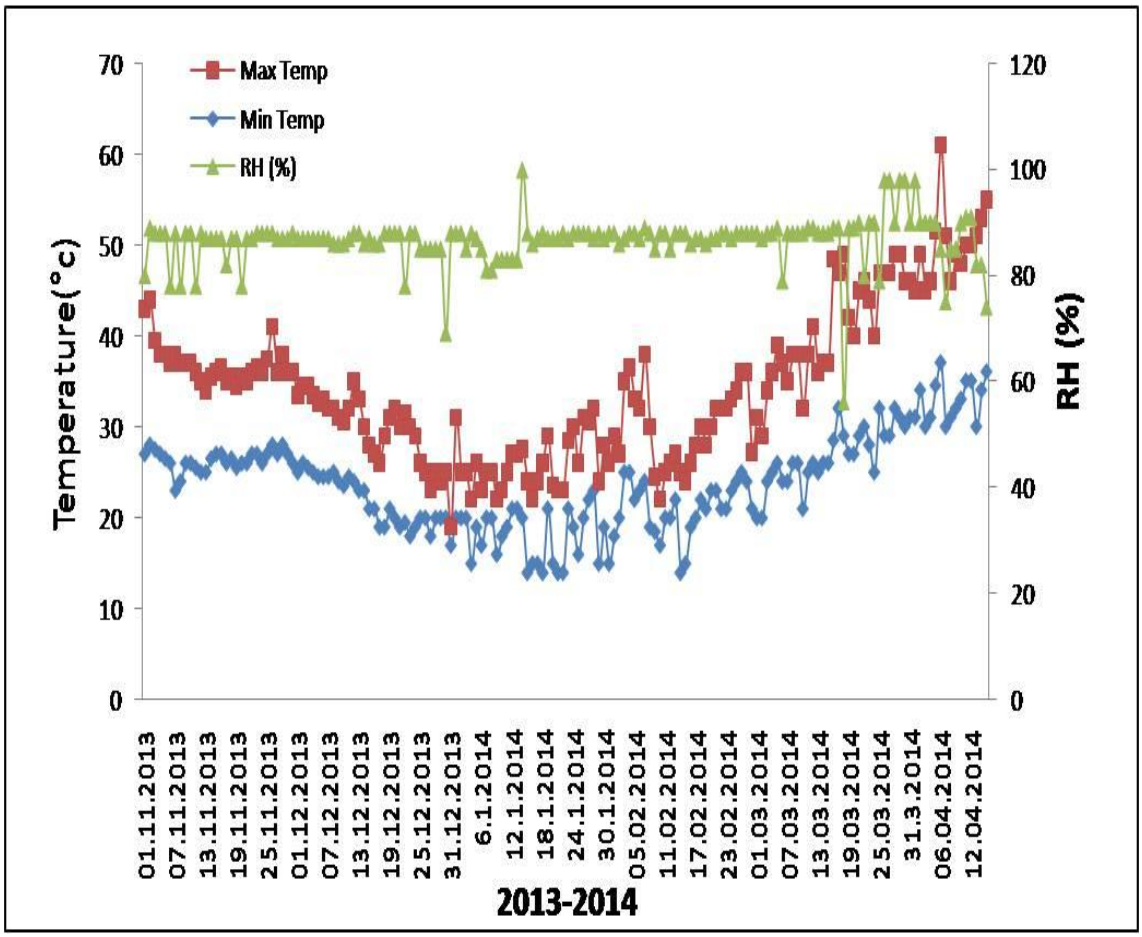

Figure 5.3: Meteorological data obtained for 2013-14

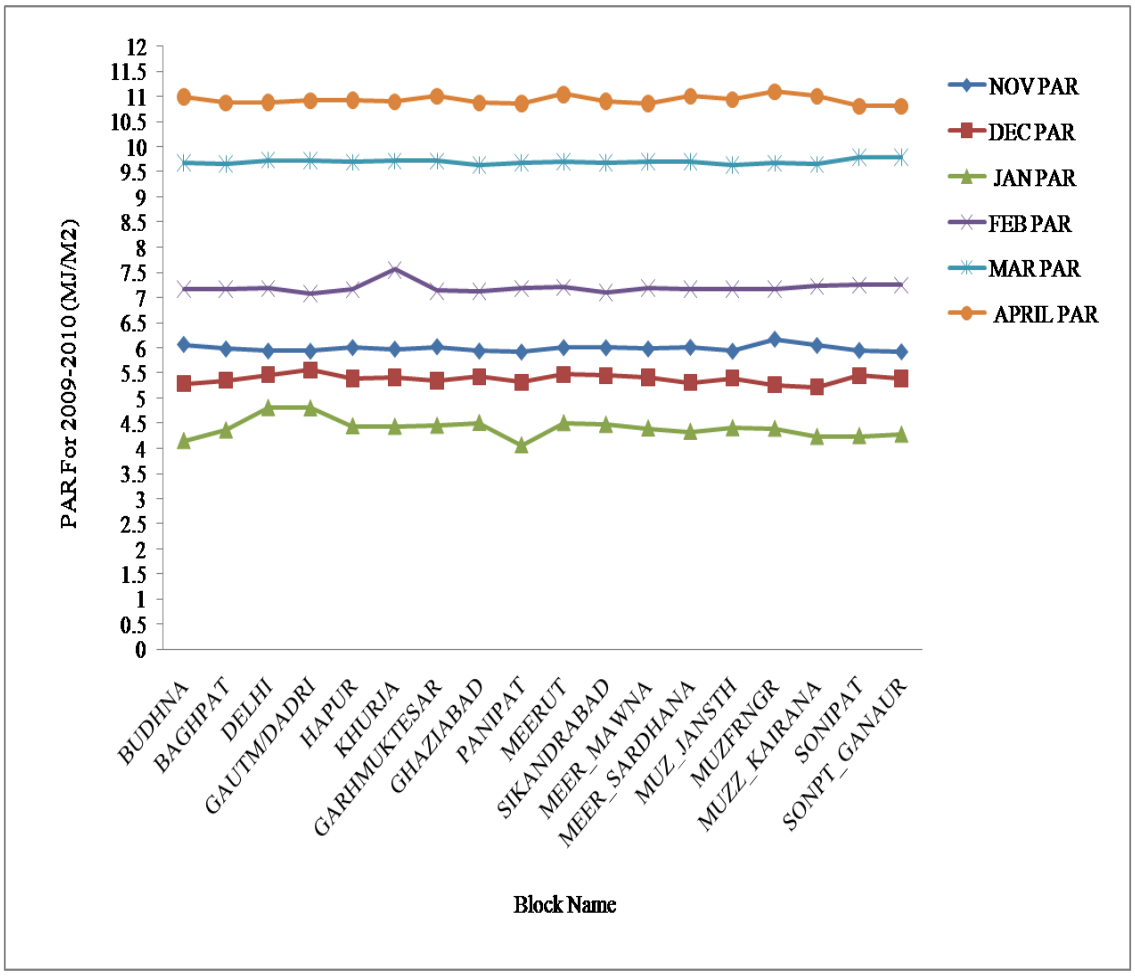

Figure 5.4: Distribution of PAR data obtained for different blocks for 2009-10

5.3 DETECTION OF WATER STRESS FROM SATELLITE BASED INDICES

Different water stress indices were used for quantitative estimation of water stress in crops. Near infrared (NIR), Short wave infrared (SWIR) and Thermal infrared (TIR) bands were used for this study. Study was carried for two year i.e. for 2009-10 and 2013-14 Rabi season.

5.3.1 VEGETATION WATER STRESS INDEX (Ws_VWSI)

Ws_VWSI is a 2-D scatter plot based water stress index, which is based on reflectance between NIR and SWIR bands. Description of VWSI has been given in methodology (Chapter-4). As per the methodology, the results of derived index ranges between 0 to 1, where higher values corresponds to stress and lower values corresponds to no or very less stress. According to (Ghulam et al., 2008a) VWSI < 0.3 implies normal growth condition , VWSI > 0.3 and < 0.5 slight stress conditions and VWSI > 0.5 show severe stress condition.

As per the temporal profiles shown below, in 2009-10 November is showing 0.5 and 0.4 value for Haryana and Meerut respectively. Haryana in comparison to Meerut has shown more higher values in November which is decreasing every month and has reached to very low value (0.15) in March indicating normal conditions or no stress condition, this indicate good vegetative growth of wheat. In April values are again higher and have reached to 0.51. The variation of values in November month is due to late sowing of wheat in Meerut region, since it has some other crop (sugarcane) already whereas in Haryana early sowing of wheat is done. VWSI values are lower in all months except November and April because of full crop growth conditions. Lower values observed in 2009-10 for Haryana and Meerut was 0.15 and 0.02 respectively.

In 2013-14 November and April higher values were observed (0.59 to 0.61) and (0.5 to 0.51) for Haryana and Meerut whereas lowest values were observed in March for Haryana (0.09) and Meerut (0.12) respectively. In April, Meerut is showing lower values than Haryana the reason behind is late harvesting of wheat crop in Meerut whereas in Haryana early harvesting takes place. The temporal profiles and spatial distribution for variation of VWSI can be seen in Figure 5.5 and Figure 5.4.In December and January 2013-14 images may show some abrupt higher VWSI values which is because of cloud cover prevailed in some part.

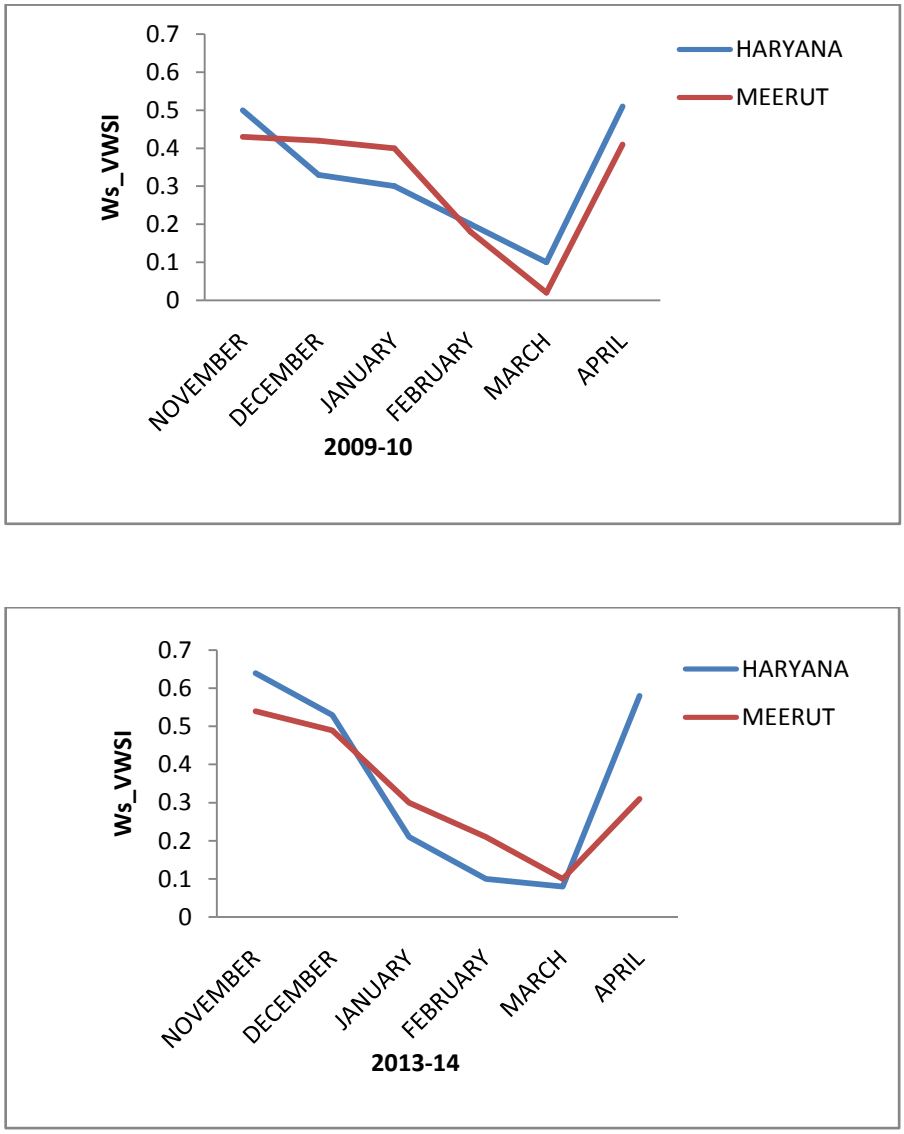

Figure 5.5: Temporal profiles of Ws_VWSI for 2009-10 and 2013-14 for parts of Haryana and Meerut

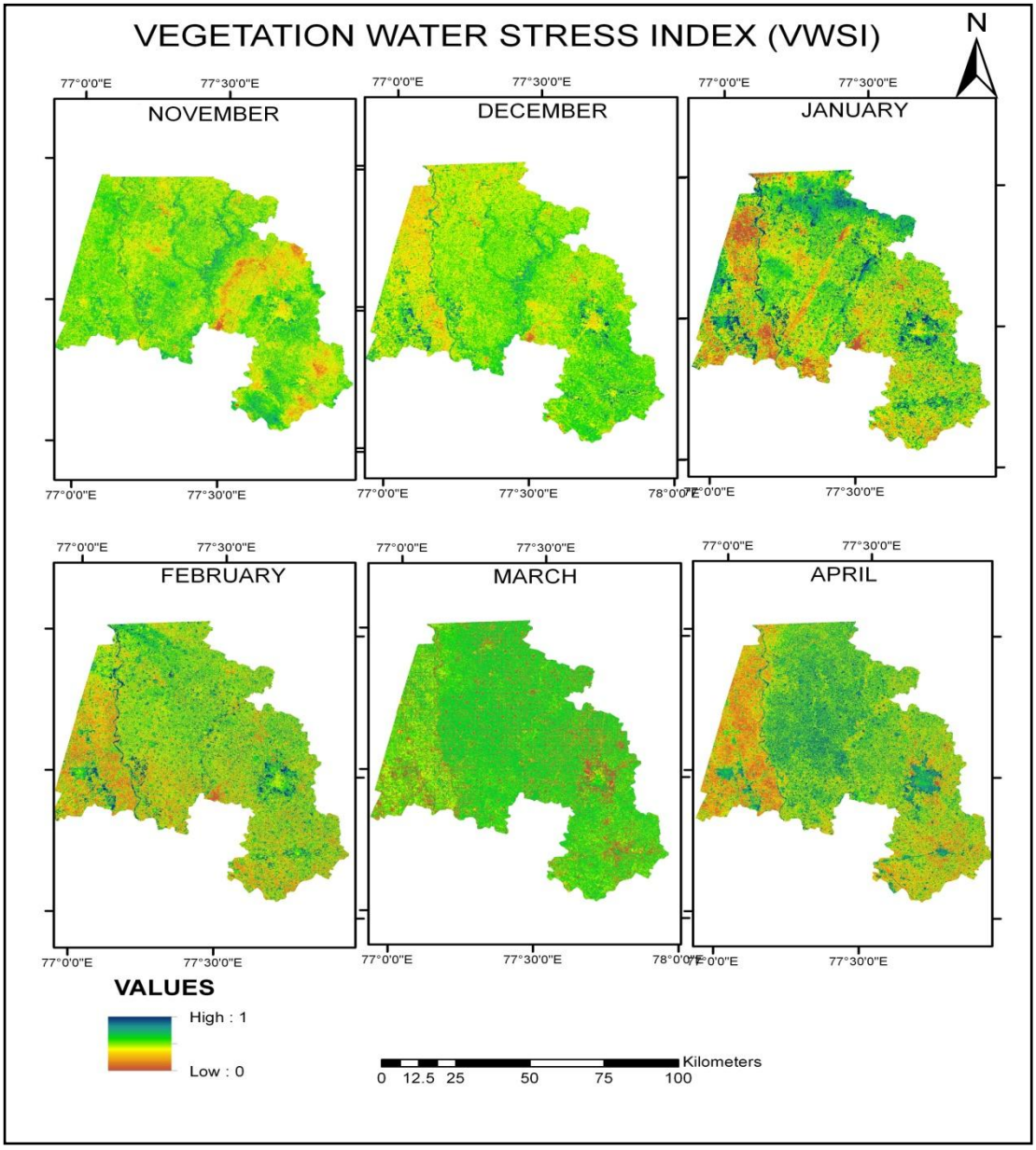

Figure 5.6: Spatial distribution of Ws_VWSI for 2009 - 10

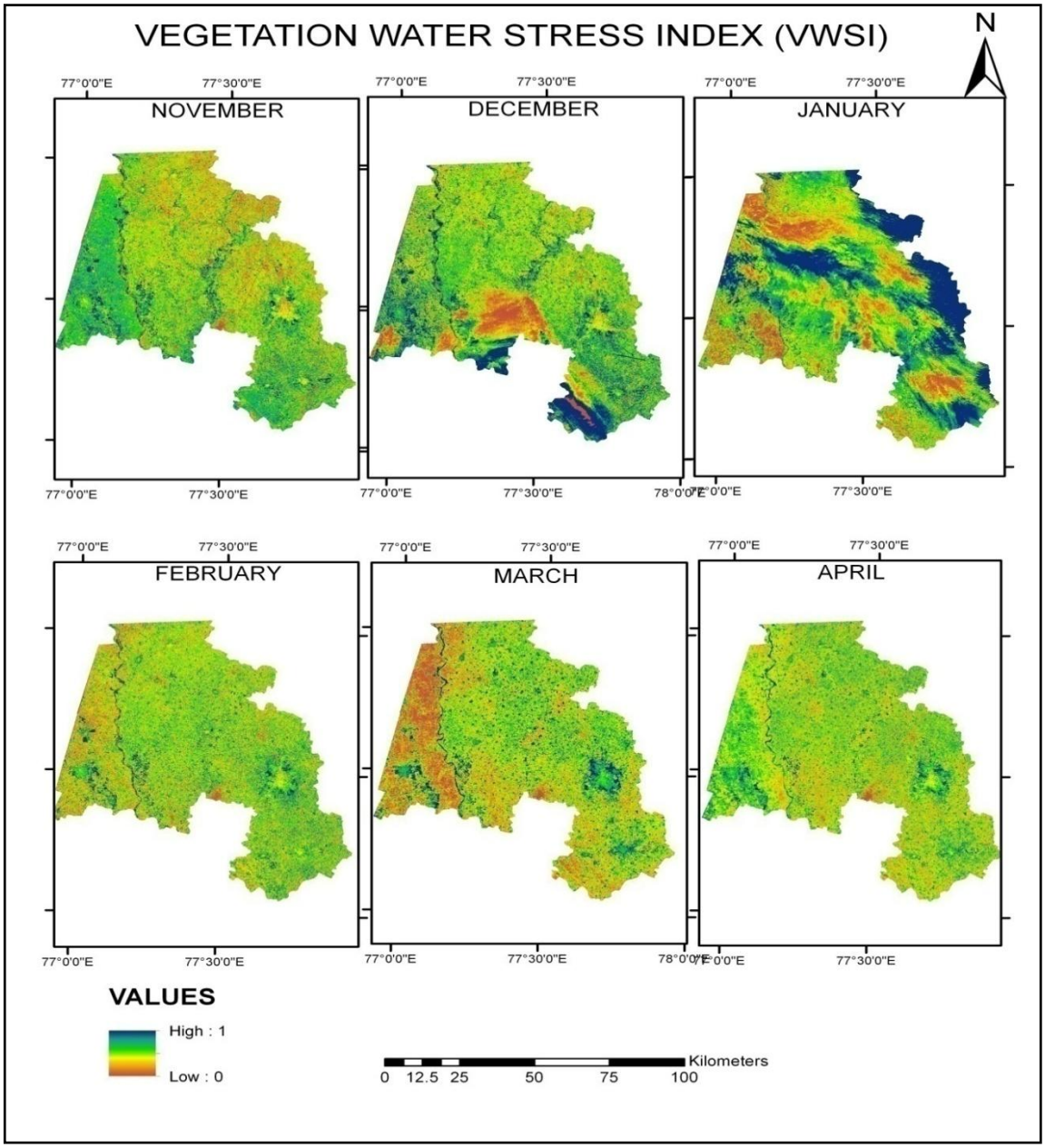

Figure 5.7: Spatial distribution of Ws_VWSI for 2013-14

5.3.2 LAND SURFACE WETNESS INDEX (Ws_LSWI)

Land surface wetness index is a linear combination of NIR and SWIR bands. Water scalar was calculated for it based on (Xiao et al., 2005) approach. This index has a value range between 0 to 1.Where 0 signifies no stress and 1 signifies severe stress. As per results obtained for 2009-10 in (Figure 5.8)In November high stress was observed in Haryana with value 0.45 and in Meerut 0.35 then in respective months i.e. January , February and march a decrease trend can be seen in stress values for both Meerut and Haryana reaching 0.05 to 0.1because of increasing vegetative growth of wheat. In 2013-14 higher values of water stress were observed in Haryana (0.51) for November whereas (0.43) for Meerut. In January value reaches to 0.2 for Haryana which constantly decrease till March and then give an abrupt change rising till 0.4 in April. Whereas in Meerut values take a dip after December signifying about less water stress as crop growth takes place. Values show small change from February to March reaching 0.1 then get lower reaching to 0.01. Overall spatial distribution of stress can be observed in figure 5.9.

5.3.3 WATER STRESS INDEX (Ws_WSI)

Water stress index is the thermal band based index which is formed by NDVI/Ts based scatter plot. It is a modified index of WDI proposed by Moran et al. The results obtained from Ws_WSI are shown in temporal profile figure 5.10 and spatial distribution is shown in figure 5.11. Availability of cloud-free Landsat data for a whole growing season (2009-10) was limited and hence it has affected interpretation of WSI. Thus, the Ws_WSI has been derived for only three months in 2009-10. During early growth stages of wheat coinciding Nov. & Dec. of 2013-14, the higher values noticed, particularly, in Haryana. Later it has decreased rapidly and reached to its lowest in February and finally again increased to 0.51 in the month of April.While in case of Meerut, WSI exhibit lowest water stress factor for March (0.2) and reaches finally to 0.3 for April month. In 2009-10 ,values for November months ranges between 0.61 for Haryana and 0.4 for Meerut showing water stress conditions for Haryana and in February decline in water stress is seen ranging between 0.1 to 0.2 for Haryana to Meerut respectively. In harvesting month of wheat i.e. April, water stress ranges 0.35 to 0.2 for Haryana and Meerut. Thus overall pattern for water stress is observed, in November more stress is seen in Haryana than Meerut area whereas in February due to high vegetative growth of wheat stress is decreased and value range become less which again rises in April due to harvesting of wheat.

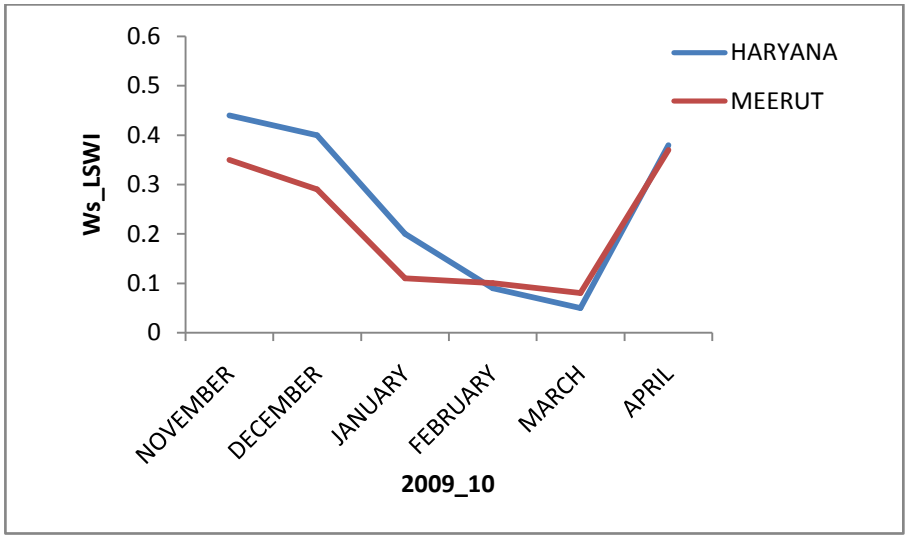

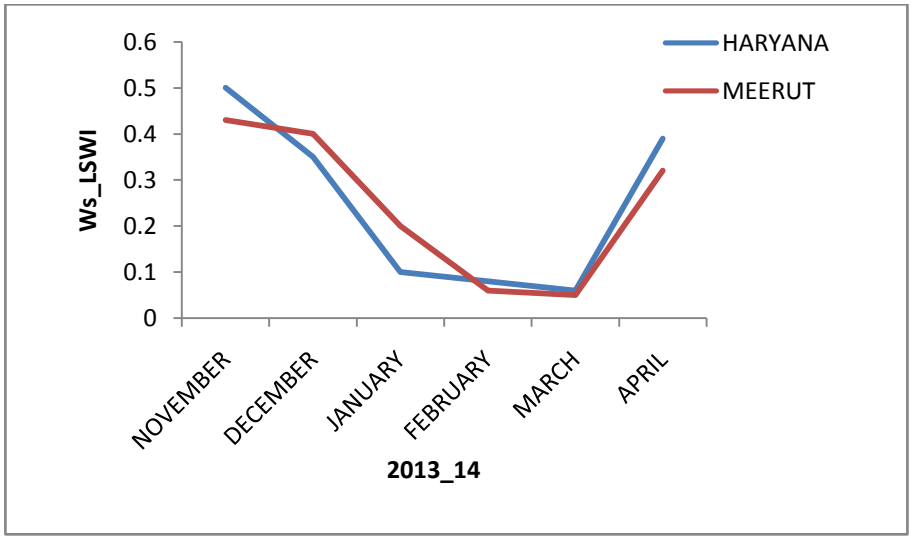

Figure 5.8: Ws_LSWI temporal profiles for 2009-10 and 2013-14

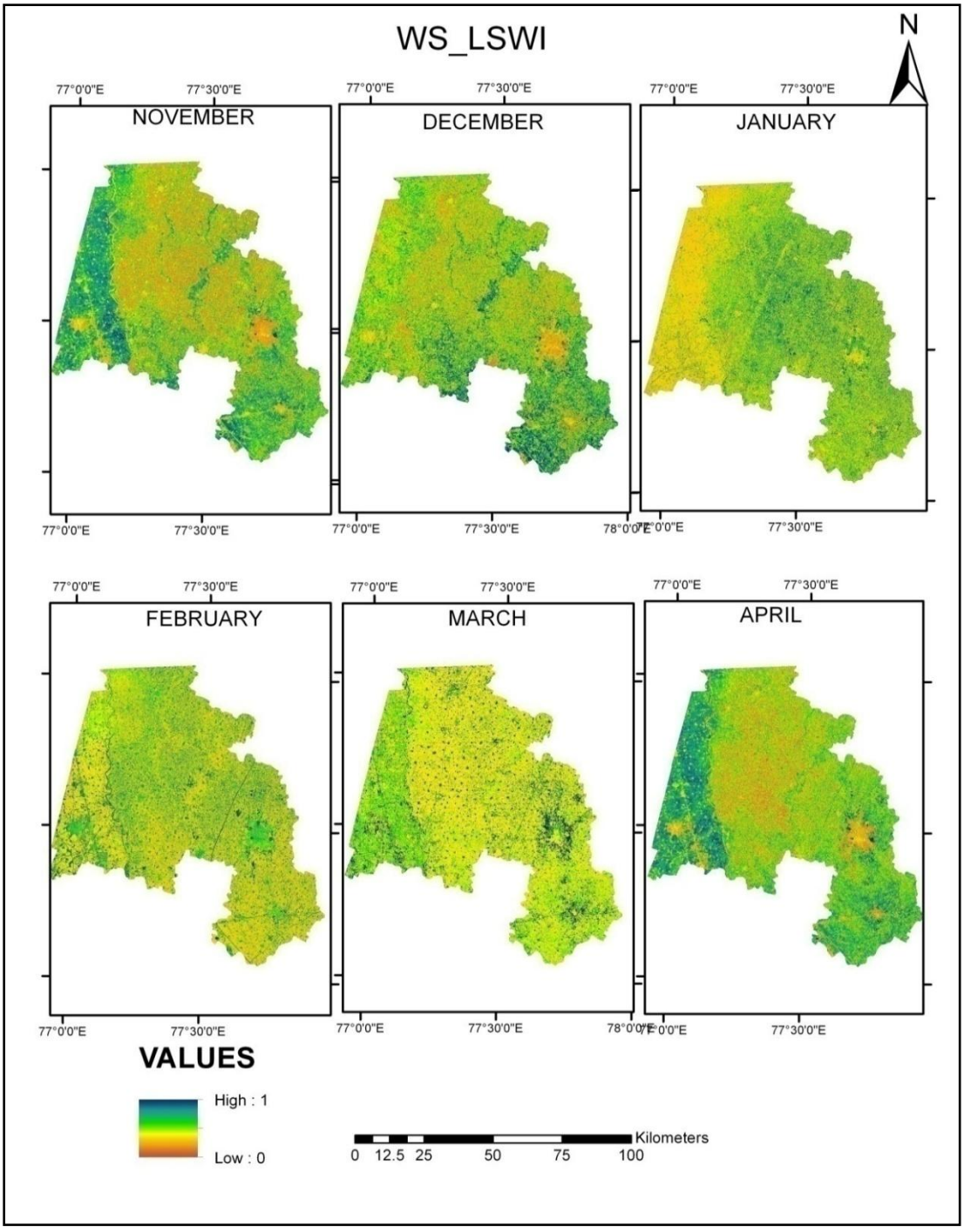

Figure 5.9: Spatial distribution of Ws_LSWI for 2009-10

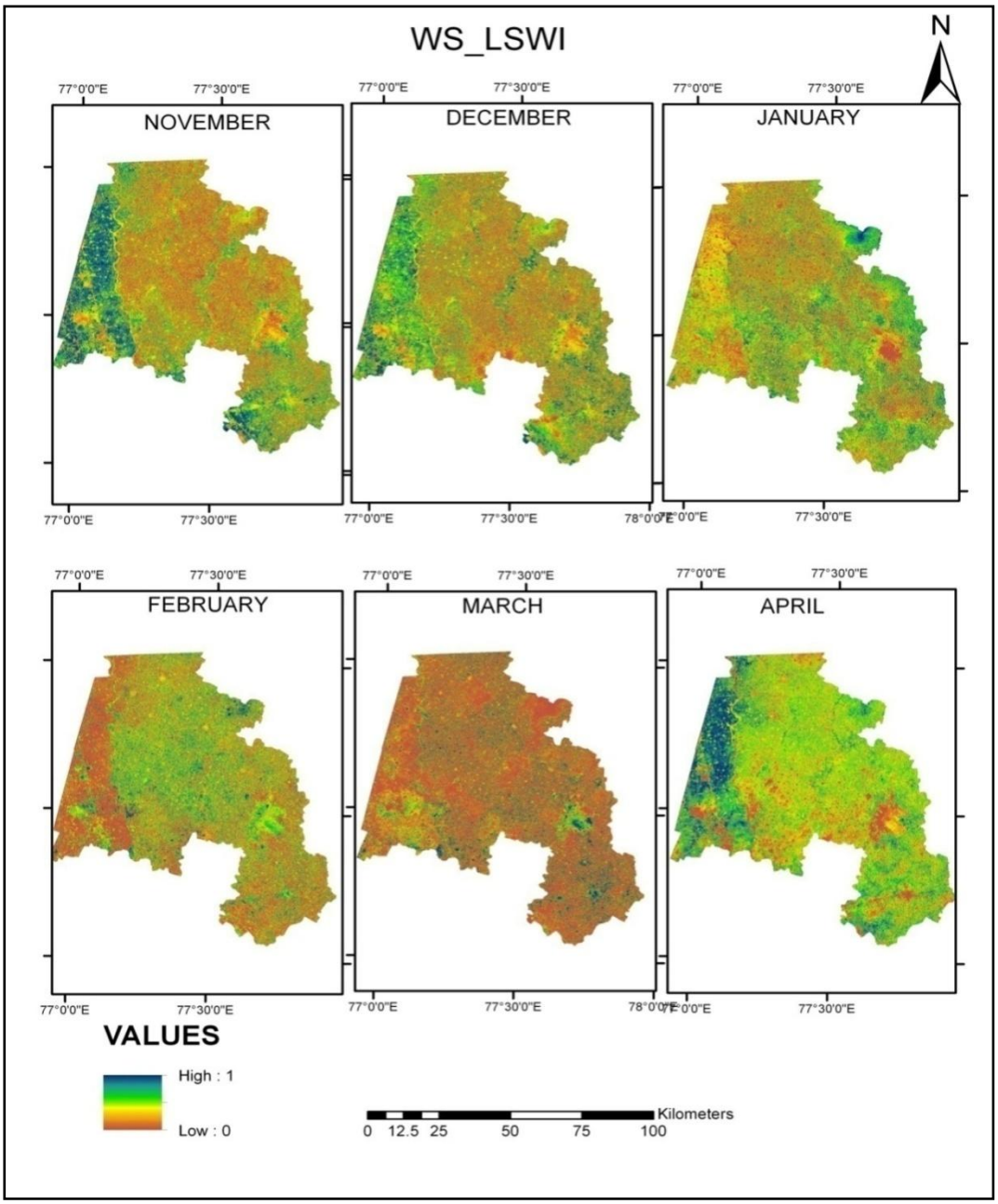

Figure 5.10: Spatial distribution of Ws_LSWI for 2013-14

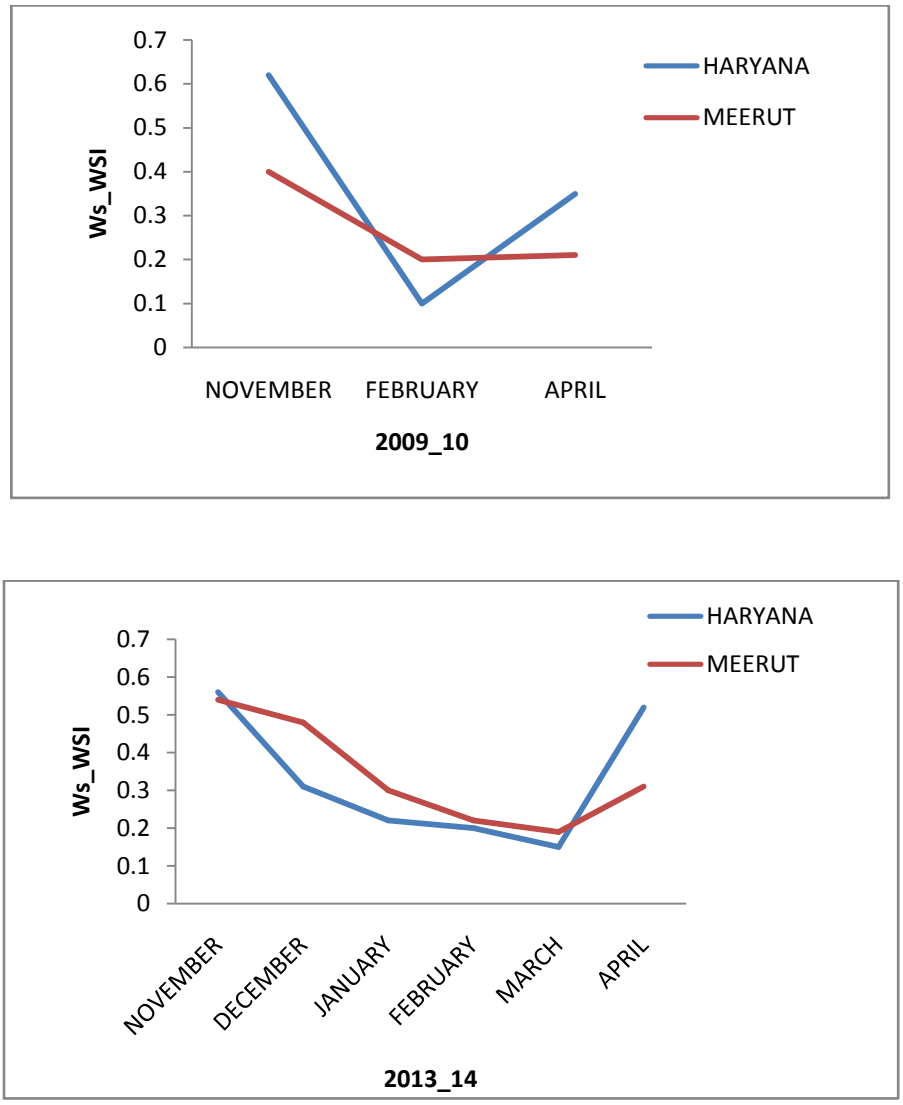

Figure 5.11: Ws_WSI temporal profiles for 2009-10 and 2013-14

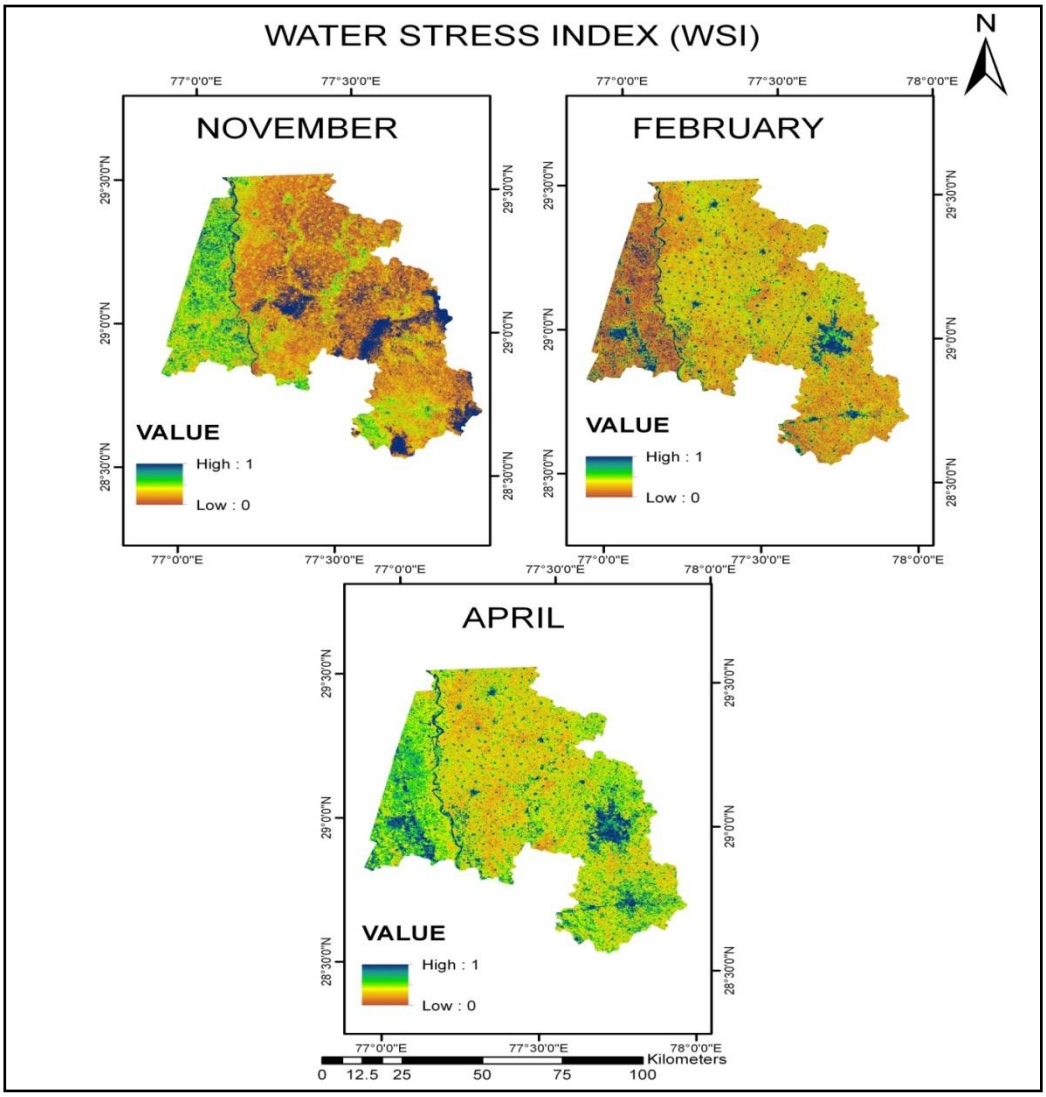

Figure 5.12: Spatial distribution of WSI for 2009-10

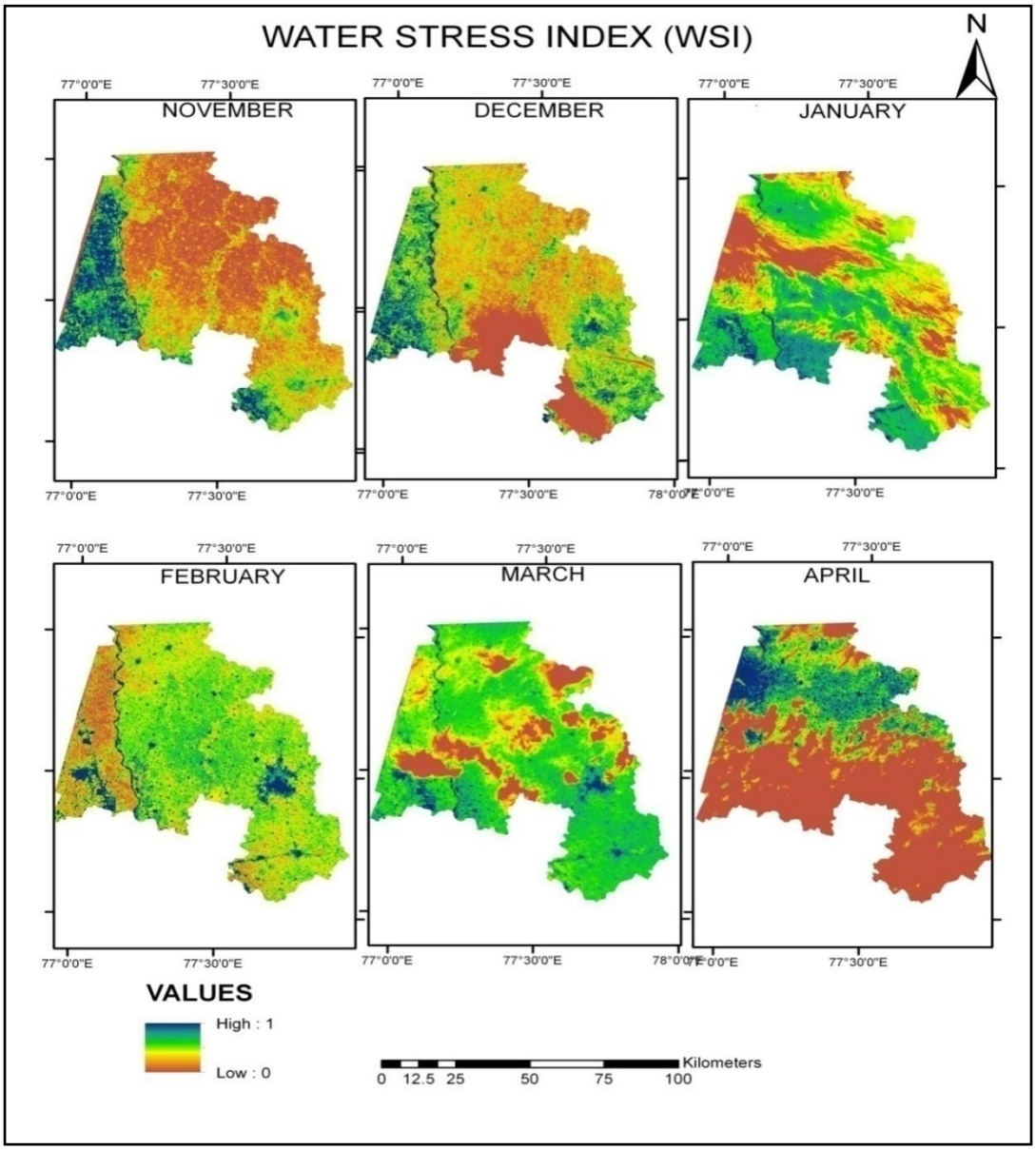

Figure 5.13: Spatial distribution of Ws_WSI for 2013-14

5.4 SATELLITE DERIVED ET

Daily Evapotranspiration has been derived by using Surface energy balance tool (SEBS tool) in ILWIS for the year 2009 and 2010 three dates of November, February and April month. The results of actual evapotranspiration around the area of interest from remote sensing data and SEBS has been indicated in figure 5.14.The SEBS calculates actual ET per pixel and the resolution of each pixel originates from resolution of LST which was estimated by Landsat 5 TM thermal infrared band (TIR).It means that resolution of actual ET is equals to 30m per pixel with respect to resolution of LST.

The retrieved results of actual ET from SEBS indicated that ET has increased in February than in November for Haryana because of increased vegetative growth of wheat while if we observe in Meerut and other region of West UP somewhere slight high values of ET can be observed which decreases in February month this is because of sugarcane growth in November and by December most of it get harvested. So due to early vegetative growth of wheat in February lower values is being observed. In April, Haryana region is showing decreased values of ET in the range (3.1to 4mm/day) and Western Uttarpradesh area is showing higher values (6.5 to 7 mm/day) this is due to the fact that wheat has been harvested in most of the part of Haryana but in western UP its in ripened stage . The overall monthly images show a proper trend in spatial distribution of ET monthly wise.

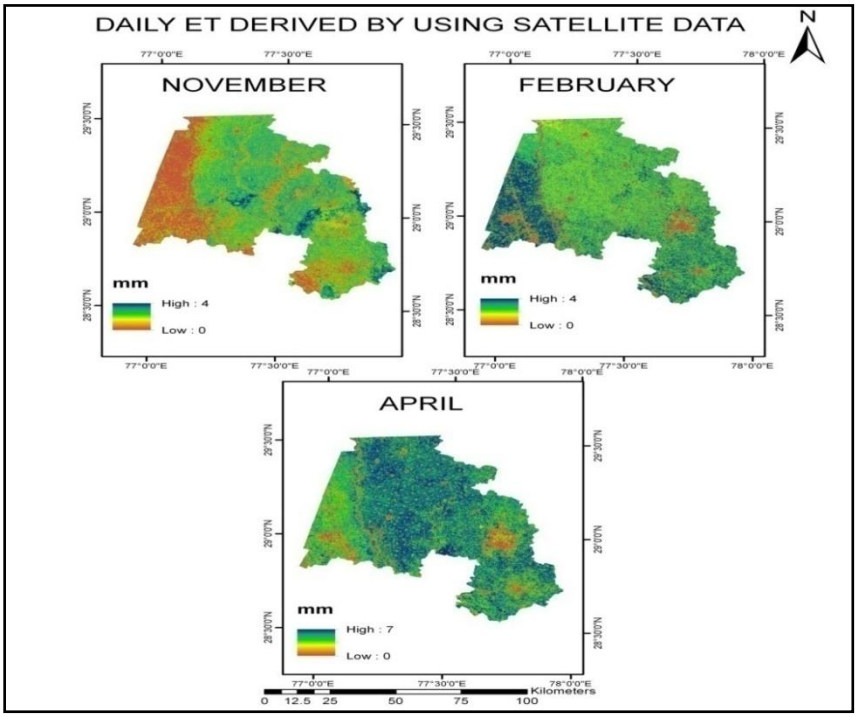

Figure 5.14: Spatial distribution of Daily ET obtained from SEBS for 2009 and 2010

5.5 COMPARISON OF FIELD WATER STRESS WITH ESTIMATED WATER STRESS

Validation is an important process to test the applicability of applied model to that particular area. Validation of water stress was done for 2009-10 data with Tower site water stress factor. The estimated water stress from Ws_LSWI and Ws_VWSI were compared with flux-tower site water stress factor using 1:1 line plot. The performance of derived index was quantified by coefficient of determination (R^2) which was quite good for Ws_LSWI with value of R^2 0.76 showing more relation with tower data than Ws_VWSI which shows less relation in comparison to Ws_LSWI with value of R^2 0.65.RMSE for Ws_LSWI and Ws_VWSI was 0.12 and 0.13 respectively. Overall Statistical details are shown in table 5.3.In figure 5.16 comparison of Ws_WSI with tower site observations has been shown, high temporal variations has been observed. Estimated water stress was highly underestimated from tower site data in November whereas in the month of February estimated water stress increases slightly which again decreases in April.

The estimated ET by SEBS model was compared with flux tower site ET (figure 5.17).The model has observed over estimated ET for all months.

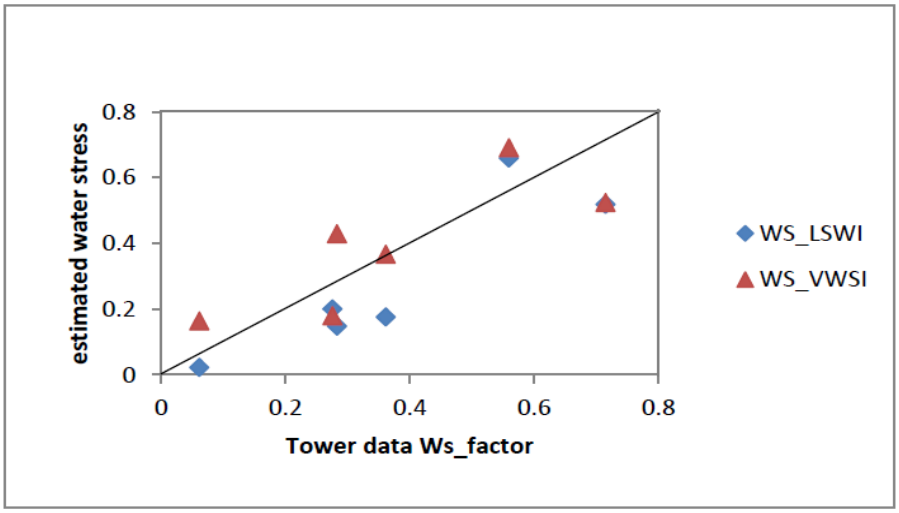

Figure 5.15: 1:1 line plot for field vs. estimated water stress

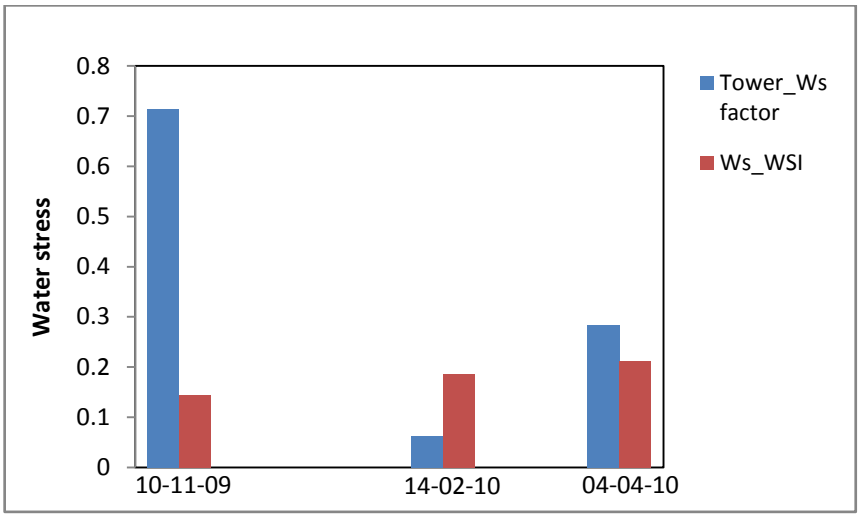

Figure 5.16: Field water stress vs. Ws_WSI for tower site

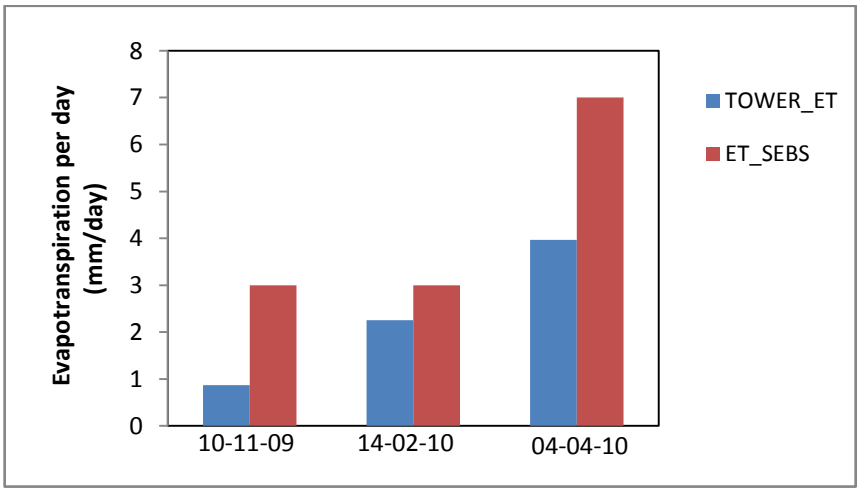

Figure 5.17: Field ET vs. SEBS derived ET for tower site

Table 5.3: Statistical details for Ws_LSWI and Ws_VWSI for Line plot

STRESS INDEX	R^2	RMSE	Agreement index	Mean RD (%)
Ws_LSWI	0.76	0.12	0.91	5.26
Ws_VWSI	0.65	0.13	0.89	-4.28

5.6 FAPAR ESTIMATION

Attempt to establish fAPAR-NDVI relationship was done for use in LUE model of yield estimation in 2013-14. For estimating FAPAR from remotely sensed data, empirical relationship between FAPAR and NDVI was constructed. Predictive functions varying in mathematical forms (linear, logarithmic, power et.) were used to determine best statistical fit between NDVI and corresponding measured FAPAR (n=58) values (2013-14) .Some independent measurements were retained for validation purpose. The statistical result revealed that NDVI shows a logarithmic relationship with FAPAR showing coefficient of determination (R^2) equal to 0.63. Figure 5.18 shows the empirical relationship between FAPAR and NDVI.

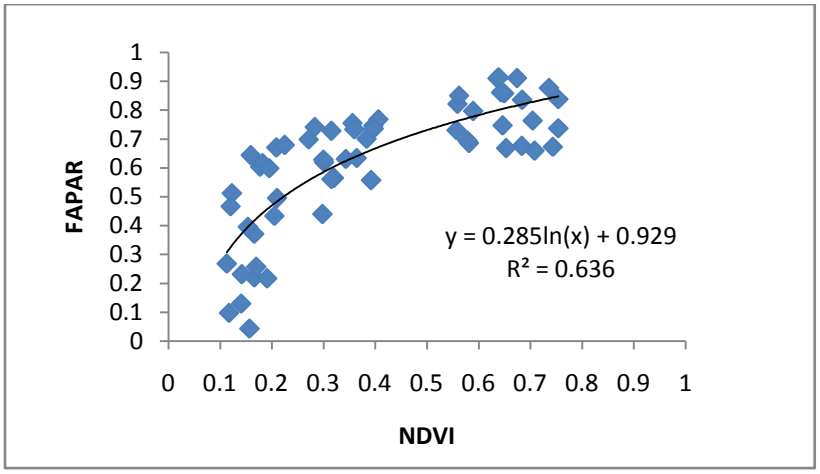

Figure 5.18: Relationship between FAPAR and NDVI of wheat crop over Western Uttarpradesh and Haryana during Rabi season 2013-14

5.7 VALIDATION OF ESTIMATED FAPAR

The estimated empirical relationship between FAPAR and NDVI was validated to test the predictive functions. The estimated FAPAR was compared with corresponding measured FAPAR values from independent sites of same season. For comparison purpose, estimated FAPAR values were plotted against measured FAPAR at independent sites and corresponding results are presented in figure 5.19.Statistical parameters show good agreement between both.

Showing coefficient of determination (R^2=0.54) and (RMSE =0.11).These results show that the predictive functions perform well for estimating FAPAR for wheat.

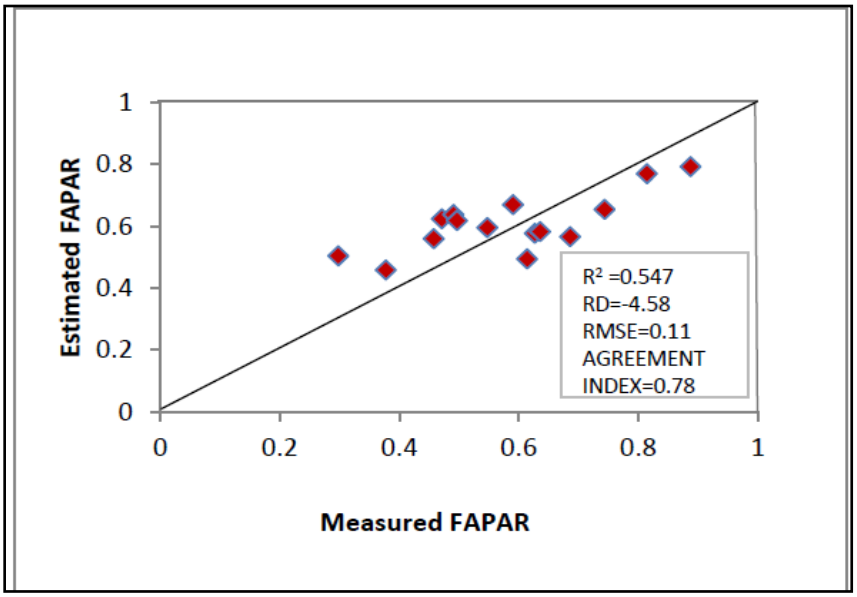

Figure 5.19: Cross validation of measured vs. estimated FAPAR of wheat (2013-14)

5.8 SPATIO-TEMPORAL OBSERVATION OF ESTIMATED FAPAR

APAR is an important biophysical parameter which is used for yield calculation in LUE model. The absorbed PAR (APAR) is both governed by both PAR and FAPAR .Since the temporal variations in APAR plays significant role in primary productivity of vegetation.LUE model is totally based on amount of APAR converted through photosynthesis of vegetation. Here, APAR was derived by available PAR and derived FAPAR (described in Chapter3). Temporal and Spatial distribution of derived FAPAR for 2009-10 and 2013-14 is presented in figure 5.20, figure 5.21 and 5.22. FAPAR values were found to be in range of 0.0 to 1.0. In 2009-10, FAPAR values observed in March were higher ranging between 0.7 to 0.8 both for Haryana and Meerut because of peak growth stage of wheat while in November values for Haryana was0.3 because of early growth stage which then increased every month showing vegetation vigor in that area. In April values again decline (0.40 to 0.45) due to harvested fields.

In Meerut region, FAPAR has shown rise in the curve after December month due to late sowing of wheat in that area. In 2013-14 same pattern was observed but value range is higher than in 2009-10. FAPAR values reaches to more than 0.8 in February and March and then decline reaching around 0.52 to 0.54 in April because of harvesting.

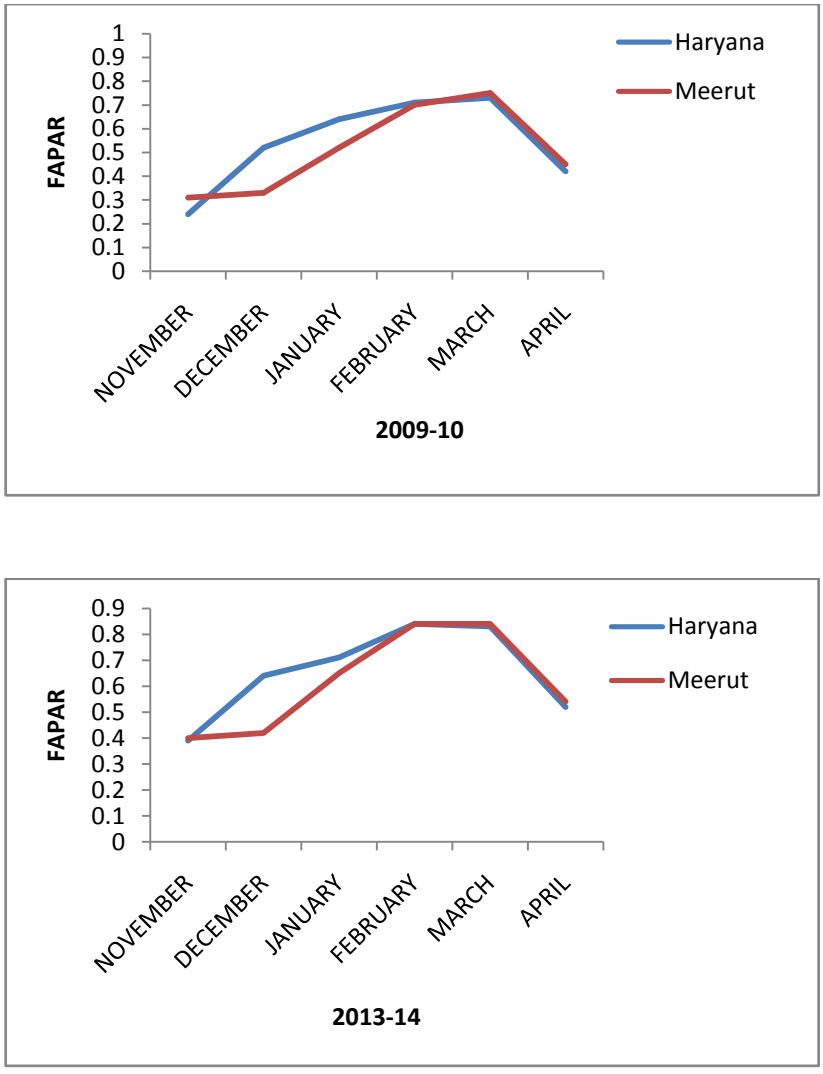

Figure 5.20: Temporal profiles for FAPAR generated in 2009-10 and 2013-14

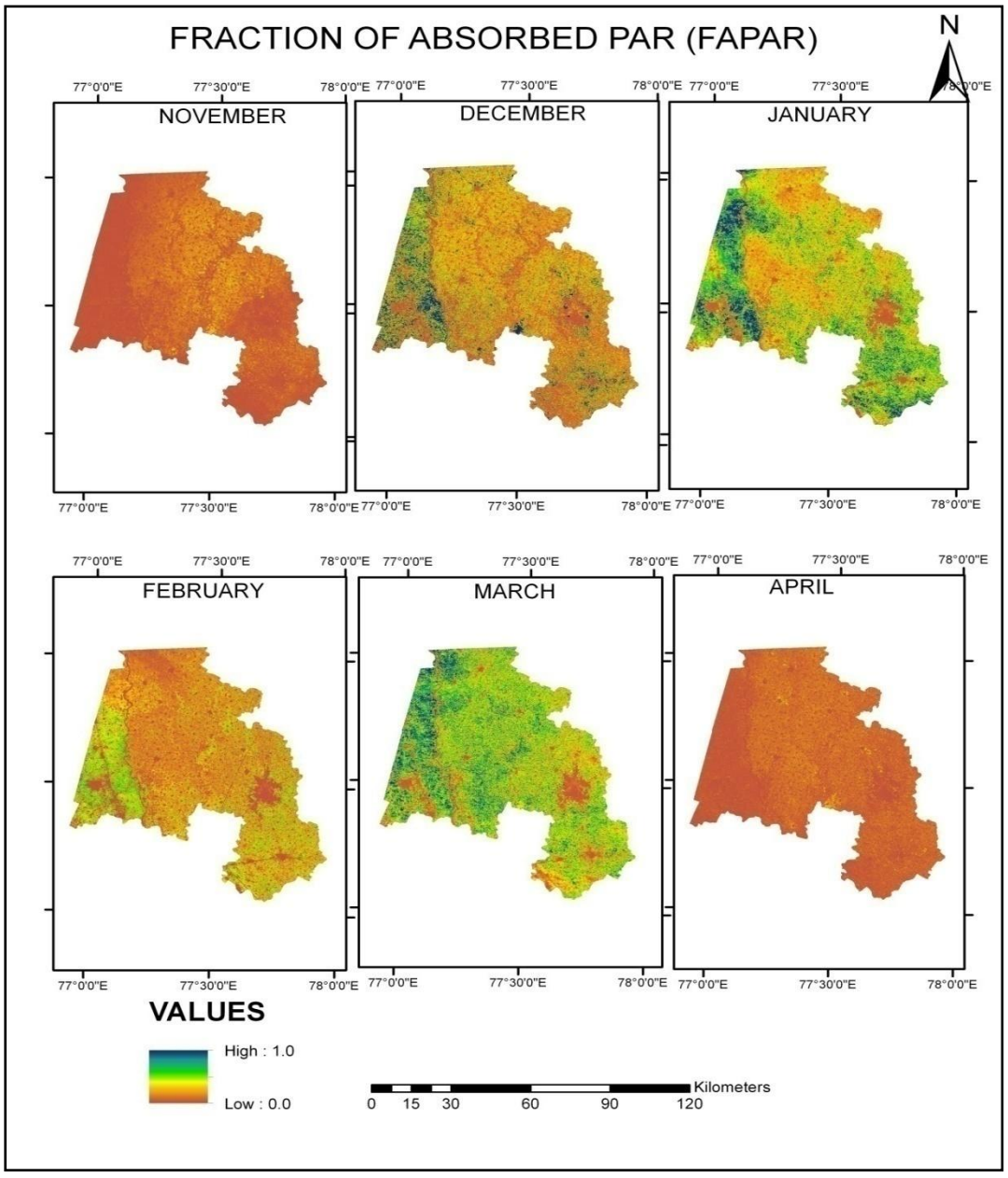

Figure 5.21: Spatial distribution of FAPAR in 2009-10

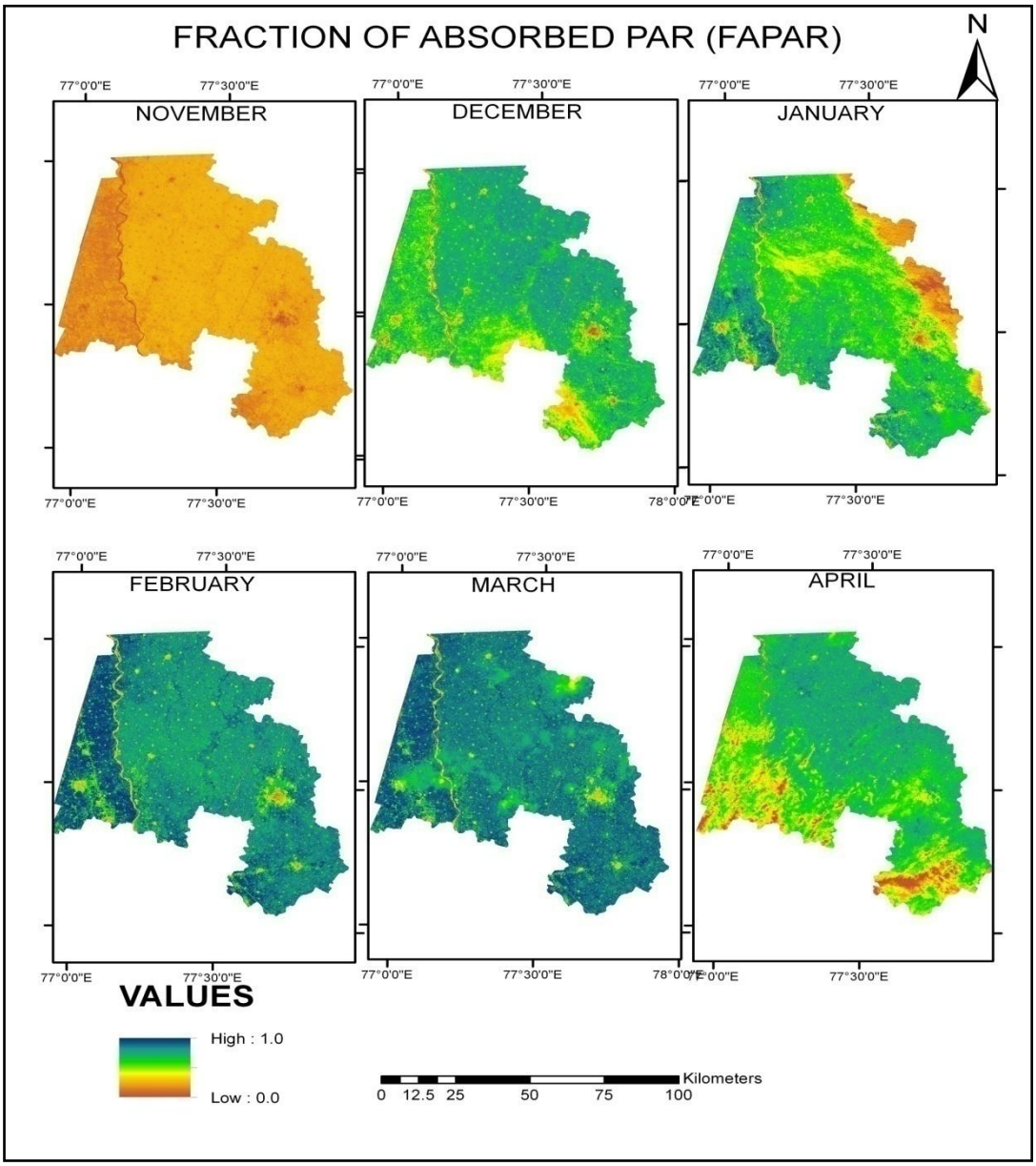

Figure 5.22: Spatial distribution of FAPAR in 2013-14

5.9 ESTIMATING LIGHT USE EFFICIENCY

Light use efficiency is the main controlling factor in LUE model for predicting productivity. The Magnitude of LUE differs across vegetation types spatially and temporally due to variable temperature and moisture conditions. Controlling factors of LUE are optimal temperature and moisture stress. Variations in temperature and water scalar can led to decline in LUE which can affect final yield. In figure 5.23 (a) and (b) February month LUE image is presented to briefly describe its concept related with two different water scalars when taken in its calculation. As we have discussed above that the moisture status of vegetation can affect LUE predictions. If crop is under stress then LUE will decline. So here we are using two different water scalars in estimating LUE. Ws_LSWI and Ws_VWSI are used in LUE calculations for all months. The difference in the estimated LUE can be seen properly in high vegetative month. So February month derived LUE is presented here. We can observe here that LUE with Ws_LSWI has shown better results than Ws_VWSI. In 2010 higher value ranges to 2.85 in both images but maximum area showing high LUE can be observed in image with Ws_LWSI as water scalar. Similarly in 2014 February image (figure 5.24) higher value reached to 1.76 for both images but spatial distribution of higher value was large for Ws_LSWI. So, with this understanding we can conclude that Ws_LSWI has shown higher LUE than Ws_VWSI.

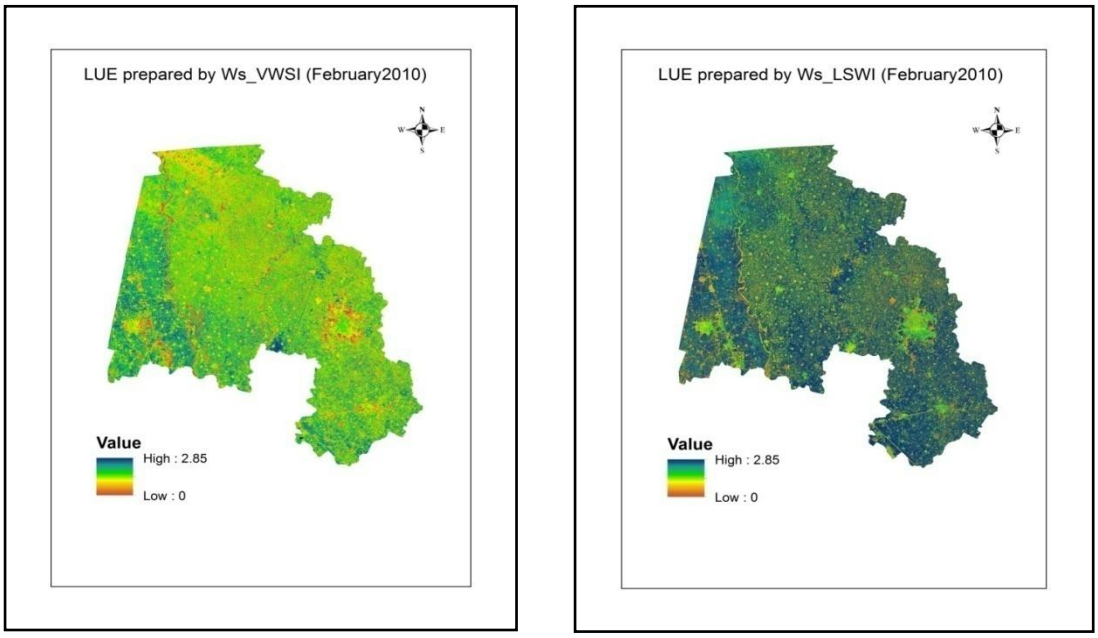

(a) **(b)**

Figure 5.23: Spatial distribution of LUE for February using different water scalar (a) Ws_VWSI (b) Ws_LSWI for 2009-10

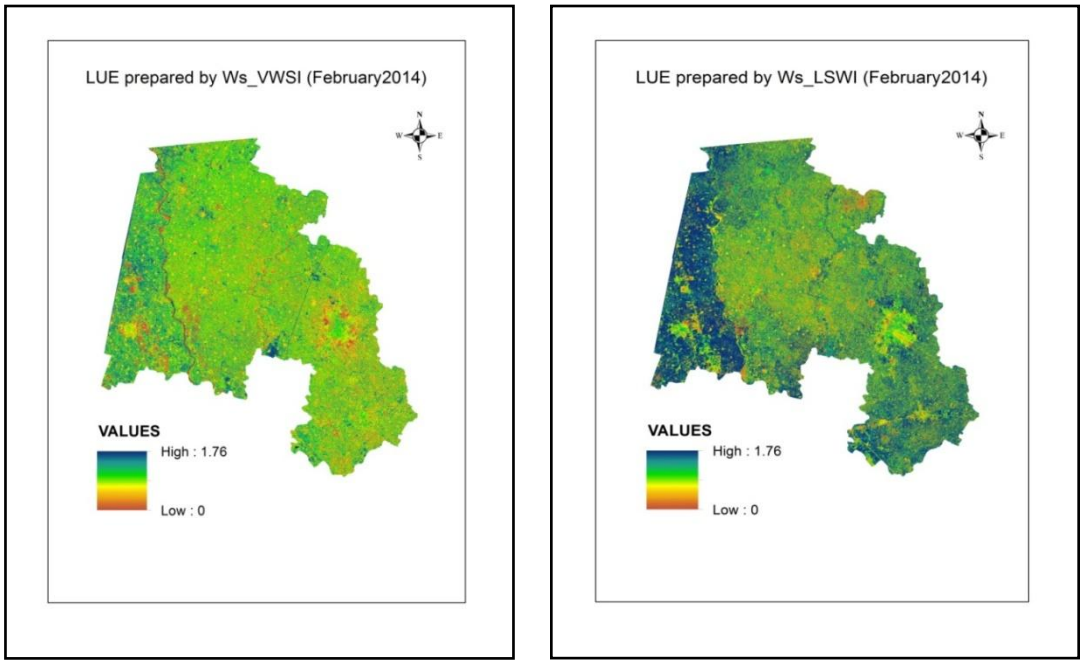

(a) **(b)**

Figure 5.24 Spatial distribution of LUE for February using different water scalar (a) Ws_VWSI (b) Ws_LSWI for 2013-14

5.10 YIELD ESTIMATION

Yield was predicted by using Light use efficiency model given by Monteith. This model uses PAR, FAPAR, LUE and Harvest index for calculating productivity. FAPAR and LUE are very important factors which show effect of crop condition over productivity. In this study productivity was estimated for two year Rabi season (2009-10) and (2013-14), derivation of parameters for LUE model has already been explained for both years.

The simulated productivity for a particular season was summed up and masked for wheat growing areas. Wide range of variations existed across western Uttarpradesh and Haryana. In 2009-10 productivity observed with LUE(LSWI) showed maximum values ranging between 3.5 -7.5 t/ha for most of the area in Haryana, while a small portion of area near Sonipat showed values between 7.5 – 9.5 t/ha. In Meerut maximum area extends to 5.5 t/ha whereas very small area near Ghaziabad ranges between 5.5 – 7.5 t/ha.

Same year, if we observe yield with LUE (VWSI), maximum area fall in the range between 2.5 to 5.5 t/ha whereas values more than 6.5 and less than 7.5 t/ha were observed near Sonipat. Maximum values reached to 3.5 t/ha for western Uttarpradesh while less area showed value range between 3.5-4.5 t/ha.

In 2013-14 productivity derived with LUE (LSWI) predicted maximum value range between 2.5-6 t/ha. In western Uttarpradesh most of the area has been observed in the range between 2.5-3.5 t/ha while Haryana covered the range between 5.5 – 9 t/ha. Values between 4.5-5.5 t/ha was observed in some part of Haryana. In western Uttarpradesh least area has been observed with productivity, ranging between 5.5-6.5 t/ha. As seen in figure 5.26(b) yield estimated using LUE (VWSI) observed values ranging more than 5.5t/ha and less than 9 t/ha for major parts of Haryana while some of the area ranges between 4.5-5.5 t/ha. Whereas major area of western Uttarpradesh falls in the range between 1.5-3.5 t/ha and minor part shows productivity range between 5.5-6.5 t/ha.

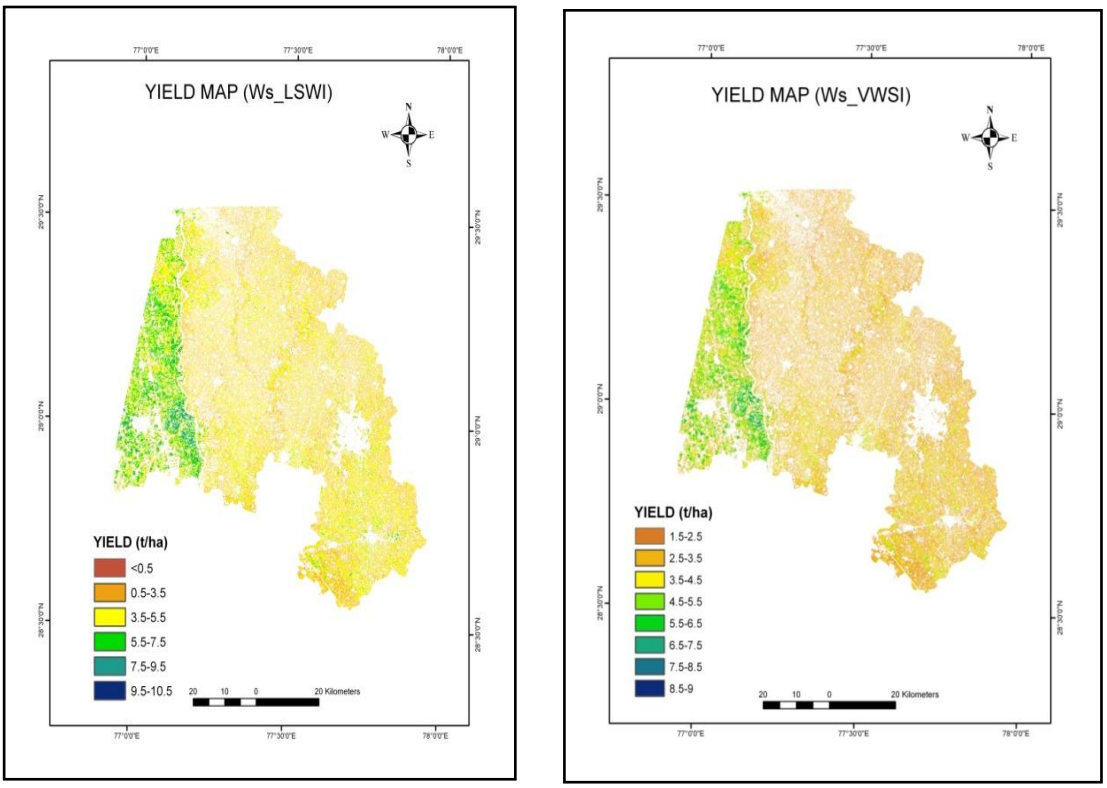

(a) (b)

Figure 5.25: Spatial pattern of wheat yield from different LUE scalar: (a) Ws (LSWI) (b) Ws_(VWSI) during 2009-10

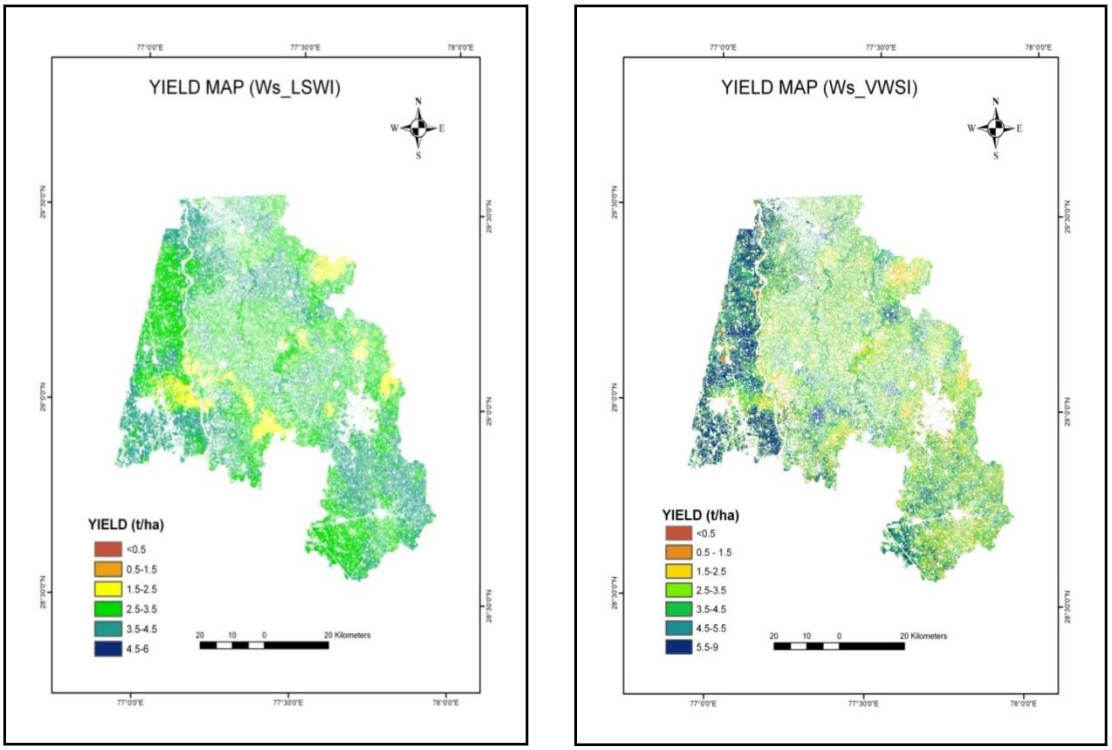

(a) **(b)**

Figure 5.26: Spatial pattern of wheat yield from different LUE scalar: (a) Ws (LSWI) (b) Ws_ (VWSI) during 2013-14

In figure 5.27 spatial distribution of productivity with histogram has been presented. Spatial distribution of productivity from LUE (LSWI) shows mean equal to 355g/m^2 for 2009-10 and 510g/m^2 for 2013-14(figure 5.27) while mean productivity obtained from LUE(VWSI) for 2009-10 were 298g/m^2 and for 2013-14 were 352g/m^2.

For 2009-10 and 2013-14 mean values are higher for LUE(LSWI) water scalar in comparison with LUE(VWSI).Moreover we can observe two peaks for LUE(LSWI) of 2013-14.The higher peak signifies Haryana region where productivity is more than Western Uttarpradesh which signify small peak. So, we can conclude that productivity of wheat simulated using water scalar from LSWI remained higher than Ws_VWSI. These differences were explained by variations in

light use efficiency resulted from different water scalars (figure 5.23 and 5.24).Higher LUE from Ws (LSWI) led to high levels of yield during period of maximum growth accumulation

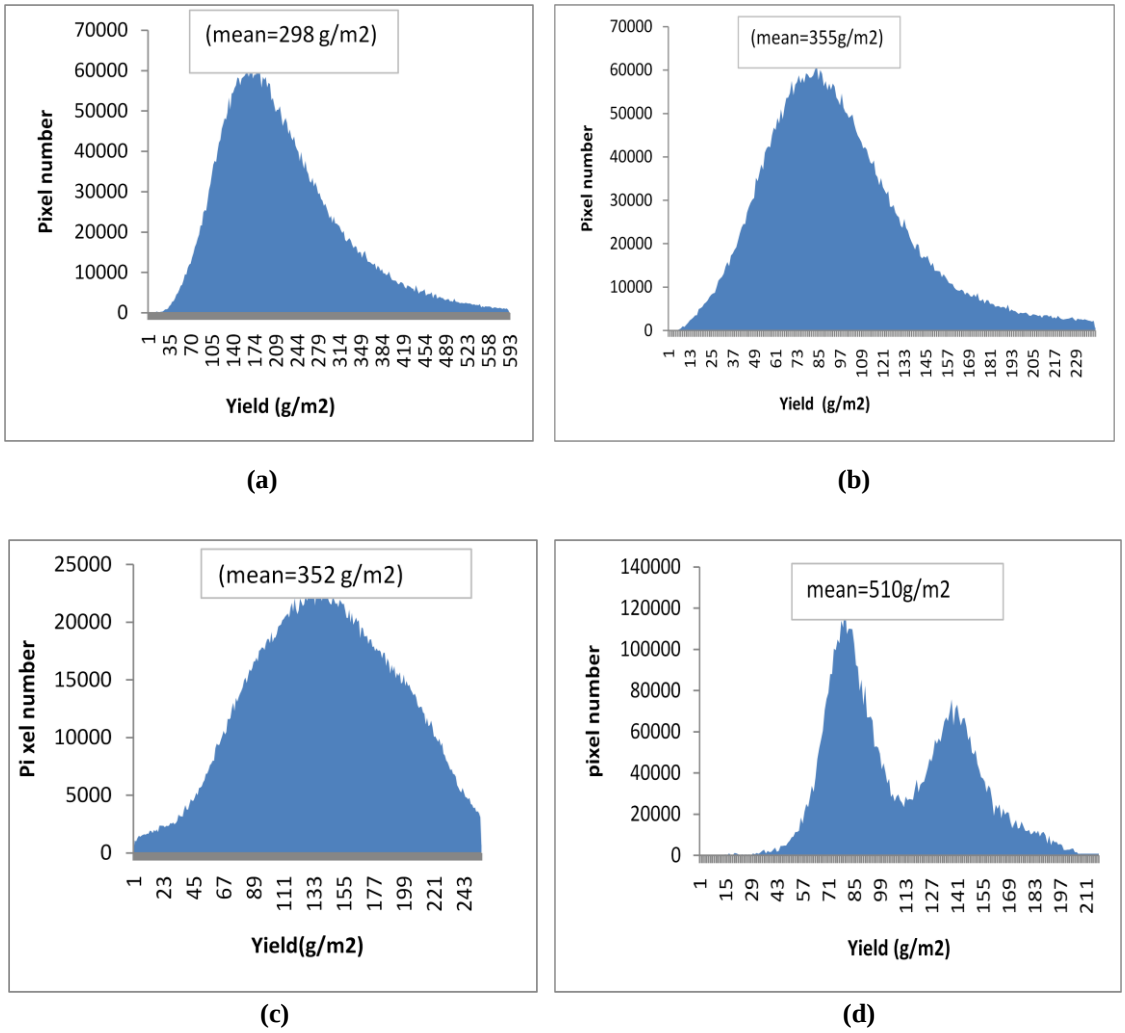

Figure 5.27: Spatial pattern with histogram frequency of productivity of wheat crop for different water stress scalars (a) LUE (VWSI),for 2009_10 (b) LUE (LSWI)for 2009_10 (c) LUE (VWSI),for 2013_14 (d) LUE (LSWI) for 2013_14

5.11 VALIDATION OF ESTIMATED YIELD

Wheat yield estimated from LUE model was validated against ground measured yield data obtained at field scale (from CCE). Whereas modeled yield for 2009-10 was compared with district-level acreage yield (BES). Water scalar from VWSI and LSWI were used down-regulating Maximum LUE and finally yield calculation. In 2009-10, yield estimated by LUE (LSWI) showed good results in comparison to LUE (VWSI) for all blocks except Sonipat (shown in figure 5.28). Predicted yield was found to be lower than observed yield.

For 2013-14, results were validated by using 1:1 statistical plot between measured and observed data. The temporal dynamics of predicted productivity agreed significantly well with observed productivity. The Coefficient of determination R^2 and RMSE observed for LUE(LSWI) based productivity was 0.65 and 1.00 showing an accepted agreement whereas productivity with LUE(VWSI) showed an R^2 of 0.46 and RMSE of 1.01.Overall statistical details are shown in table 5.4. Moreover predicted productivity was found to be higher than observed productivity showing an overestimated value of 14% for productivity with LUE(LSWI) whereas 3% for LUE(VWSI).

Hence, we can conclude that close relationship was observed between simulated productivity obtained from LUE based on LSWI and observed productivity of wheat in parts of Haryana and western Uttarpradesh.

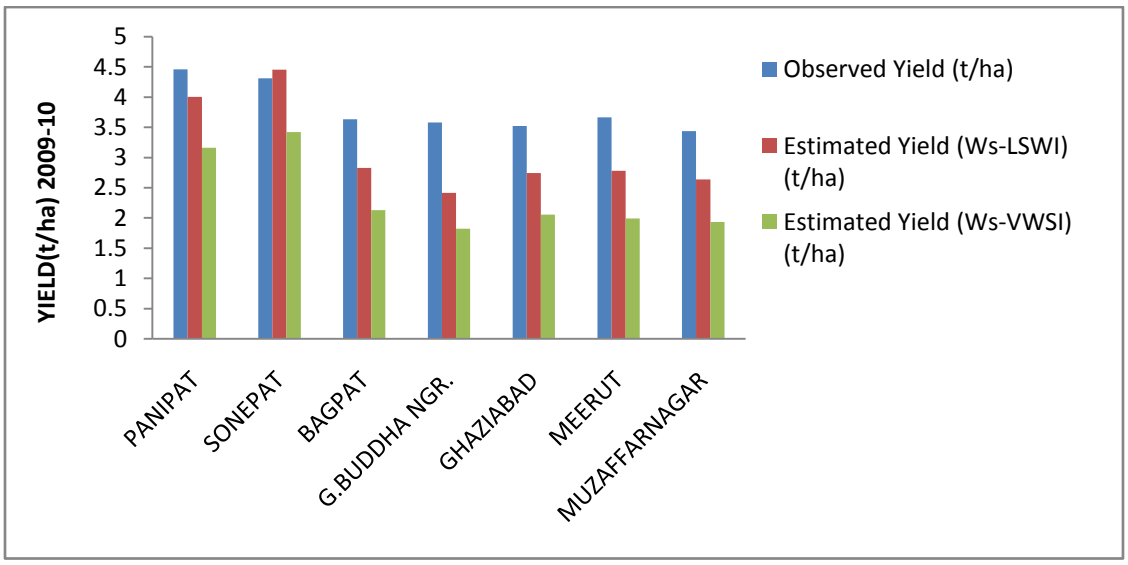

Figure 5.28: Comparison of estimated yield with different water scalars with observed yield for 2009-10

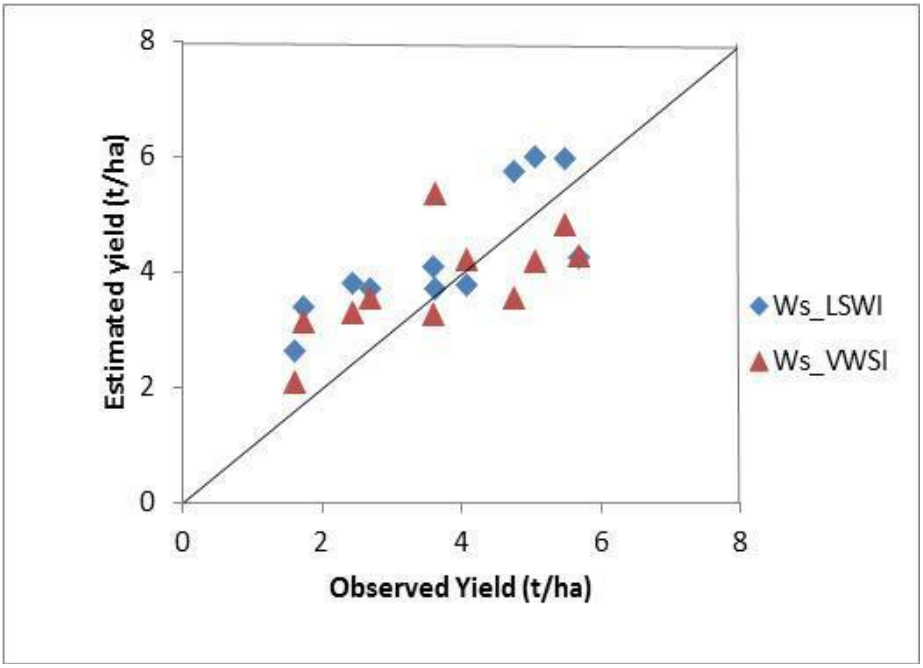

Figure 5.29: Line plot for observed vs. estimated yield for 2013-14

Table 1.4: Statistical relation details

YIELD	AGREEMENT INDEX	RMSE (t/ha)	R^2	Mean RD (%)
Ws_LSWI	0.82	1.00	0.65	-14.89
WS_VWSI	0.77	1.01	0.46	-3.67

SUMMARY AND CONCLUSION *Chapter 6*

Global water scarcity and unavailability of fresh water including many other biological factors has led to affect crop water status influencing its growth. The study was focused on detecting crop water stress and observing its impacts over productivity of wheat. The prime objective of the study was to assess performance of different approaches of water stress detection from satellite data and validating with Eddy Covariance measurements and to analyze the importance of water stress factor in controlling cropland productivity over space and time.

The Study was conducted in parts of Haryana and western Uttarpradesh falling under 26.4 degree and 30.1 degree latitude and 77.3 degree and 80.44 degree longitude. Wheat and Sugarcane are the dominant crop practiced in the study area during Rabi season. Landsat data for 2009-10 and 2013-14 Rabi season was used in this study. Since study was specified for wheat crop, crop discrimination was done using rule based classification technique. Using rule based classifier wheat was properly discriminated from other classes showing individual accuracy of wheat as 85% and overall accuracy of 90%. Different satellite based water stress indices viz., Ws_LSWI, Ws_VWSI, Ws_WSI were derived individually from optical and thermal dataset. SEBS model was also used for deriving daily ET using multi temporal landsat data. Predicted water stress for 2009-10 were compared with flux tower based ET.

To assess the impact of water stress over productivity LUE model was used. Water scalar, temperature scalar and maximum light use efficiency were used for deriving productivity. APAR and LUE were the two important inputs used in LUE model. Water scalars Ws_LSWI and Ws_VWSI were used in LUE model for assessing impact of water stress over productivity of wheat. Estimated FAPAR was developed by using ground readings taken during field visit and showing a logarithmic relation between FAPAR and NDVI which was validated and used for productivity calculation (2013-14) and final productivity was validated with yield estimated by crop cutting experiment (CCE) for 2013-14 and by crop statistics (BES) for 2009-10. The impact of water stress was observed over productivity of wheat by using two different water scalar viz., Ws_LSWI, Ws_VWSI amongst them Ws_LSWI proved to be better indices for estimating water stress and showing its impact over productivity.

From this study the following conclusions were made:

- Overall accuracy of classified map was 90.12% whereas kappa coefficient was 0.87. Accuracy individually for wheat was 85%.

- Different water stress indices were used for quantifying water stress by satellite data. Out of all, Ws_LSWI was found superior over other indices. It showed an RMSE of 0.12, R^2 of 0.65 whereas observed R^2 for Ws_VWSI was 0.76.
- SEBS model derived daily ET values were over estimated for all months when compared to Flux Tower ET.
- Water stress observed was more over Haryana region in November and April when compared to Meerut. Water stress observed for February and March was less due to good wheat growth.
- Estimated FAPAR model when validated with ground measured FAPAR showed an R^2= 0.54.
- LUE was derived using two different water scalar. Ws_LSWI based estimated LUE showed better results for February month than Ws_VWSI.
- Final yield detected was higher for Haryana region than compared to western UP. Productivity obtained using Ws_LSWI proved to be superior over Ws_VWSI showing R^2 0.65 but overestimation of yield was observed for both.

REFERENCES

Allen, R.G., Tasumi, M., Trezza, R., 2007. Satellite-based energy balance for mapping evapotranspiration with internalized calibration (METRIC)—Model. J. Irrig. Drain. Eng. 133, 380–394.

Almhab, A., Busu, I., n.d. Decision Support System for Estimation of Regional Evapotranspiration in arid areas: Application to the Republic of Yemen.

Asrar, G., Fuchs, M., Kanemasu, E.T., Hatfield, J.L., 1984. Estimating absorbed photosynthetic radiation and leaf area index from spectral reflectance in wheat. Agron. J. 76, 300–306.

Asrar, G., Kanemasu, E.T., Yoshida, M., 1985. Estimates of leaf area index from spectral reflectance of wheat under different cultural practices and solar angle. Remote Sens. Environ. 17, 1–11.

Baret, F., Guyot, G., 1991. Potentials and limits of vegetation indices for LAI and APAR assessment. Remote Sens. Environ. 35, 161–173.

Bastiaanssen, W.G.M., Menenti, M., Feddes, R.A., Holtslag, A.A.M., 1998. A remote sensing surface energy balance algorithm for land (SEBAL). 1. Formulation. J. Hydrol. 212, 198–212.

Biggs, T.W., Mishra, P.K., Turral, H., 2008. Evapotranspiration and regional probabilities of soil moisture stress in rainfed crops, southern India. Agric. For. Meteorol. 148, 1585–1597.

Black, M., Fleming, A., Riley, T., Ferrier, G., Fretwell, P., McFee, J., Achal, S., Diaz, A.U., 2014. On the Atmospheric Correction of Antarctic Airborne Hyperspectral Data. Remote Sens. 6, 4498–4514.

Campbell, J.B., 1987. Introduction to remote sensing, 1987. Fung T Drew E PERS 53, l649–l658.

Carlson, T.N., Buffum, M.J., 1989. On estimating total daily evapotranspiration from remote surface temperature measurements. Remote Sens. Environ. 29, 197–207.

Carlson, T.N., Gillies, R.R., Schmugge, T.J., 1995a. An interpretation of methodologies for indirect measurement of soil water content. Agric. For. Meteorol. 77, 191–205.

Carlson, T.N., Gillies, R.R., Schmugge, T.J., 1995b. An interpretation of methodologies for indirect measurement of soil water content. Agric. For. Meteorol. 77, 191–205.

Carlson, T.N., Perry, E.M., Schmugge, T.J., 1990. Remote estimation of soil moisture availability and fractional vegetation cover for agricultural fields. Agric. For. Meteorol. 52, 45–69.

Chavez, P.S., 1996. Image-based atmospheric corrections-revisited and improved. Photogramm. Eng. Remote Sens. 62, 1025–1035.

Chen, J.M., 1996. Canopy architecture and remote sensing of the fraction of photosynthetically active radiation absorbed by boreal conifer forests. Geosci. Remote Sens. IEEE Trans. On 34, 1353–1368.

Chen, J.M., Chen, X., Ju, W., Geng, X., 2005. Distributed hydrological model for mapping evapotranspiration using remote sensing inputs. J. Hydrol. 305, 15–39.

Claudio, H.C., Cheng, Y., Fuentes, D.A., Gamon, J.A., Luo, H., Oechel, W., Qiu, H.-L., Rahman, A.F., Sims, D.A., 2006. Monitoring drought effects on vegetation water content and

fluxes in chaparral with the 970 nm water band index. Remote Sens. Environ. 103, 304–311.
Clawson, K.L., Blad, B.L., 1982. Infrared thermometry for scheduling irrigation of corn. Agron. J. 74, 311–316.
Cohen, W.B., 1991. Response of vegetation indices to changes in three measures of leaf water stress.
Consoli, S., D'Urso, G., Toscano, A., 2006. Remote sensing to estimate ET-fluxes and the performance of an irrigation district in southern Italy. Agric. Water Manag. 81, 295–314.
De Troch, F.P., Troch, P.A., Su, Z., Lin, D.S., 1996. Application of remote sensing for hydrological modelling, in: Distributed Hydrological Modelling. Springer, pp. 165–191.
DeFries, R., Hansen, M., Townshend, J., 1995. Global discrimination of land cover types from metrics derived from AVHRR Pathfinder data. Remote Sens. Environ. 54, 209–222.
Dodds, P.E., Barton, A., Meyer, W.S., 2005. Review of Methods to Estimate Irrigated Reference Crop Evapotranspiration Across Australia.
Du, J.P., Sun, R., 2012. Estimation of evapotranspiration for ungauged areas using MODIS measurements and GLDAS data. Procedia Environ. Sci. 13, 1718–1727.
Dubey, R.P., Ajwani, N.D., Navalgund, R.R., 1991. Relation of wheat yield with parameters derived from a spectral growth profile. J. Indian Soc. Remote Sens. 19, 27–44.
Elhag, M., Psilovikos, A., Manakos, I., Perakis, K., 2011. Application of the SEBS water balance model in estimating daily evapotranspiration and evaporative fraction from remote sensing data over the Nile Delta. Water Resour. Manag. 25, 2731–2742.
FAO. 2008. Expert meeting on Climate change, water and food security. 26–28 February 2008. Contribution to the High Level Conference on World Food Security and the Challenge of Climate Change and Bio-energy on Water and Climate Change.
FAO. 2011a. Climate change, water and food security. Prepared by H. Turral, J. Burke and J.-M. Faurès. FAO Water Reports, no. 36.
FAO. 2011b. Global food losses and food waste; extend causes and prevention. Study conducted for the International Congress "Save Food!" at Interpack2011, Düsseldorf, Germany.
FAO. 2012. Crop yield response to water. Prepared by P. Steduto, T.C. Hsiao, E. Fereres and D. Raes. FAO Irrigation and Drainage Paper, no. 66. 500 p.

Gallagher, J.N., Biscoe, P.V., 1978. Radiation absorption, growth and yield of cereals. J. Agric. Sci. 91, 47–60.
Gao, B.-C., 1996. NDWI—a normalized difference water index for remote sensing of vegetation liquid water from space. Remote Sens. Environ. 58, 257–266.
Ghulam, A., Li, Z.-L., Qin, Q., Yimit, H., Wang, J., 2008. Estimating crop water stress with ETM+ NIR and SWIR data. Agric. For. Meteorol. 148, 1679–1695.
Gillies, R.R., Carlson, T.N., 1995. Thermal remote sensing of surface soil water content with partial vegetation cover for incorporation into climate models. J. Appl. Meteorol. 34, 745–756.

Goward, S.N., Xue, Y., Czajkowski, K.P., 2002. Evaluating land surface moisture conditions from the remotely sensed temperature/vegetation index measurements: an exploration with the simplified simple biosphere model. Remote Sens. Environ. 79, 225–242.

Gower, S.T., Kucharik, C.J., Norman, J.M., 1999. Direct and indirect estimation of leaf area index,< i> f</i>< sub> apar</sub>, and net primary production of terrestrial ecosystems. Remote Sens. Environ. 70, 29–51.

Hardisky, M.A., Klemas, V., Smart, M., 1983. The influence of soil salinity, growth form, and leaf moisture on the spectral radiance of. Spartina Alterniflora 77–83.

Hooda, R.S., DYE, D., 1995. Identification and mapping irrigated vegetation using NDVI-Climatological modeling: In: Proceeding of ACRS. Thiland.

Hope, A.S., Petzold, D.E., Goward, S.N., Ragan, R.M., 1986. SIMULATED RELATIONSHIPS BETWEEN SPECTRAL REFLECTANCE, THERMAL EMISSIONS, AND EVAPOTRANSPIRATION OF A SOYBEAN CANOPY1. JAWRA J. Am. Water Resour. Assoc. 22, 1011–1019.

Hunt, E.R., Running, S.W., 1992. Effects of Climate and Lifeporm on Dry Matter Yield (E) from Simulations Using Biome-BGC, in: Geoscience and Remote Sensing Symposium, 1992. IGARSS'92. International. IEEE, pp. 1631–1633.

Hunt Jr, R., Rock, B.N., Nobel, P.S., 1987. Measurement of leaf relative water content by infrared reflectance. Remote Sens. Environ. 22, 429–435.

Idso, S.B., 1982. Non-water-stressed baselines: a key to measuring and interpreting plant water stress. Agric. Meteorol. 27, 59–70.

Idso, S.B., Jackson, R.D., Reginato, R.J., 1977. Remote sensing for agricultural water management and crop yield prediction. Agric. Water Manag. 1, 299–310.

IPCC. 2008. Climate Change and Water. Edited by B.C. Bates, Z.W. Kundzewicz, S. Wu and J.P. Palutikof. IPCC Technical Paper VI. IPCC Secretariat, Geneva. 210 p.

Irmak, A., 2008. Estimation of Land Surface Energy Fluxes: An Application of Satellite Remote Sensing Procedure.

Jackson, R.D., Idso, S.B., Reginato, R.J., Pinter, P.J., 1981. Canopy temperature as a crop water stress indicator. Water Resour. Res. 17, 1133–1138.

Jacob, F., Olioso, A., Gu, X.F., Su, Z., Seguin, B., 2002. Mapping surface fluxes using airborne visible, near infrared, thermal infrared remote sensing data and a spatialized surface energy balance model. Agronomie 22, 669–680.

Jensen, M.E., Burman, R.D., Allen, R.G., 1990. Evapotranspiration and irrigation water requirements. ASCE.

Jiang, L., Islam, S., 2001. Estimation of surface evaporation map over southern Great Plains using remote sensing data. Water Resour. Res. 37, 329–340.

Kalma, J.D., McVicar, T.R., McCabe, M.F., 2008. Estimating land surface evaporation: A review of methods using remotely sensed surface temperature data. Surv. Geophys. 29, 421–469.

Kim, H.J., 2006. Combined use of vegetation and water indices from remotely-sensed AVIRIS and MODIS data to monitor riparian and semiarid vegetation.

Kustas, W.P., Li, F., Jackson, T.J., Prueger, J.H., MacPherson, J.I., Wolde, M., 2004. Effects of remote sensing pixel resolution on modeled energy flux variability of croplands in Iowa. Remote Sens. Environ. 92, 535–547.

Landsberg, J.J., Waring, R.H., 1997. A generalised model of forest productivity using simplified concepts of radiation-use efficiency, carbon balance and partitioning. For. Ecol. Manag. 95, 209–228.

Law, B.E., Waring, R.H., 1994. Combining remote sensing and climatic data to estimate net primary production across Oregon. Ecol. Appl. 4, 717–728.

Legg, B.J., Day, W., Lawlor, D.W., Parkinson, K.J., 1979. The effects of drought on barley growth: models and measurements showing the relative importance of leaf area and photosynthetic rate. J. Agric. Sci. 92, 703–716.

Li, S.Z., Singh, S., 2009. Markov random field modeling in image analysis. Springer.

Liang, S., Fang, H., Chen, M., 2001. Atmospheric correction of Landsat ETM+ land surface imagery. I. Methods. Geosci. Remote Sens. IEEE Trans. On 39, 2490–2498.

Lillesand, T.M., Kiefer, R.W., Chipman, J.W., 2004. Remote sensing and image interpretation. John Wiley & Sons Ltd.

López López, R., Arteaga Ramírez, R., Vázquez Peña, M.A., López Cruz, I., Sánchez Cohen, I., 2009. Índice de estrés hídrico como un indicador del momento de riego en cultivos agrícolas. Agric. Téc. En México 35, 97–111.

Menenti, M., Choudhury, B.J., 1993. Parameterization of land surface evaporation by means of location dependent potential evaporation and surface temperature range.

Monteith, J.L., 1972. Solar radiation and productivity in tropical ecosystems. J. Appl. Ecol. 9, 747–766.

Monteith, J.L., Moss, C.J., 1977. Climate and the efficiency of crop production in Britain [and discussion]. Philos. Trans. R. Soc. Lond. B Biol. Sci. 281, 277–294.

Moran, M.S., Clarke, T.R., Inoue, Y., Vidal, A., 1994. Estimating crop water deficit using the relation between surface-air temperature and spectral vegetation index. Remote Sens. Environ. 49, 246–263.

Mu, Q., Heinsch, F.A., Zhao, M., Running, S.W., 2007. Development of a global evapotranspiration algorithm based on MODIS and global meteorology data. Remote Sens. Environ. 111, 519–536.

Mu, Q., Zhao, M., Running, S.W., 2011. Improvements to a MODIS global terrestrial evapotranspiration algorithm. Remote Sens. Environ. 115, 1781–1800.

Myneni, R.B., Williams, D.L., 1994. On the relationship between FAPAR and NDVI. Remote Sens. Environ. 49, 200–211.

Navalgund, R.R., Parihar Ajai, J.S., Nageshwara Rao, P.P., 1991a. Crop inventory using remotely sensed data. Curr. Sci. 61, 162–171.

Navalgund, R.R., Parihar Ajai, J.S., Nageshwara Rao, P.P., 1991b. Crop inventory using remotely sensed data. Curr. Sci. 61, 162–171.

Nemani, R.R., Running, S.W., 1989. Estimation of regional surface resistance to evapotranspiration from NDVI and thermal-IR AVHRR data. J. Appl. Meteorol. 28, 276–284.

Nouvellon, Y., Seen, D.L., Rambal, S., Bégué, A., Moran, M.S., Kerr, Y., Qi, J., 2000. Time course of radiation use efficiency in a shortgrass ecosystem: consequences for remotely sensed estimation of primary production. Remote Sens. Environ. 71, 43–55.

Patel, N.R., Mehta, A.N., Shekh, A.M., 2001. Canopy temperature and water stress quantificaiton in rainfed pigeonpea (< i> Cajanus cajan</i>(L.) Millsp.). Agric. For. Meteorol. 109, 223–232.

Potter, C.S., Randerson, J.T., Field, C.B., Matson, P.A., Vitousek, P.M., Mooney, H.A., Klooster, S.A., 1993. Terrestrial ecosystem production: A process model based on global satellite and surface data. Glob. Biogeochem. Cycles 7, 811–841.

Price, J.C., 1987. Calibration of satellite radiometers and the comparison of vegetation indices. Remote Sens. Environ. 21, 15–27.

Price, J.C., 1990. Using spatial context in satellite data to infer regional scale evapotranspiration. Geosci. Remote Sens. IEEE Trans. On 28, 940–948.

Priestley, C.H.B., Taylor, R.J., 1972. On the assessment of surface heat flux and evaporation using large-scale parameters. Mon. Weather Rev. 100, 81–92.

Prince, S.D., Goward, S.N., 1995. Global primary production: a remote sensing approach. J. Biogeogr. 815–835.

Qi, J., Chehbouni, A., Huete, A.R., Kerr, Y.H., Sorooshian, S., 1994. A modified soil adjusted vegetation index. Remote Sens. Environ. 48, 119–126.

Reynolds, C.A., Yitayew, M., Slack, D.C., Hutchinson, C.F., Huete, A., Petersen, M.S., 2000. Estimating crop yields and production by integrating the FAO Crop Specific Water Balance model with real-time satellite data and ground-based ancillary data. Int. J. Remote Sens. 21, 3487–3508.

Ridd, M.K., 1995. Exploring a VIS (vegetation-impervious surface-soil) model for urban ecosystem analysis through remote sensing: comparative anatomy for cities†. Int. J. Remote Sens. 16, 2165–2185.

Ripple, W.J., 1986. Spectral reflectance relationships to leaf water stress.

Roerink, G.J., Su, Z., Menenti, M., 2000. S-SEBI: A simple remote sensing algorithm to estimate the surface energy balance. Phys. Chem. Earth Part B Hydrol. Oceans Atmosphere 25, 147–157.

Rouse Jr, J.W., Haas, R.H., Schell, J.A., Deering, D.W., 1974. Monitoring vegetation systems in the Great Plains with ERTS. NASA Spec. Publ. 351, 309.

Ruimy, A., Kergoat, L., Bondeau, A., Intercomparison, T., Model, P.O.T.P.N., 1999. Comparing global models of terrestrial net primary productivity (NPP): Analysis of differences in light absorption and light-use efficiency. Glob. Change Biol. 5, 56–64.

Ruimy, A., Saugier, B., Dedieu, G., 1994. Methodology for the estimation of terrestrial net primary production from remotely sensed data. J. Geophys. Res. Atmospheres 1984–2012 99, 5263–5283.

Running, S.W., Nemani, R.R., Heinsch, F.A., Zhao, M., Reeves, M., Hashimoto, H., 2004. A continuous satellite-derived measure of global terrestrial primary production. Bioscience 54, 547–560.

Runyon, J., Waring, R.H., Goward, S.N., Welles, J.M., 1994. Environmental limits on net primary production and light-use efficiency across the Oregon transect. Ecol. Appl. 4, 226–237.
Sabins Jr, F.F., n.d. Remote Sensing, Principles and Interpretation. 1978. San Francisco, WH Freeman & Co.
Sandholt, I., Rasmussen, K., Andersen, J., 2002. A simple interpretation of the surface temperature/vegetation index space for assessment of surface moisture status. Remote Sens. Environ. 79, 213–224.
Sands, P.J., 1996. Modelling canopy production. III. Canopy light-utilisation efficiency and its sensitivity to physiological and environmental variables. Funct. Plant Biol. 23, 103–114.
Sellers, P.J., 1985. Canopy reflectance, photosynthesis and transpiration. Int. J. Remote Sens. 6, 1335–1372.
Senay, G.B., Leake, S., Nagler, P.L., Artan, G., Dickinson, J., Cordova, J.T., Glenn, E.P., 2011. Estimating basin scale evapotranspiration (ET) by water balance and remote sensing methods. Hydrol. Process. 25, 4037–4049.
Senay, G.B., Verdin, J.P., Lietzow, R., Melesse, A.M., 2008. Global Daily Reference Evapotranspiration Modeling and Evaluation1. Wiley Online Library.
ŞENCAN, S., 2004. DECISION TREE CLASSIFICATION OF MULTI-TEMPORAL IMAGES FOR FIELD-BASED CROP MAPPING. MIDDLE EAST TECHNICAL UNIVERSITY.
Slater, P.N., 1980. Remote sensing: optics and optical systems. Read. Mass Addison-Wesley Publ. CoRemote Sens. No 1 1980 593 P 1.
Smyth, A.J., Dumanski, J., 1993. FESLM: An international framework for evaluating sustainable land management. FAO Rome,, Italy.
Stisen, S., Sandholt, I., Nørgaard, A., Fensholt, R., Jensen, K.H., 2008. Combining the triangle method with thermal inertia to estimate regional evapotranspiration—Applied to MSG-SEVIRI data in the Senegal River basin. Remote Sens. Environ. 112, 1242–1255.
Straschnoy, J.V., Di Bella, C.M., Jaimes, F.R., Oricchio, P.A., Rebella, C.M., 2006. Caracterización espacial del estrés hídrico y de las heladas en la región pampeana a partir de información satelital y complementaria. Rev. Investig. Agropecu. 35, 117–141.
Su, Z., 1999. The Surface Energy Balance System (SEBS) for estimation of turbulent heat fluxes. Hydrol. Earth Syst. Sci. 6, 85–100.
Su, Z.B., 2002. A Surface Energy Balance System (SEBS) for estimation of turbulent heat fluxes from point to continental scale, in: Spectra Workshop. p. 23.
Tang, R., Li, Z.-L., Tang, B., 2010. An application of the< i> T</i>< sub> s</sub>–VI triangle method with enhanced edges determination for evapotranspiration estimation from MODIS data in arid and semi-arid regions: Implementation and validation. Remote Sens. Environ. 114, 540–551.
Tian, Y., Zhang, Y., Knyazikhin, Y., Myneni, R.B., Glassy, J.M., Dedieu, G., Running, S.W., 2000. Prototyping of MODIS LAI and FPAR algorithm with LASUR and LANDSAT data. Geosci. Remote Sens. IEEE Trans. On 38, 2387–2401.
Tucker, C.J., 1979. Red and photographic infrared linear combinations for monitoring vegetation. Remote Sens. Environ. 8, 127–150.

Tucker, C.J., 1980. Remote sensing of leaf water content in the near infrared. Remote Sens. Environ. 10, 23–32.

Usman, M., Ahmad, A., Ahmad, S., Arshad, M., Khaliq, T., Wajid, A., Hussain, K., Nasim, W., Chattha, T.M., Trethowan, R., 2009. Development and application of crop water stress index for scheduling irrigation in cotton (Gossypium hirsutum L.) under semiarid environment. J. Food Agric. Environ. 7, 386–391.

Venturini, V., Islam, S., Rodriguez, L., 2008. Estimation of evaporative fraction and evapotranspiration from MODIS products using a complementary based model. Remote Sens. Environ. 112, 132–141.

Vermote, E.F., El Saleous, N.Z., Justice, C.O., 2002. Atmospheric correction of MODIS data in the visible to middle infrared: first results. Remote Sens. Environ. 83, 97–111.

Veroustraete, F., Sabbe, H., Eerens, H., 2002. Estimation of carbon mass fluxes over Europe using the C-Fix model and Euroflux data. Remote Sens. Environ. 83, 376–399.

Wright, G.C., Bell, M.J., Hammer, G.L., 1993. Leaf nitrogen content and minimum temperature interactions affect radiation-use efficiency in peanut. Crop Sci. 33, 476–481.

Xiao, X., Boles, S., Liu, J., Zhuang, D., Frolking, S., Li, C., Salas, W., Moore III, B., 2005. Mapping paddy rice agriculture in southern China using multi-temporal MODIS images. Remote Sens. Environ. 95, 480–492.

Xiao, X., Zhang, Q., Braswell, B., Urbanski, S., Boles, S., Wofsy, S., Moore III, B., Ojima, D., 2004. Modeling gross primary production of temperate deciduous broadleaf forest using satellite images and climate data. Remote Sens. Environ. 91, 256–270.

Zarco-Tejada, P. J., Miller, J. R., Mohammed, G. H., and No land, T. L. (2000), Chlorophyll fluorescence effects on vege tation apparent reflectance: I. Leaf-level measurements and model simulation. Remote Sens. Environ. (this issue).

Zhang, B., Kang, S., Li, F., Zhang, L., 2008. Comparison of three evapotranspiration models to Bowen ratio-energy balance method for a vineyard in an arid desert region of northwest China. Agric. For. Meteorol. 148, 1629–1640.

Zhang, X.C., WU, J., WU, H., Li, Y., 2011. Simplified SEBAL method for estimating vast areal evapotranspiration with MODIS data. Water Sci Eng 4, 24–35.